Phenotype-genotype distinctions among clones of the pine pitch canker pathogen *Fusarium circinatum*

by

Ongeziwe Mbhele

Submitted in partial fulfilment of the requirements for the degree

Magister Scientiae

In the Faculty of Natural & Agricultural Sciences,
Department of Biochemistry, Genetics, and Microbiology

University of Pretoria, Pretoria, South Africa

May 2022

Supervisor: Prof Emma Steenkamp

Co-supervisors: Prof. Almuth Hammerbacher, Dr. Felix Fru, Dr. Quentin Santana and Dr. Magrieta van der Nest

Table of contents

DECLARATION

I declare that the dissertation, which I hereby submit for the degree of **Master of Science** at the University of Pretoria, is my work and has not previously been submitted for a degree at another university. Where secondary material is used, this has been carefully acknowledged and referenced in accordance with university requirements. I am aware of university policy and its implications regarding plagiarism.

SIGNATURE: DATE: **17 May 2022**

ACKNOWLEDGEMENTS

I would like to thank everyone who contributed in any way significant to the completion of this dissertation. I am grateful to my supervisors, Professors Emma Steenkamp and Almuth Hammerbacher, Doctors Quentin Santana, Felix Fru, and Magrieta van der Nest. Your patience and guidance have made it possible to overcome all challenges, not only in this dissertation but also in many other aspects of my life.

I would like to further thank my funding bodies, The National Research Foundation (NRF), the University of Pretoria (UP), and the Tree Protection Cooperative Programme (TPCP) for financial support.

I would like to also extend my gratitude to my church and cell leader Lerato Pheeha, my family, and friends for their continued love and support.

PREFACE

The genomic information of an organism is expressed in its phenotypic traits. Therefore, to uncover the nature of its apparent/behavioural characteristics, thorough investigations of its gene and genomic characteristics are required. These traits can also be used to gain valuable information regarding the population biology of the organism. In fungi, two widely used traits include microsatellite-based typing and vegetative compatibility group designation. Both these methods are multilocus in nature, and thus have the potential to identify groups of individuals potentially representing clones. The work described in this dissertation represents a foundational study in which specific strains of the pine pitch canker pathogen *Fusarium circinatum* were characterized at the molecular level. The finding presented are intended to inform future research on how to identify and study clones of this fungus, when vegetative compatibility and microsatellites are considered. Such baseline data would be crucial not only for source-tracking of the pathogen during epidemics, but also in understanding the reproductive biology of the *F. circinatum*.

Chapter One provides a literature review of what is known about vegetative incompatibility, which is a phenomenon unique to fungi. It also summarizes the current techniques used to study this vegetative incompatibility. Particular attention is given to vegetative incompatibility in ascomycetes, as the molecular basis of this trait is best understood in the model species *Neurospora crassa*, *Podospora anserina*, *Aspergillus oryzae*, and *Cryphonectria parasitica*. Genes involved in vegetative incompatibility in these species have been molecularly characterised and are available for use as models for characterising other species with the aim to better understand their populations.

Chapter Two investigates whether the apparent microsatellite-based clonality observed in *F. circinatum* is also reflected at the phenotypic level. This was achieved by assaying the virulence of four distinct groups of isolates that are each characterized by distinct microsatellite-based genotypes. Different inoculation techniques that included tip, stem, and root inoculations were used on three months

old *P. patula* seedlings. The growth rates and sporulating capacities on ½ PDA and pine extract medium of the isolates were assessed. After these experiments, it was established that microsatellite-based clonality among isolates does not always extend to phenotype. Therefore, further molecular and phenotypic analyses are required to study genotype-phenotype relations in *F. circinatum*.

Chapter Three of this dissertation provides an *in silico* characterization of vegetative incompatibility genes in the genome of the reference strain (FSP34) of *F. circinatum* by making use of the genic information available for *N. crassa*, *P. anserina*, *A. oryzae*, and *C. parasitica*. Sequence similarity, phylogeny, and protein domain structure were used to identify the known genes in FSP34, and to determine the relationship of *F. circinatum* and the four model species in terms of *het/vic* genes distribution. The result of this study showed that the *het/vic* gene repertoire of *F. circinatum* is potentially shaped by gene duplication, followed by gene loss/multiplication and a variety of domain fusion/shuffling events.

The information in this dissertation adds to the body of knowledge about the reproductive mode of *F. circinatum*. Further integration of the data generated in this study into population genomics studies could potentially reveal which of the *het/vic* genes (if any) could serve as markers for delineating VCGs and whether these groupings are congruent with those inferred using microsatellite markers. This study enhanced our understanding of the fungus and may be used to optimize its control.

CHAPTER ONE

Vegetative compatibility and microsatellite as markers for delineation of fungal groups with special reference to *Fusarium circinatum*

Introduction

Microsatellites and vegetative compatibility have informative characteristics that have often been used for studying the population biology of fungi (Giraud et al., 2008; Shamim et al., 2016). These markers are useful in investigating genetic distribution and change among individuals due to forces such as mutation, genetic drift, reproduction and mating system, gene flow, and natural selection within and between populations (McDonald & Linde, 2002b; Nicolaus & Edelaar, 2018; Ottenburghs et al., 2019). In the understanding of the population biology of an organism: knowledge of their origin, introduction routes, dispersal, and distribution are established. Numerous studies and particularly on fungi have been conducted addressing these important biological concepts (Aneja, 2007; Baltrus et al., 2017; Castillo et al., 2021; McDonald & Linde, 2002a; McDonald et al., 1989). Findings from such studies are invaluable in developing effective strategies to limit the spread of pathogens and manage the disease they can cause (McDonald & Linde, 2002a).

A good example of how microsatellites and vegetative compatibility have aided in the study of a plant pathogen is *Fusarium circinatum*, the causal agent of pitch canker disease of pine. Populations of this fungus were first analysed using compatibility of strains during vegetative growth as an indication that they have the same set of alleles at all or most of the molecular loci determining this trait (Leslie, 1993). During assays based on this principle, strains are assigned to the so-called vegetative compatibility groups (VCGs) (Leslie & Summerell, 2006; Leslie, 1993). Analyses of VCGs of *F. circinatum* thus allowed for comparisons of the genetic diversity and makeup of different populations and aided in the development of disease management strategies (Drenkhan et al., 2020). Later, with the advent of next-generation sequencing technologies, a set of highly polymorphic microsatellite markers were developed by Santana et al. (2009) for this fungus. Various studies reviewed by Drenkhan et al., 2020 have since used these markers to reveal potential sources and introduction routes of this pathogen.

Methodologies involving microsatellites and vegetative compatibility can both be used to study the extent of clonality in populations (Leslie & Summerell, 2006; Leslie,

1993). Clonality refers to where a group contains genetically identical individuals, likely because they were produced asexually from the same ancestor (Hiebert et al., 2021; Stoeckel et al., 2021). In other words, microsatellite markers and VCG assays can allow for assembling individuals into groups that potentially represent distinct clones, because both approaches involve the "scoring" of multiple genetic loci (either individually as in the case of microsatellites, or collectively in the form of a distinct VCG phenotype as in the case of vegetative compatibility). From a plant pathology perspective, the identification of such groups is valuable in that it allows for the "tracking" of particular clones of a fungal pathogen within and between particular environments (Milgroom & Fry, 1997). Also, the ability to identify clones within populations is fundamental to studies aimed at inferring a pathogen's mating system, which represents fundamental information for disease management strategies (McDonald & Linde, 2002a).

This chapter aims to elucidate the vegetative compatibility and microsatellite markers in *F. circinatum* and how they are used to infer clonality. This is done by first describing the molecular basis of these two characters, and then explaining how they are used in the laboratory for population genetic studies. In both cases, I also consider their overall value for accurately delineating clones. Because my research project focuses on *F. circinatum*, I include a section on this fungus to briefly describe general aspects of its biology and pathological importance, as well as what we know about its population biology. I conclude the chapter by highlighting notable gaps in our knowledge and outlining potential future avenues for study.

Vegetative compatibility

Filamentous fungi are multicellular, multinucleate, interconnected networks of tube-shaped hyphae. In vegetative growth (Glass & Kuldau, 1992; Mela et al., 2020; Read & Roca, 2006), the hyphae communicate and chemotropically grow towards each other and establish contact. Cell fusion is then initiated, which results in the modification of the cell walls and fusion of the plasma membranes to form a heterokaryotic cell containing two different nuclei in a single cytoplasm. The fusion

process is referred to as hyphal anastomosis which allows for the formation of a "hallmark of interconnected colony" (Fischer & Glass, 2019). With such a colony, efficient movement of nutrients and other organelles are possible from one hypha to another (Hickey et al., 2002; Roper et al., 2015; Roper et al., 2013; Simonin et al., 2012). The process is essential for growth (Fischer & Glass, 2019) and enhances fitness through increased colony growth rates, and improves the production of asexual spores (Bastiaans et al., 2015; Richard et al., 2012; Simonin et al., 2012).

Anastomosis is possible between the hyphae of different individuals optimizing resource-sharing and collaboration (Bastiaans et al., 2015). In such cases, the interacting individuals need to be genetically similar because fusion between genetically dissimilar hyphae results in compartmentalisation and programmed cell death (PCD) (Glass & Kaneko, 2003; Gonçalves et al., 2017; Saupe, 2000). During PCD, septal pores are plugged to compartmentalise dying hyphal segments, the cytoplasm is vacuolized, organelles are degraded, and the plasma membrane then shrinks from the cell wall (Paoletti, 2016; Paoletti & Clave, 2007). This helps to avoid the transfer of nuclei and other organelles between incompatible strains (Daskalov et al., 2017; Gonçalves et al., 2020). However, if the incompatibility reaction is slow or defective, organelles, viruses or plasmids may be transferred to the adjacent cells before PCD takes place (Gonçalves et al., 2020).

The process that controls the outcome of hyphal fusion events is a self/non-self-recognition system that is often referred to as vegetative, heterokaryon, or post-fusion compatibility/incompatibility (Giovannetti et al., 2015; Sbrana et al., 2018; Strom & Bushley, 2016). It is controlled by the genes encoded at multiple *vic* (vegetative incompatibility) loci that are often also referred to as *het* (heterokaryon incompatibility) loci (Glass et al., 2000; Leslie, 1993; Paoletti, 2016; Saupe, 2000; Zhang et al., 2014). Individuals carrying the same alleles at all or most of these loci are usually able to establish stable vegetative heterokaryons, while those with different alleles at these loci cannot (Glass et al., 2000; Paoletti, 2016; Saupe, 2000; Zhang et al., 2014). Individuals capable of forming heterokaryotic hyphal cells are diagnosed as belonging to the same VCG (Leslie & Summerell, 2006; Leslie, 1993),

while those in which cytoplasmic exchange after the initial hyphal interaction is prevented through the PCD response belong to different VCGs.

Known *het* loci and genes in model fungi

The molecular mechanisms controlling vegetative compatibility all appear to represent a module containing a domain that recognizes like/unlike elements from the two interacting strains, together with a cell death-inducing/executing domain involved in PCD (Paoletti, 2016). These two interacting domains may be present on the same protein or on separate proteins (Paoletti, 2016). To date, the genes encoded at *het* loci have been characterized only in a small number of fungi. These include the two model fungi *Neurospora crassa* and *Podospora anserina,* as well as *Aspergillus oryzae* and *Cryphonectria parasitica*. Among these, *N. crassa* and *P. anserina* stand out as they are the ones in which most *het* genes have been identified and characterised at the molecular level (Clavé et al., 2022a; Daskalov et al., 2019). Below I provide a brief overview of the structure and function the *het* loci in the two model fungi, and where known, information regarding their allele diversity.

Podospora anserina

There are at least seven known *het* genes in *P. anserina* that have been characterized molecularly (Clavé et al., 2022b; Daskalov, Dyrka, et al., 2020b; Glass et al., 2000; Saupe et al., 2000). These vegetative incompatibility mediating loci are named *het-d*, *het-e*, *het-c*, *het-r*, *het-v*, *het-s and het-q* (Choi et al., 2012; Daskalov et al., 2019). They are all discussed in the following sub sections based on the relationship between them.

het-d and het-e

The *het-d* and *het-e* genes code for the HET-D and HET-E proteins which are members of the STAND (<u>s</u>ignal <u>t</u>ransduction <u>A</u>TPase with <u>n</u>umerous <u>d</u>omains) class of nucleotide binding proteins known to control PCD (Paoletti & Clave, 2007). They comprise a C-terminal WD-repeat domain, a central NACHT nucleotide binding-

oligomerization domain, and an N-terminal HET domain with guanosine triphosphate (GTP)-binding activity (Jain & Pandey, 2018). The HET domain is responsible for cell death execution, while allelic recognition is conferred by the WD-repeats. The latter are motifs made of about 40 amino acids terminating in a Trp-Asp (W-D) dipeptide. These repeats each make a 7-8 bladed beta-propeller fold (Hudson & Cooley, 2008), and with each protein containing about 4-16 of these repeated units in a circularised beta-propeller structure. WD-repeat containing proteins are a large family found in all eukaryotes (Hu et al., 2017; Jain & Pandey, 2018; Kim & Kim, 2020; Zhang et al., 2014). Also common to eukaryotes, is the GTP-binding domain which has a highly conserved "G-domain" that hydrolyses GTP to guanosine diphosphate (Wittinghofer & Vetter, 2011). The fact that HET-E and HET-D contain WD-repeats and a GTP-binding site that mediate protein-protein interaction (Jain & Pandey, 2018), suggest that they likely function in cellular mechanisms such as signal transduction, gene regulation and RNA processing (Seet et al., 2006). The *het-d* and *het-e* genes are regarded as paralogs and form part of the *hnwd* gene family, which also contain known *het* genes characterised in *N. crassa* (see below).

het-c

The *het-c* gene of *P. anserina* is also termed *hch* (for <u>h</u>et-<u>c</u> <u>h</u>omolog) and encodes a polypeptide with glycolipid transfer activity and that is 52% identical to Het-C in *N. crassa* (see below) (Saupe, 2000). Despite initial suggestions, some authors doubted its involvement in vegetative compatibility in *P. anserina* due to a general lack of variation in its sequences (Milgroom & Cortesi, 1999). However, polymorphism was eventually found when extensive populations of the fungus were analysed (Bastiaans et al., 2014). Interestingly, the authors of the study concluded that Het-C plays a possible role, not only in vegetative compatibility, but also in the recognition of its hosts. Nevertheless, it has experimentally been demonstrated that non-allelic interactions between *het-c* and *het-e* loci and between *het-c* and *het-e* loci can trigger PCD (Espagne et al., 2002; Paoletti & Clave, 2007).

het-r/het-v

The *het-r* gene (initially named *hnwd2*) is another member of the *hnwd* gene family (Chevanne et al., 2009). Incompatible *het-r* alleles are divided into active (*het-R*) and inactive (*het-r*) forms based on the number of WD-repeats in the C-terminal domain (Daskalov, Dyrka, et al., 2020a). However, Het-r establishes an incompatibility system with the closely linked *het-v* locus (see below), the details of which are still being investigated (Chevanne et al., 2009; Hutchison & Glass, 2012).

The *het-v* locus contains two genes, one encoding a methyltransferase and the other proteins with the domains TUDOR (named after a protein in *Drosophila*) and MLKL (for mixed lineage kinase domain-like) (Ament-Velásquez, 2020; Auxier et al., 2021). The alternate allele of this locus is a null allele, containing neither of the two genes. In this system, the methyltransferase methylates certain protein targets, which is sensed by the second protein's TUDOR domain (via its ability to bind methylated lysine and arginine residues). If there is no methylation (as would be the case when strains with different *het-v* loci fuse), its MLKL domain would activate cell death (Auxier et al., 2021).

het-s

The *het-s* locus of *P. anserina* encodes for two antagonistic allelic variants, with HET-S having prion activity and HET-s incapable of prion formation (Daskalov et al., 2015; Saupe, 2011). The two proteins are 95% similar in sequence and both have an N-terminal α-helical domain (the so-called Helo domain) and the C-terminal unstructured prion-forming domain (Balguerie et al., 2003; Greenwald et al., 2010; Seuring et al., 2012). When strains with these different alleles fuse, PCD is activated. This is because the HET-s/HET-S interaction triggers the unstructured prion-forming domain of HET-S to transition to a polymeric β-solenoid structure, which in turn activates refolding of the protein's HeLo domain responsible for cell death execution (Daskalov & Saupe, 2021; Otzen & Riek, 2019; Riek & Saupe, 2016). The latter happens because the refolded HeLo domain is relocated to the cell membrane where it has pore-forming activity (Daskalov & Saupe, 2021).

het-q

The het-Q locus is idiomorphic, encoding either the Het-Q1 gasdermin-like protein or the Het-Q2 protease, which together regulate cell death in *P. anserina* (Clave et al., 2021). Gasdermin is a protein family implicated in controlling cell death and inflammation in mammals and fungi (Clavé et al., 2022a). HET-Q1 has been identified in more than 180 fungal species (Cao & Kagan, 2021; Clavé et al., 2021; Clavé et al., 2022a; Daskalov & Glass, 2021). Het-Q2 encodes a subtilisin-like serine protease. When strains with different idiomorphs interact, the protease activity of HET-Q2 removes an approximately 5 kDa fragment from the C-terminal of HET-Q1, which activates its cytotoxic gasdermin pore-forming activity (Clave et al., 2021).

Neurospora crassa

There are at least eight known *het* genes in *N. crassa* that have been characterized molecularly (Glass et al., 2000; Saupe et al., 2000). These vegetative incompatibility mediating loci are named *her-c, pin-c*, *sec-9*, *plp-1*, *rcd-1*, *het-6*, *mat*, *and tol* (Choi et al., 2012; Daskalov et al., 2019). They are all discussed in the following sub sections based on the relationship between them.

het-c/pin-c

The *het-c* locus of *N. crassa* is closely linked to the *pin-c* (for p̲artner in i̲ncompatibility of *het-c*) locus. The *het-c* locus encodes a single-pass membrane protein, that bears a C-terminal signal peptide with repeated glycine-rich units. The *pin-c* locus encodes a HET domain. The outcome of interactions between different strains of the fungus is dependent on allelic interactions at the *het-c* locus, as well as nonallelic interactions between the two loci (Kaneko et al., 2006).

sec-9/plp-1

PLP-1 is a patatin-like phospholipase-1 resembling a STAND class nucleotide binding activity, while SEC-9 is a SNARE (s̲oluble N̲SF [N-ethylmaleimide-sensitive

factor] attachment protein receptor) protein involved in secretory vesicle or plasma membrane fusion (Heller et al., 2018). They mediate vegetative compatibility via a nonallelic, physical interaction between them. The nucleotide binding domain of PLP-1 is responsible for activating cell death and the polymorphic SNARE domain at the C-terminal of SEC-9 is responsible for allelic specificity (Heller et al., 2018).

rcd-1

The *rcd-1* locus encodes a gasdermin-like protein domain RCD-1 (Clave et al., 2021; Daskalov, Mitchell, et al., 2020). It was shown that RCD-1 probably localizes and interacts with the cell's plasma membrane via a secondary structure motif with amphipathic α-helices having positively charged residues. The exact mechanism of cell death execution is still unclear, but vegetative incompatibility is mediated by allelic interactions between antagonistic versions of RCD (Daskalov, Dyrka, et al., 2020a; Richman, 2000).

het-6

This locus of *N. crassa* consist of two tightly linked genes, *het-6* and *un-24* (Lafontaine & Smith, 2012). While *het-6* encodes a HET domain protein, *un-24* encodes the large subunit of a type 1 ribonucleotide reductase (Nourparvar, 2016). Both genes have two variants that can mediate vegetative compatibility (Lafontaine, 2010). During an allelic *un-24* interaction, cell death is thought to be initiated when antagonistic variants of the polypeptide become covalently bound, thereby inactivating the reductase (Smith et al., 2013). Cell death can also be mediated via non-allelic interactions between the products of the two genes (Lafontaine & Smith, 2012; Smith et al., 2013).

mat/tol

The two idiomorphs of the mating type locus encodes two sets of genes involved in sexual reproduction (Wallen & Perlin, 2018). These are *mat-1-2-1* in the one idiomorph, and *mat-1-1-1* and *mat-1-3-1* in the other idiomorph, of which *mat-1-2-1* and *mat-1-1-1* encode transcriptional regulators with DNA binding domains involved

in sexual development (Staben & Yanofsky, 1990). However, these two genes also function in vegetative incompatibility (Daskalov et al., 2017; Wallen & Perlin, 2018). Initially, Beadle & Coonradt, (1944) and Garnjobst (1953) indicated that expression of these idiomorphs in the same cytoplasm is detrimental. Recent work suggests that this vegetative incompatibility function is due to direct interaction between the *mat-1-2-1* and *mat-1-1-1* proteins, and is apparently independent of their role in transcription (Strom & Bushley, 2016). Furthermore, it has been reported that a mutation in either of the two genes restores the growth of the incompatible heterokaryon (Strom & Bushley, 2016). This mutation is driven by the product of the *tol* gene, which is a suppressor of mating-type associated incompatibility reactions and encodes part of a HET protein domain (Shiu, 1999).

Experimental inferences of Vegetative Compatibility Groups

Three methods have been developed to assay for VCGs in filamentous ascomycetes (Leslie, 1993). The first involves direct observation of heterokaryon formation using auxotrophy or pigmentation markers (Leslie, 1993), while the second involves direct observation of the inability to form vegetative heterokaryons (Brooker et al., 1991; Ford et al., 1995; Leslie & Zeller, 1996). The third method involves the use of partial diploids for assess incompatibility between individuals. These methods are all relevant in the study of the biology of fungi especially in the study of population genetics.

Direct observation of vegetative compatibility/incompatibility

Vegetative compatibility/incompatibility of fungal isolates can be determined directly on agar plates (Zeynali Bari et al., 2021). Isolates can be allocated to the same VCG in this manner if their hyphae can anastomose with each other. Here, a dark pigmented barrage is formed at the point of contact if isolates are not compatible, while normal

growth is observed if they are compatible. This method works for many fungal groups, except for pigmented fungi such as *Fusarium* and *Aspergillus* species where the barrage is typically not observable (Leslie & Summerell, 2008). These markers are necessary to verify vegetative compatibility in these species. In both groups of fungi the preferred marker is nitrate utilization among laboratory-generated nitrate-non utilizing (*nit*) mutants (Bayman & Cotty, 1991; Leslie & Summerell, 2008), an approach that was first developed by Puhalla in 1985.

Nit mutants are generated by growing the fungus on medium containing one nitrogen source (NaNO$_3$) and its toxic analogue K$_2$ClO$_3$. However, the production of *nit* mutants on solid media using conventional methods is laborious and time-consuming. To mitigate the impact of these setbacks, Papaioannou et al. (2015) devised a high-throughput approach for producing *nit* mutants and performing complementation assays, which accelerates the development of *nit* mutants by exposing them to UV light while growing on K$_2$ClO$_3$-containing medium.

Putative *nit* mutants are observable on solid medium because their growth is different from the remainder of the culture, i.e., they form distinct growth 'sectors'. Depending on their growth on media (i.e., containing different nitrogen sources), three different kinds of *nit* mutants (i.e., Nit1, Nit3, or NitM) may be isolated. Identified *nit* mutants are paired to determine their vegetative compatibility (Leslie, 1993; Leslie & Zeller, 1996). The Nit1 or Nit3 mutants would then complement NitM mutants for re-establishing functional nitrate utilization. In other words, same-VCG strains would be characterized by wild-type growth in the area where the Nit1 or Nit3 mutants of one strain interacts with the NitM mutant of another strain.

Partial diploids for assessing vegetative incompatibly

Partial diploids are cells containing two copies of a subset of its genes (Papaioannou et al., 2015). Partially diploid cells are produced by complementing missing, mutated or non-functional genes in a cell via transformation with a plasmid harbouring functional copies of the mutated genes. For partially diploid isolates to be used in assessing vegetative incompatibility they must be heterozygous for the genes responsible for the incompatibility reaction (Xiang & Glass, 2004). For example,

partially diploid strains of *N. crassa* that are heterozygous for a single heterokaryon incompatibility (het) gene would be viable but grow at a drastically reduced rate (Jacobson et al., 1998). Although it is possible to produce partially diploid strains, they are not used often, due to their limited growth, and the laborious methodologies for generating them.

Using VCGs in population genetic analyses

Members of a population can be genetically similar or diverse, but this is often not apparent as some genetic features do not always extend to the phenotype (Dawkins, 2016; Pollard et al., 2009). Consequently, in many fungal population studies, VCGs can be used to group isolates based on their ability to anastomose and extend growth (Jiménez-Gasco et al., 2014). A well-known example in which populations were extensively studied using VCGs is the chestnut blight pathogen, *C. parasitica* (Bissegger et al., 1997; JaNkoVSký et al., 2011; Pérez-Sierra et al., 2019). In this fungus, the VCG analysis was a valuable tool for studying genetic diversity and population biology (Zeynali Bari et al., 2021), as well as for predicting the occurrence of recombination (Milgroom, 1996) and for estimating population differentiation (McDermott & McDonald, 1993). In this fungus, mycoviruses may represent a significant factor in structuring populations (Nuss, 1992; Van Alfen et al., 1975; Zeynali Bari et al., 2021) as vegetative compatibility may allow for virus transmission within and among populations (Huber & Fulbright, 1994; Liu & Milgroom, 1996). However, knowledge of the molecular basis of vegetative compatibility and the nature of *het* loci has grown considerably over the last few decades, and ultimately allowed for the development of mycovirus-based biological control of the pathogens (García-Pedrajas, 2019; Wu, 2017).

The value of VCGs as population marker lies in the fact that, depending on the species, filamentous ascomycetes contain 5 -11 genetically unlinked *het* loci, each with 2 - 4 allelic specificities (Glass and Kaneko 2003). This has the consequence of large numbers of vegetatively incompatible individuals likely characterize even populations of sexually reproducing fungi. The fact that certain *het* loci also interact in a non-allelic manner would increase the number of potentially incompatible

individuals in such populations even more (Glass and Kaneko 2003). Accordingly, the likelihood that two strains are from the same VCG becomes less with an increase in the number of *het* loci, the number of allelic specificities at these loci, and the occurrence of non-allelic interactions among *het* loci. If strains are of the same VCG-based "genotype", they could also potentially be clonal, especially if the predominant mode of reproduction is asexual.

Microsatellites

Having the same set of *het* alleles is not the only approach to measure clonality or lack thereof, and characterisation using other methods could give more insights on whether fungal strains are genetically diverse or clonal. For this reason, the use of microsatellite markers (sometimes also called simple sequence repeats; SSRs) have become commonplace in population studies (Abdul-Muneer, 2014; Bruford & Wayne, 1993; Brumfield et al., 2003; Cavalli-Sforza, 2005; Oliveira et al., 2006b).

A microsatellite locus is represented by a DNA sequence that consists of simple sequence motifs (i.e., units containing 1 to 6 nucleotides) that are tandemly repeated 5-50 times (Bennett, 2000; Shia, 2021). These loci can be found at multiple locations across an organism's genome in both coding and non-coding regions and they are usually highly polymorphic (Ellegren, 2004). The polymorphisms arise as a consequence of replication slippage, a process during which the replicating strands are temporarily disassociated and then reassociated, but in such a fashion that the correct units of the repeats are misaligned, causing either deletion or insertion of repeat units, relative to the original strand (Ellegren, 2004). Their highly polymorphic nature makes microsatellites ideal markers for studying relatedness among organisms of a population or between populations (Amiteye, 2021; Parker et al., 1998; Yang et al., 2020).

Development of microsatellite markers

The amplification of microsatellites is based on the use of polymerase chain reaction (PCR) with DNA extracted from a specific fungal species. The DNA sequence

flanking a microsatellite locus is used to design primers for PCR amplifications (Gupta et al., 2021). Different alleles of a locus are then reflected in the variation of amplicon sizes (Zane et al., 2002).

The identification of microsatellites in a genome based on PCR primers can be complex. Sometimes extensive DNA enrichment steps are involved to have DNA libraries with microsatellite sequences. Molecular cloning and sanger sequencing are also used to establish suitable nucleotide positions for primer design (Zane et al., 2002). Recently, the next generation sequencing is being used in addition to SSRs but they remain an important tool in population studies. Also, various computer software packages are now available for identifying microsatellites from genome data and primer design (Mokhtar & Atia, 2019). Recently, Lepais et al. (2020) introduced a rapid bioinformatic workflow for sequence-based genotyping of microsatellites, but this approach has not yet been used extensively in fungi.

Using microsatellite markers in population genetic studies

Analogous to the molecular principle underlying VCG assays, strains characterized by the same set of alleles at all the microsatellite loci targeted are regarded as representing a particular multilocus genotype (MLG). In other words, strains yielding the same sized amplicon for each of the loci examined, form part of a group having the same MLG. As with VCG-based "genotype", strains of an MLG could also potentially be clonal, especially if they occur in populations where asexuality is the predominant mode of reproduction.

Various fungi, particular pathogenic species, have been subjected to microsatellite-based studies for inferences regarding population biology (Lepais et al., 2020). These also included *C. parasitica* where microsatellite-based studies revealed similar patterns regarding population diversity, structuring and overall dynamics of the pathogen in regions of Europe and North America (e.g., (García-Pedrajas et al., 2019; Ježić et al., 2021; Stauber et al., 2022). Most studies that compared microsatellites-based patterns with those observed using vegetative compatibility report broad congruence between VCGs and microsatellite-based groups; for example some populations of *Sclerotinia homoeocarpa* (Chang et al., 2014) and of

Verticillium dahliae (Dung et al., 2013). In these examples, however, the two types of groupings do not necessarily match exactly, because a small set of closely related microsatellite based MLGs often represent a single VCG (i.e., microsatellites resolve more groups within a VCG). Populations of *Aspergillus flavus* present examples of even more pronounced microsatellite-based differentiation within particular VCGs, which is thought to result from the continued asexual reproduction (likely involving mutation at microsatellite loci) within particular VCGs following their initial emergence (Grubisha & Cotty, 2010). Such patterns are thus expected given the different nature of these two marker types, as well as the varying evolutionary processes (especially those involved in the formation and maintenance of *het* and microsatellite loci) acting upon them (Oliveira et al., 2006a).

Fusarium circinatum

Fusarium circinatum is a necrotrophic pathogen that is widely distributed in almost all pine-growing regions around the world (Drenkhan et al., 2020). At least 67 *Pinus* species and 18 *Pinus* hybrids have been shown to be susceptible to the pathogen (Drenkhan et al., 2020). A range of current studies also presented that this fungus can also infect and colonize tissues of various non-pine tree species, herbaceous plants and a range of grass species (Drenkhan et al., 2020; Herron et al., 2020; Swett et al., 2014).

As a pathogen of *Pinus*, *F. circinatum* causes significant economic losses of about R11-12 million per annum (Mitchell, 2011) as it can infect all tissue types (Mitchell, 2011; Gordon, 2015; Steenkamp, 2012). However, in the commercial forestry setting, infection of seedlings in nurseries represent a major concern (Mitchell et al., 2011; Wingfield et al., 2008). This is because fungus has been reported to be responsible for devasting root disease resulting in substantial seedling mortality (Dwinell et al., 1985; Wingfield et al., 2008). Seedlings may be asymptomatically infected, where the pathogen is introduced in the field and gets to develop when conditions are favourable. This can then lead to the successful establishment of the pathogen limiting the establishment of plants in the field due to post-planting

mortality. Another important concern in the commercial forestry environment is infection of established trees which typically result in resinous cankers on stems and branches (Dwinell et al., 1985). In these situations, *F. circinatum* is associated with significant timber yield and quality losses (Drenkhan et al., 2020).

The pathogen *F. circinatum* is capable of both sexual and asexual reproduction (Dwinell et al., 1985; Wingfield et al., 2008). VCG analysis has been used to show heterothallism which is when two mating types Mat 1 and Mat 2 idiomorphs are present in a population (Britz et al. 1999). Where sexual reproduction is possible, individuals of opposite mating type are present in a population (Martin et al., 2011). However, sexual structure of this fungus has never been observed in nature though sexual crosses between compatible individuals has been shown in the laboratory environment that led to the production of perithecia (Britz et al. 1999).

Understanding the population genetics of *F. circinatum* using VCG and microsatellite markers

VCG assays and microsatellite-based analyses have been used extensively to study population biology of the fungus in various regions. For example, in-depth VCG studies have been conducted on populations from California and the south-eastern United States (Correll et al. 1992; Gordon et al. 2006), while extensive microsatellite-based data are available for populations of the fungus from Spain (Berbegal et al 2013). For populations from South Africa, both VCG and microsatellite-based studies have been conducted, and thus provide a valuable opportunity for assessing the congruence between groupings based on vegetative compatibility and microsatellites (Fru et al., 2019; Fru et al., 2017; Santana et al., 2016; Steenkamp et al., 2014).

Following the discovery of *F. circinatum* in South Africa, Viljoen et al. (1997) reported the existence of 23 different VCGs in the summer rainfall region in the country. A few years later, Britz et al. (2005) reported 29 different VCGs from the region, of which 23 matched those reported by Viljoen et al. (1997). Note, both these initial studies focussed on strains originating in the nursery environment and hypothesized that the observed diversity was due to sexual reproduction by the fungus in the region. Subsequently, an investigation from the winter rainfall region of the country reported

the existence of 46 different VCGs, which the authors attributed to multiple introductions of the fungus into the region, as well as potentially sexual reproduction (Steenkamp et al., 2014). The strains used in the latter study mostly originated from cankers in plantation trees, and it is still unknown whether VCGs from the two regions overlap. However, it might be possible that there is limited overlap, as many VCGs would be possible for *F. circinatum*. This is because the fungus is thought to have 6-10 *het* loci (Gordon et al., 2006; Gordon et al., 2021), which means that at least 64 VCGs would be possible if a minimum of 6 loci, only two allelic specificities and only allelic interactions are assumed. But such a level of simplicity is likely not the case, as was shown for the model fungi discussed above.

Since the development of a set of 10 microsatellite markers for *F. circinatum* (Santana et al., 2009), various studies have reported the existence of various MLGs within SA populations of the fungus (Fru et al., 2019; Fru et al., 2017; Santana et al., 2016; Steenkamp et al., 2014; Steenkamp et al., 2012; Wingfield et al., 2008). These studies showed that most plantation disease outbreaks in the country are associated with relatively few MLGs. Additionally, none of these microsatellite-based studies found any evidence of sexual reproduction within the plantation populations, because recombination at the examined microsatellite loci appeared to be largely absent. These studies suggested that multiple introductions into the country remains the most plausible explanation for the observed diversity of the pathogen, and that asexuality is the dominant mode of reproduction in the plantation environment.

Only one SA study, so far, attempted to compare VCG and microsatellite data. The collection of strains examined by Santana et al (2016) included representatives of VCGs from previous studies in the summer and winter rainfall regions of South Africa (Viljoen et al., 1997; Britz et al., 2005; Steenkamp et al., 2014). The 43 known VCGs examined by Santana et al (2016), represented only 29 MLGs and they argued that, in the absence of sexual reproduction, this likely reflects mutational changes affecting the compatibility among isolates, as also suggested by Wikler et al. (2000) and Gordon et al. (2006). Indeed, it was confirmed in a recent genomics study that spontaneous changes in vegetative compatibility can occur in 5-8 of every million

spores (Gordon et al. 2021). Therefore, different from the examples listed in the previous section above, it seems as if VCG assays provide more resolution within *F. circinatum* populations than microsatellite markers. However, more extensive studies are required to fully understand the congruence between VCG and microsatellite data in this fungus.

Way forward

Previous research on *F. circinatum* demonstrated that VCGs and MLGs can be used to answer questions about the relatedness and diversity of strains in and between populations. Given the predominance of asexual reproduction, the hypothesis is that strains from the same microsatellite-based genotype represent clonal individuals (Carleson et al., 2021; Fru et al., 2019; Fru et al., 2017; Santana et al., 2016; Steenkamp et al., 2014; Steenkamp et al., 2012; Wingfield et al., 2008). Although this might not be the case for all VCGs, the genetic nature of single VCGs and MLGs has not been tested in this fungus. The latter is important, because true clonality between strains (i.e., having similar genome sequences) would mostly also be reflected in phenotype, of which vegetative compatibility would be one example (Davila-Velderrain & Alvarez-Buylla, 2014; Lewis et al., 2012; Wagner & Zhang, 2011). In other words, except for potential expression differences among clones, their phenotypes are expected to be broadly similar. Therefore, the two experimental chapters of this dissertation serve to provide the foundation for addressing this research gap.

In the South African *F. circinatum* population, intensive research has been conducted to uncover the genetic status of isolates from various areas and hosts (Berbegal et al., 2013; Fru et al., 2017; Santana et al., 2016). However, only a limited number of isolates of the entire population have been studied, and the correlation between genotypic variation patterns in populations and phenotypic patters. We therefore utilized different sets of multi-strain microsatellite based MLGs to evaluate the level of phenotypic differences among them. The latter includes various traits

commonly examined in plant pathology laboratories. The overall question was to determine whether strains from the same MLG and/or VCG indeed display similar phenotypic traits. This study also had the benefit of allowing a deeper understanding of previous work on the fungus, where virulence and growth among apparently clonal strains were compared.

Ideally, an investigation of the phenotypic and genotypic diversity within single VCGs would have complemented the work conducted in the first research chapter. However, much is still unknown about the molecular basis of VCGs in *F. circinatum*. A recent genome-based study in *F. circinatum* showed that *F. circinatum* encodes homologs of all the known *het* genes in *P. anserina* and *N. crassa* in the fungus (Gordon et al., 2021), but it is not yet known how many homologs of these genes are present in *F. circinatum*, and which of these represent likely orthologs of the known genes. Also, the repertoire of homologs of these known genes are not known in *F. circinatum*. Therefore, the second research chapter of this dissertation seeks to expand on the study by Gordon et al (2021), by aiming to fully characterize putative orthologs of the *het* genes from *P. anserina*, *N. crassa*, *A. oryzae* and *C. parasitica*.

References

Abdul-Muneer, P. (2014). Application of microsatellite markers in conservation genetics and fisheries management: recent advances in population structure analysis and conservation strategies. *Genetics Research International*, *2014*.

Ament-Velásquez, S. L. (2020). Drivers of evolutionary change in *Podospora anserina* [Acta Universitatis Upsaliensis].

Amiteye, S. (2021). Basic concepts and methodologies of DNA marker systems in plant molecular breeding. *Heliyon*, *7*(10), e08093.

Aneja, K. (2007). Experiments in microbiology, plant pathology and biotechnology. *New Age International*.

Auxier, B., Scholtmeijer, K., van Peer, A. F., Baars, J. J., Debets, A. J., & Aanen, D. K. (2021). Cytoplasmic mixing, not nuclear coexistence, can explain somatic incompatibility in basidiomycetes. *Microorganisms*, *9*(6), 1248.

Balguerie, A., Dos Reis, S., Ritter, C., Chaignepain, S., Coulary-Salin, B., Forge, V., Bathany, K., Lascu, I., Schmitter, J. M., & Riek, R. (2003). Domain organization and structure–function relationship of the HET-s prion protein of *Podospora anserina*. *The EMBO Journal*, *22*(9), 2071-2081.

Baltrus, D. A., McCann, H. C., & Guttman, D. S. (2017). Evolution, genomics and epidemiology of *Pseudomonas syringae*: challenges in bacterial molecular plant pathology. *Molecular Plant Pathology*, *18*(1), 152-168.

Bastiaans, E., Debets, A. J., & Aanen, D. K. (2015). Experimental demonstration of the benefits of somatic fusion and the consequences for allorecognition. *Evolution*, *69*(4), 1091-1099.

Bastiaans, E., Debets, A. J., Aanen, D. K., van Diepeningen, A. D., Saupe, S. J., & Paoletti, M. (2014). Natural variation of heterokaryon incompatibility gene het-c in *Podospora anserina* reveals diversifying selection. *Molecular Biology and Evolution*, *31*(4), 962-974.

Bayman, P., & Cotty, P. J. (1991). Vegetative compatibility and genetic diversity in the *Aspergillus flavus* population of a single field. *Canadian Journal of Botany*, *69*(8), 1707-1711.

Beadle, G., & Coonradt, V. L. (1944). Heterocaryosis in *Neurospora crassa*. *Genetics*, *29*(3), 291.

Bennett, P. (2000). Demystified…: Microsatellites. *Molecular Patholog 53*(4), 177.

Berbegal, M., Pérez-Sierra, A., Armengol, J., & Grünwald, N. (2013). Evidence for multiple introductions and clonality in Spanish populations of *Fusarium circinatum*. *Phytopathology*, *103*(8), 851-861.

Bissegger, M., Rigling, D., & Heiniger, U. (1997). Population structure and disease development of *Cryphonectria parasitica* in European chestnut forests in the presence of natural hypovirulence. *Phytopathology*, *87*(1), 50-59.

Brooker, N. L., Leslie, J. F., & Dickman, M. B. (1991). Nitrate non-utilizing mutants of Colletotrichum and their use in studies of vegetative compatibility and genetic relatedness. *Phytopathology*, *81*(6), 672-677.

Bruford, M. W., & Wayne, R. K. (1993). Microsatellites and their application to population genetic studies. *Current Opinion in Genetics & Development*, *3*(6), 939-943.

Brumfield, R. T., Beerli, P., Nickerson, D. A., & Edwards, S. V. (2003). The utility of single nucleotide polymorphisms in inferences of population history. *Trends in Ecology & Evolution*, *18*(5), 249-256.

Cao, A., & Kagan, J. C. (2021). Gasdermin pore forming activities that promote inflammation from living and dead cells. *Journal of Molecular Biology*, *434*(4), 167427.

Carleson, N. C., Daniels, H. A., Reeser, P. W., Kanaskie, A., Navarro, S. M., LeBoldus, J. M., & Grünwald, N. J. (2021). Novel introductions and epidemic dynamics of the sudden oak death pathogen *Phytophthora ramorum* in Oregon forests. *Phytopathology*, *111*(4), 731-740.

Castillo, A. I., Bojanini, I., Chen, H., Kandel, P. P., De La Fuente, L., & Almeida, R. P. (2021). Allopatric plant pathogen population divergence following disease emergence. *Applied and Environmental Microbiology*, *87*(7), e02095-e02020.

Cavalli-Sforza, L. L. (2005). The human genome diversity project: past, present and future. *Nature Reviews Genetics*, *6*(4), 333-340.

Chang, S. W., Jo, Y.-K., Chang, T., & Jung, G. (2014). Evidence for genetic similarity of vegetative compatibility groupings in *Sclerotinia homoeocarpa*. *The Plant Pathology Journal* , *30*(4), 384.

Chevanne, D., Bastiaans, E., Debets, A., Saupe, S. J., Clavé, C., & Paoletti, M. (2009). Identification of the het-r vegetative incompatibility gene of *Podospora anserina* as a member of the fast evolving HNWD gene family. *Current Genetics*, *55*(1), 93-102.

Choi, G. H., Dawe, A. L., Churbanov, A., Smith, M. L., Milgroom, M. G., & Nuss, D. L. (2012). Molecular characterization of vegetative incompatibility genes that restrict hypovirus transmission in the chestnut blight fungus *Cryphonectria parasitica*. *Genetics*, *190*(1), 113-127.

Clave, C., Dyrka, W., Granger-Farbos, A., Pinson, B., Saupe, S. J., & Daskalov, A. (2021). Fungal gasdermin-like proteins are controlled by proteolytic cleavage. *Proceedings of the National Academy of Sciences*, *119*(7), e2109418119.

Clavé, C., Dyrka, W., Turcotte, E. A., Granger-Farbos, A., Ibarlosa, L., Pinson, B., Vance, R. E., Saupe, S. J., & Daskalov, A. (2022). Fungal gasdermin-like proteins are controlled by proteolytic cleavage. *Proceedings of the National Academy of Sciences*, *119*(7), e2109418119.

Daskalov, A., Dyrka, W., & Saupe, S. J. (2020a). 6 NLR function in fungi as revealed by the study of self/non-self recognition systems. In *Genetics and Biotechnology* (pp. 123-141). Springer.

Daskalov, A., Dyrka, W., & Saupe, S. J. (2020b). NLR function in fungi as revealed by the study of self/non-self recognition systems. In *Genetics and biotechnology* (pp. 123-141). Springer.

Daskalov, A., Gladieux, P., Heller, J., & Glass, N. L. (2019). Programmed cell death in *Neurospora crassa* is controlled by the allorecognition determinant rcd-1. *Genetics*, *213*(4), 1387-1400.

Daskalov, A., & Glass, N. L. (2021). Gasdermin and gasdermin-like pore-forming proteins in invertebrates, fungi and bacteria. *Journal of Molecular Biology*, 167273.

Daskalov, A., Habenstein, B., Martinez, D., Debets, A. J., Sabate, R., Loquet, A., & Saupe, S. J. (2015). Signal transduction by a fungal NOD-like receptor based on propagation of a prion amyloid fold. *PLoS Biology*, *13*(2), e1002059.

Daskalov, A., Heller, J., Herzog, S., Fleißner, A., & Glass, N. L. (2017). Molecular mechanisms regulating cell fusion and heterokaryon formation in filamentous fungi. *Microbiology Spectrum*, *5*(2), 5.2. 02.

Daskalov, A., Mitchell, P. S., Sandstrom, A., Vance, R. E., & Glass, N. L. (2020). Molecular characterization of a fungal gasdermin-like protein. *Proceedings of the National Academy of Sciences*, *117*(31), 18600-18607.

Daskalov, A., & Saupe, S. J. (2021). The expanding scope of amyloid signalling. *Prion*, *15*(1), 21-28.

Davila-Velderrain, J., & Alvarez-Buylla, E. R. (2014). Bridging genotype and phenotype. *Frontiers in Ecology, Evolution and Complexity*, 144-154.

Dawkins, R. (2016). The extended phenotype: the long reach of the gene. [Oxford University Press].

Drenkhan, R., Ganley, B., Martín-García, J., Vahalík, P., Adamson, K., Adamčíková, K., Ahumada, R., Blank, L., Bragança, H., & Capretti, P. (2020). Global geographic distribution and host range of *Fusarium circinatum*, the causal agent of pine pitch canker. *Forests, 11*(7), 724.

Dung, J. K., Peever, T. L., & Johnson, D. A. (2013). *Verticillium dahliae* populations from mint and potato are genetically divergent with predominant haplotypes. *Phytopathology*, *103*(5), 445-459.

Dwinell, L. D., Barrows-Broaddus, J. B., & Kuhlman, E. G. (1985). Pitch canker: a disease complex. *Plant Disease*, *69*, 270-276.

Ellegren, H. (2004). Microsatellites: simple sequences with complex evolution. *Nature Reviews Genetics*, *5*(6), 435-445.

Espagne, E., Balhadere, P., Penin, M.-L., Barreau, C., & Turcq, B. (2002). HET-E and HET-D belong to a new subfamily of WD40 proteins involved in vegetative incompatibility specificity in the fungus *Podospora anserina*. *Genetics*, *161*(1), 71-81.

Fischer, M. S., & Glass, N. L. (2019). Communicate and fuse: how filamentous fungi establish and maintain an interconnected mycelial network. *Frontiers in Microbiology*, *10*, 619.

Ford, E., Miller, R., Gray, H., & Sherwood, J. (1995). Heterokaryon formation and vegetative compatibility in *Sclerotinia sclerotiorum*. *Mycological Research*, *99*(2), 241-247.

Fru, F. F., Steenkamp, E. T., Wingfield, M. J., & Roux, J. (2019). High genetic diversity of *Fusarium circinatum* associated with the first outbreak of pitch canker on *Pinus patula* in South Africa. *Southern Forests: a Journal of Forest Science*, *81*(1), 69-78.

Fru, F. F., Steenkamp, E. T., Wingfield, M. J., Santana, Q. C., & Roux, J. (2017). Unique clones of the pitch canker fungus, *Fusarium circinatum*, associated with a new disease outbreak in South Africa. *European Journal of Plant Pathology*, *148*(1), 97-107.

García-Pedrajas, M., Cañizares, M., Sarmiento-Villamil, J. L., Jacquat, A. G., & Dambolena, J. S. (2019). Mycoviruses in biological control: From basic research to field implementation. *Phytopathology*, *109*(11), 1828-1839.

Garnjobst, L. (1953). Genetic control of heterocaryosis in *Neurospora crassa*. *American Journal of Botany*, 607-614.

Giovannetti, M., Avio, L., & Sbrana, C. (2015). Functional significance of anastomosis in arbuscular mycorrhizal networks. In *Mycorrhizal Networks* (pp. 41-67). Springer.

Giraud, T., Enjalbert, J., Fournier, E., Delmotte, F., & Dutech, C. (2008). Population genetics of fungal diseases of plants. *Parasite*, *15*(3), 449-454.

Glass, N. L., Jacobson, D. J., & Shiu, P. K. (2000). The genetics of hyphal fusion and vegetative incompatibility in filamentous ascomycete fungi. *Annual Review of Genetics*, *34*(1), 165-186.

Glass, N. L., & Kaneko, I. (2003). Fatal attraction: nonself recognition and heterokaryon incompatibility in filamentous fungi. *Eukaryotic Cell*, *2*(1), 1-8.

Glass, N. L., & Kuldau, G. A. (1992). Mating type and vegetative incompatibility in filamentous ascomycetes. *Annual Review of Phytopathology*, *30*(1), 201-224.

Gonçalves, A. P., Heller, J., Daskalov, A., Videira, A., & Glass, N. L. (2017). Regulated forms of cell death in fungi. *Frontiers in Microbiology*, *8*, 1837.

Gonçalves, A. P., Heller, J., Rico-Ramírez, A. M., Daskalov, A., Rosenfield, G., & Glass, N. L. (2020). Conflict, competition, and cooperation regulate social interactions in filamentous fungi. *Annual Review of Microbiology*, *74*, 693-712.

Gordon, T. R., Henry, P. M., Jenner, B. N., & Scott, J. C. (2021). Spontaneous changes in somatic compatibility in *Fusarium circinatum*. *Fungal Biology 125*(9), pp.725-732

Greenwald, J., Buhtz, C., Ritter, C., Kwiatkowski, W., Choe, S., Maddelein, M.-L., Ness, F., Cescau, S., Soragni, A., & Leitz, D. (2010). The mechanism of prion inhibition by HET-S. *Molecular Cell*, *38*(6), 889-899.

Grubisha, L., & Cotty, P. (2010). Genetic isolation among sympatric vegetative compatibility groups of the aflatoxin-producing fungus *Aspergillus flavus*. *Molecular Ecology*, *19*(2), 269-280.

Gupta, M. K., Donde, R., Sabarinathan, S., Gouda, G., Dash, G. K., Pati, P., Rathore, S. K., Vadde, R., Sanghamitra, P., & Parameswaran, C. (2021).

Microsatellite markers from whole genome and transcriptomic sequences. In *Bioinformatics in Rice Research* (pp. 387-412). Springer.

Heller, J., Clavé, C., Gladieux, P., Saupe, S. J., & Glass, N. L. (2018). NLR surveillance of essential SEC-9 SNARE proteins induces programmed cell death upon allorecognition in filamentous fungi. *Proceedings of the National Academy of Sciences*, *115*(10), e2292-e2301.

Herron, D. A., Wingfield, M. J., Fru, F., Wingfield, B. D., & Steenkamp, E. T. (2020). Grasses as a refuge for *Fusarium circinatum* L.–evidence from South Africa. *Southern Forests: a Journal of Forest Science*, *82*(3), 253-262.

Hickey, P. C., Jacobson, D. J., Read, N. D., & Glass, N. L. (2002). Live-cell imaging of vegetative hyphal fusion in *Neurospora crassa*. *Fungal Genetics and Biology*, *37*(1), 109-119.

Hiebert, L. S., Simpson, C., & Tiozzo, S. (2021). Coloniality, clonality, and modularity in animals: The elephant in the room. *Journal of Experimental Zoology Part B: Molecular and Developmental Evolution*, *336*(3), 198-211.

Hu, X.-J., Li, T., Wang, Y., Xiong, Y., Wu, X.-H., Zhang, D.-L., Ye, Z.-Q., & Wu, Y.-D. (2017). Prokaryotic and highly-repetitive WD40 proteins: A systematic study. *Scientific Reports*, *7*(1), 1-13.

Huber, D., & Fulbright, D. (1994). Preliminary investigations on the effect of individual vic genes upon the transmission of dsRNA in *Cryphonectria parasitica*. Proceedings of the International Chestnut Conference, (pp. 15-19). Morgantown: West Virginia University Press.

Hudson, A. M., & Cooley, L. (2008). Phylogenetic, structural and functional relationships between WD-and Kelch-repeat proteins. *The Coronin Family of Proteins*, 6-19.

Hutchison, E. A., & Glass, N. L. (2012). Programmed cell death and heterokaryon incompatibility in filamentous fungi. In *Biocommunication of Fungi* (pp. 115-138). Springer.

Jacobson, D., Beurkens, K., & Klomparens, K. (1998). Microscopic and ultrastructural examination of vegetative incompatibility in partial diploids heterozygous at het loci in *Neurospora crassa*. *Fungal Genetics and Biology*, *23*(1), 45-56.

Jain, B. P., & Pandey, S. (2018). WD40 repeat proteins: signalling scaffold with diverse functions. *The Protein Journal*, *37*(5), 391-406.

JaNkoVSký, L., Palovčíková, D., & Haltofová, P. (2011). Some new findings of *Cryphonectria parasitica* (Murrill) ME Barr in the Czech Republic. *Plant Protection Science*, *46*(1), 19-24.

Ježić, M., Schwarz, J. M., Prospero, S., Sotirovski, K., Risteski, M., Ćurković-Perica, M., Nuskern, L., Krstin, L., Katanić, Z., & Maleničić, E. (2021). Temporal and spatial genetic population structure of *Cryphonectria parasitica* and its associated hypovirus across an invasive range of chestnut blight in Europe. *Phytopathology*, *111*(8), 1327-1337.

Jiménez-Gasco, M. d. M., Malcolm, G. M., Berbegal, M., Armengol, J., & Jiménez-Díaz, R. M. (2014). Complex molecular relationship between vegetative compatibility groups (VCGs) in *Verticillium dahliae*: VCGs do not always align with clonal lineages. *Phytopathology*, *104*(6), 650-659.

Kaneko, I., Dementhon, K., Xiang, Q., & Glass, N. L. (2006). Nonallelic interactions between het-c and a polymorphic locus, pin-c, are essential for nonself recognition and programmed cell death in *Neurospora crassa*. *Genetics*, *172*(3), 1545-1555.

Kim, Y., & Kim, S.-H. (2020). WD40-repeat proteins in ciliopathies and congenital disorders of endocrine system. *Endocrinology and Metabolism*, *35*(3), 494.

Lafontaine, D. (2010). Genetic and epigenetic control of a nonself recognition complex in *Neurospora crassa* [Carleton University].

Lafontaine, D. L., & Smith, M. L. (2012). Diverse interactions mediate asymmetric incompatibility by the het-6 supergene complex in *Neurospora crassa*. *Fungal Genetics and Biology*, *49*(1), 65-73.

Lepais, O., Chancerel, E., Boury, C., Salin, F., Manicki, A., Taillebois, L., Dutech, C., Aissi, A., Bacles, C. F., & Daverat, F. (2020). Fast sequence-based microsatellite genotyping development workflow. *PeerJ*, *8*, e9085.

Leslie, J., & Summerell, B. (2006). Fusarium laboratory workshops—a recent history. *Mycotoxin Research*, *22*(2), 73-74.

Leslie, J. F. (1993). Fungal vegetative compatibility. *Annual Review of Phytopathology*, *31*(1), 127-150.

Leslie, J. F., & Summerell, B. A. (2008). *The Fusarium laboratory manual*. John Wiley & Sons.

Leslie, J. F., & Zeller, K. A. (1996). Heterokaryon incompatibility in fungi—more than just another way to die. *Journal of Genetics*, *75*(3), 415-424.

Lewis, N. E., Nagarajan, H., & Palsson, B. O. (2012). Constraining the metabolic genotype–phenotype relationship using a phylogeny of in silico methods. *Nature Reviews Microbiology*, *10*(4), 291-305.

Liu, Y., & Milgroom, M. G. (1996). Correlation between hypovirus transmission and the number of vegetative incompatibility (vic) genes different among isolates from a natural population of *Cryphonectria parasitica*. *Phytopathology*, *86*(1), 79-86.

Martin, S. H., Wingfield, B. D., Wingfield, M. J., & Steenkamp, E. T. (2011). Structure and evolution of the Fusarium mating type locus: new insights from the *Gibberella fujikuroi* complex. *Fungal Genetics and Biology*, *48*(7), 731-740.

McDermott, J. M., & McDonald, B. A. (1993). Gene flow in plant pathosystems. *Annual Review of Phytopathology*, *31*(1), 353-373.

McDonald, B. A., & Linde, C. (2002a). Pathogen population genetics, evolutionary potential, and durable resistance. *Annual Review of Phytopathology*, *40*(1), 349-379.

McDonald, B. A., & Linde, C. (2002b). The population genetics of plant pathogens and breeding strategies for durable resistance. *Euphytica*, *124*(2), 163-180.

McDonald, B. A., McDermott, J. M., Goodwin, S. B., & Allard, R. W. (1989). The population biology of host-pathogen interactions. *Annual Review of Phytopathology*, *27*(1), 77-94.

Mela, A. P., Rico-Ramírez, A. M., & Glass, N. L. (2020). Syncytia in fungi. *Cells*, *9*(10), 2255.

Milgroom, M., & Fry, W. E. (1997). Contributions of population genetics to plant disease epidemiology and management. In *Advances in Botanical Research* (Vol. 24, pp. 1-30). Elsevier.

Milgroom, M. G. (1996). Recombination and the multilocus structure of fungal populations. *Annual Review of Phytopathology*, *34*(1), 457-477.

Milgroom, M. G., & Cortesi, P. (1999). Analysis of population structure of the chestnut blight fungus based on vegetative incompatibility genotypes. *Proceedings of the National Academy of Sciences*, *96*(18), 10518-10523.

Mitchell, R. G., Steenkamp, E. T., Coutinho, T. A., & Wingfield, M. J. (2011). The pitch canker fungus, *Fusarium circinatum*: implications for South African forestry. *Southern Forests: a Journal of Forest Science*, *73*(1), 1-13.

Mokhtar, M. M., & Atia, M. A. M. (2019). SSRome: an integrated database and pipelines for exploring microsatellites in all organisms. *Nucleic Acids Research*, *47*(D1), e244-e252.

Nicolaus, M., & Edelaar, P. (2018). Comparing the consequences of natural selection, adaptive phenotypic plasticity, and matching habitat choice for phenotype–environment matching, population genetic structure, and reproductive isolation in meta-populations. *Ecology and Evolution*, *8*(8), 3815-3827.

Nourparvar, G. (2016). Genetic Interactions and Biochemical Pathway Involved in Escape from het-6 Incompatibility in *Neurospora crassa* [Carleton University].

Nuss, D. L. (1992). Biological control of chestnut blight: an example of virus-mediated attenuation of fungal pathogenesis. *Microbiological Reviews*, *56*(4), 561-576.

Oliveira, E. J., Pádua, J. G., Zucchi, M. I., Vencovsky, R., & Vieira, M. L. C. (2006a). Origin, evolution and genome distribution of microsatellites. *Genetics and Molecular Biology*, *29*(2), 294-307.

Oliveira, E. J., Pádua, J. G., Zucchi, M. I., Vencovsky, R., & Vieira, M. L. C. (2006b). Origin, evolution and genome distribution of microsatellites. *Genetics and Molecular Biology*, *29*, 294-307.

Ottenburghs, J., Lavretsky, P., Peters, J. L., Kawakami, T., & Kraus, R. H. (2019). Population genomics and phylogeography. In *Avian Genomics in Ecology and Evolution* (pp. 237-265). Springer.

Otzen, D., & Riek, R. (2019). Functional amyloids. *Cold Spring Harbor Perspectives in Biology*, *11*(12), a033860.

Paoletti, M. (2016). Vegetative incompatibility in fungi: From recognition to cell death, whatever does the trick. *Fungal Biology Reviews*, *30*(4), 152-162.

Paoletti, M., & Clave, C. (2007). The fungus-specific HET domain mediates programmed cell death in *Podospora anserina*. *Eukaryotic Cell*, *6*(11), 2001-2008.

Papaioannou, G., Vasiliades, L., & Loukas, A. (2015). Multi-criteria analysis framework for potential flood prone areas mapping. *Water Resources Management*, *29*(2), 399-418.

Parker, P. G., Snow, A. A., Schug, M. D., Booton, G. C., & Fuerst, P. A. (1998). What molecules can tell us about populations: choosing and using a molecular marker. *Ecology*, *79*(2), 361-382.

Pérez-Sierra, A., Romón-Ochoa, P., Gorton, C., Lewis, A., Rees, H., Van Der Linde, S., & Webber, J. (2019). High vegetative compatibility diversity of *Cryphonectria parasitica* infecting sweet chestnut (*Castanea sativa*) in Britain indicates multiple pathogen introductions. *Plant Pathology*, *68*(4), 727-737.

Pollard, S. M., Yoshikawa, K., Clarke, I. D., Danovi, D., Stricker, S., Russell, R., Bayani, J., Head, R., Lee, M., & Bernstein, M. (2009). Glioma stem cell lines expanded in adherent culture have tumor-specific phenotypes and are suitable for chemical and genetic screens. *Cell stem cell*, *4*(6), 568-580.

Read, N. D., & Roca, M. G. (2006). Vegetative hyphal fusion in filamentous fungi. In *Cell-Cell Channels* (pp. 87-98). Springer.

Richard, F., Glass, N., & Pringle, A. (2012). Cooperation among germinating spores facilitates the growth of the fungus, *Neurospora crassa*. *Biology Letters*, *8*(3), 419-422.

Richman, A. (2000). Evolution of balanced genetic polymorphism. *Molecular Ecology*, *9*(12), 1953-1963.

Riek, R., & Saupe, S. J. (2016). The HET-S/s prion motif in the control of programmed cell death. *Cold Spring Harbor Perspectives in Biology*, *8*(9), a023515.

Roper, M., Lee, C., Hickey, P. C., & Gladfelter, A. S. (2015). Life as a moving fluid: fate of cytoplasmic macromolecules in dynamic fungal syncytia. *Current Opinion in Microbiology*, *26*, 116-122.

Roper, M., Simonin, A., Hickey, P. C., Leeder, A., & Glass, N. L. (2013). Nuclear dynamics in a fungal chimera. *Proceedings of the National Academy of Sciences*, *110*(32), 12875-12880.

Santana, Q. C., Coetzee, M. P., Steenkamp, E. T., Mlonyeni, O. X., Hammond, G. N., Wingfield, M. J., & Wingfield, B. D. (2009). Microsatellite discovery by deep sequencing of enriched genomic libraries. *Biotechniques*, *46*(3), 217-223.

Santana, Q. C., Coetzee, M. P. A., Wingfield, B. D., Wingfield, M. J., & Steenkamp, E. T. (2016). Nursery-linked plantation outbreaks and evidence for multiple introductions of the pitch canker pathogen *Fusarium circinatum* into South Africa. *Plant Pathology, 65*(3), 357-368.

Saupe, S. J. (2000). Molecular genetics of heterokaryon incompatibility in filamentous ascomycetes. *Microbiology and Molecular Biology Reviews*, *64*(3), 489-502.

Saupe, S. J. (2011). The [Het-s] prion of *Podospora anserina* and its role in heterokaryon incompatibility. *Seminars in Cell and Developmental Biology*, *22*(5), 460-468.

Saupe, S. J., Clavé, C., & Bégueret, J. (2000). Vegetative incompatibility in filamentous fungi: *Podospora* and *Neurospora* provide some clues. *Current Opinion in Microbiology*, *3*(6), 608-612.

Sbrana, C., Strani, P., Pepe, A., de Novais, C. B., & Giovannetti, M. (2018). Divergence of *Funneliformis mosseae* populations over 20 years of laboratory cultivation, as revealed by vegetative incompatibility and molecular analysis. *Mycorrhiza*, *28*(4), 329-341.

Seet, B. T., Dikic, I., Zhou, M.-M., & Pawson, T. (2006). Reading protein modifications with interaction domains. *Nature reviews Molecular cell biology*, *7*(7), 473-483.

Seuring, C., Greenwald, J., Wasmer, C., Wepf, R., Saupe, S. J., Meier, B. H., & Riek, R. (2012). The mechanism of toxicity in HET-S/HET-s prion incompatibility. *PLoS Biology*, *10*(12), e1001451.

Shamim, M., Kumar, M., Kumar, R. R., Pandey, P., Srivastava, D., Kumar, D., Khan, N., Kumar, R. R., & Singh, K. (2016). Understanding the diversity of aspergillus by next-generation sequencing. In *New and Future Developments in Microbial Biotechnology and Bioengineering* (pp. 29-40). Elsevier.

Shia, J. (2021). The diversity of tumours with microsatellite instability: molecular mechanisms and impact upon microsatellite instability testing and mismatch repair protein immunohistochemistry. *Histopathology*, *78*(4), 485-497.

Simonin, A., Palma-Guerrero, J., Fricker, M., & Glass, N. L. (2012). Physiological significance of network organization in fungi. *Eukaryotic cell*, *11*(11), 1345-1352.

Smith, R. P., Wellman, K., Haidari, L., Masuda, H., & Smith, M. L. (2013). Nonself recognition through intermolecular disulfide bond formation of ribonucleotide reductase in *Neurospora*. *Genetics*, *193*(4), 1175-1183.

Staben, C., & Yanofsky, C. (1990). *Neurospora crassa* a mating-type region. *Proceedings of the National Academy of Sciences*, *87*(13), 4917-4921.

Stauber, L., Croll, D., & Prospero, S. (2022). Temporal changes in pathogen diversity in a perennial plant-pathogen-hyperparasite system. *Molecular Ecology*, *31*(7), 2073-2088.

Steenkamp, E., Makhari, O., Coutinho, T., Wingfield, B., & Wingfield, M. (2014). Evidence for a new introduction of the pitch canker fungus *Fusarium circinatum* in South A frica. *Plant Pathology*, *63*(3), 530-538.

Steenkamp, E. T., Rodas, C., Kvas, M., & Wingfield, M. J. (2012). *Fusarium circinatum* and pitch canker of *Pinus* in Colombia. *Australasian Plant Pathology*, *41*(5), 483-491.

Stoeckel, S., Porro, B., & Arnaud-Haond, S. (2021). The discernible and hidden effects of clonality on the genotypic and genetic states of populations: improving our estimation of clonal rates. *Molecular Ecology Resources*, *21*(4), 1068-1084.

Strom, N. B., & Bushley, K. E. (2016). Two genomes are better than one: history, genetics, and biotechnological applications of fungal heterokaryons. *Fungal Biology and Biotechnology*, *3*(1), 1-14.

Swett, C. L., Porter, B., Fourie, G., Steenkamp, E. T., Gordon, T. R., & Wingfield, M. J. (2014). Association of the pitch canker pathogen *Fusarium circinatum* with grass hosts in commercial pine production areas of South Africa. *Southern Forests: a Journal of Forest Science*, *76*(3), 161-166.

Van Alfen, N., Jaynes, R., Anagnostakis, S., & Day, P. (1975). Chestnut blight: biological control by transmissible hypovirulence in *Endothia parasitica*. *Science*, *189*(4206), 890-891.

Wagner, G. P., & Zhang, J. (2011). The pleiotropic structure of the genotype–phenotype map: the evolvability of complex organisms. *Nature Reviews Genetics*, *12*(3), 204-213.

Wallen, R. M., & Perlin, M. H. (2018). An overview of the function and maintenance of sexual reproduction in dikaryotic fungi. *Frontiers in microbiology*, *9*, 503.

Wingfield, M., Hammerbacher, A., Ganley, R., Steenkamp, E., Gordon, T., Wingfield, B., & Coutinho, T. (2008). Pitch canker caused by *Fusarium circinatum*—A growing threat to pine plantations and forests worldwide. *Australasian Plant Pathology*, *37*(4), 319-334.

Wittinghofer, A., & Vetter, I. R. (2011). Structure-function relationships of the G domain, a canonical switch motif. *Annual Review of Biochemistry*, *80*, 943-971.

Wu, S., Cheng, J., Fu, Y., Chen, T., Jiang, D., Ghabrial, S. A., & Xie, J. (2017). Virus-mediated suppression of host non-self recognition facilitates horizontal transmission of heterologous viruses. *PLoS Pathogens*, *13*(3), e1006234.

Xiang, Q., & Glass, N. L. (2004). The control of mating type heterokaryon incompatibility by vib-1, a locus involved in het-c heterokaryon incompatibility in *Neurospora crassa*. *Fungal Genetics and Biology*, *41*(12), 1063-1076.

Yang, M., Abdalrahman, H., Sonia, U., Mohammed, A. I., Vestine, U., Wang, M., Ebadi, A. G., & Toughani, M. (2020). The application of DNA molecular markers in the study of Codonopsis species genetic variation, a Review. *Cellular and Molecular Biology*, *66*(2), 23-30.

Zane, L., Bargelloni, L., & Patarnello, T. (2002). Strategies for microsatellite isolation: a review. *Molecular Ecology*, *11*(1), 1-16.

Zeynali Bari, R., Abrinbana, M., & Ghosta, Y. (2021). Genetic variation, vegetative compatibility, and aggressiveness diversity of Diplodia bulgarica isolates from apple orchards in West Azarbaijan province of Iran. *Plant Pathology*, *70*(6), 1326-1341

Zhang, D.-X., Spiering, M. J., Dawe, A. L., & Nuss, D. L. (2014). Vegetative incompatibility loci with dedicated roles in allorecognition restrict mycovirus transmission in chestnut blight fungus. *Genetics*, *197*(2), 701-714.

CHAPTER TWO

Microsatellite-based clonality among isolates
of *Fusarium circinatum* does not always extend to phenotype

Abstract

Fusarium circinatum is an important pine pathogen globally. In a commercial forestry setting, it causes pitch canker on plantation trees and root disease in nursery seedlings. Although this fungus is heterothallic, its sexual stage has only been widely observed in the laboratory. Population genetics data from regions where the fungus has been introduced also suggested that it reproduces asexually, with clonality observed for certain groups of isolates based on microsatellite alleles. In this study, we aimed to determine whether these genetic similar isolates also shared important phenotypic traits. For this purpose, we assayed the virulence of four distinct groups of isolates that share the same genotype within each group. Three different inoculation techniques that included tip, stem, and root inoculations were used on three months old *P. patula* seedlings. We also assessed their growth rates and sporulating capacities in ½ PDA and pine extract medium. As was expected, there were significant differences ($P > 0.05$) in lesion lengths, growth rates and sporulating capacity between the clonal groups. However, the isolates that shared the same genotype within a group also differed significantly for all these traits. Results of this study, therefore, suggested that the isolates are not clonal and the initial genotyping method did not provide sufficient resolution for identifying true clones. However, it is also possible that the phenotypic variance could be due to differences in gene regulation. If these isolates are not true clones, it would mean that the South African population might be both genetically and phenotypically diverse. Future research can investigate the hypotheses using genomic and transcriptomic approaches. These analyses will provide valuable insight into the *F. circinatum-Pinus* interaction.

Keywords: Virulence, Lesion lengths, Clones, Growth, Sporulation capacity.

Introduction

Pine pitch canker is an economically important disease infecting both natural stands and commercial plantations of *Pinus* species worldwide (Wingfield et al., 2008). *Fusarium circinatum* (phylum Ascomycota, class Sordariomycetes, order Sordariales and a member of the Nectriaceae family), the causal agent of this disease, causes root and collar rot in seedlings, with high levels of mortality in commercial nurseries where *Pinus* seedlings are produced (Drenkhan et al., 2020; Dwinell et al., 1985; Wingfield et al., 2008). In commercial plantations, the fungus also causes symptoms that included pitch-soaked or resinous cankers on the stems and branches on mature trees (Drenkhan et al., 2020; Dwinell et al., 1985). As a result, *F. circinatum* outbreaks are linked to substantial commercial losses, especially in South Africa, in the form of seedling mortality and low establishment of trees in the field (Mitchell et al., 2011; Wingfield et al., 2008). This loss of profit may lead to increased costs for the consumers, and subsequently a reduction in the forestry sector's contribution to the economy.

Fusarium circinatum is thought to originate from Mexico/Central America (Berbegal et al., 2013; Britz et al., 2001; Wikler & Gordon, 2000) where it is associated with economical losses to pine plantations (Guerra-Santos & Cibrian-Tovar, 1998; Wikler & Gordon, 2000). The fung3us has also spread to other countries. According to the geo-database (http://bit.do/phytoportal) by Drenkhan et al. (2020), *F. circinatum* has been confirmed in 41 countries and affects 106 different host species. To date, South Africa is the only country in Africa with *F. circinatum* incidences (Viljoen et al., 1994) which could mean that the South African pine industry sourced infected pine seedlings during plantation establishment in the regions where the pathogen is reported. Among the 106 different host species, the fungus has been associated with incidences of 67 *Pinus* species and 18 *Pinus* hybrids (Drenkhan et al., 2020). However, previous studies also presented that this fungus can infect and colonize the tissues of various non-pine tree species, certain herbaceous species and a range of grass species (Drenkhan et al., 2020; Herron et al., 2020; Swett et al., 2014).

Because of its socio-economic importance, there is an ongoing quest for innovative and effective measures to control the spread and establishment of *F. circinatum*. As a result, several studies have focused on its population biology, and sought to understand how this is related to its evolutionary biology, spread and distribution, and reproductive biology (McDonald & Linde, 2002). The latter is particularly important, as it represents a key factor in determining the population dynamics of a pathogen (McDonald & Linde, 2002). Each pathogen's effectiveness in breaking host resistance depends on its population genetic diversity which is determined by its reproductive mode, mutation rate, genotype flow, and effective population size (McDonald & Linde, 2002).

In terms of reproductive mode, *F. circinatum* is a heterothallic pathogen that can reproduce both sexually and asexually (Nirenberg & O'Donnell, 1998; Pfenning et al., 2014). Sexual reproduction involves interaction between compatible individuals to form viable and fertile offspring (Nieuwenhuis et al., 2018; Wilson et al., 2019), while asexual reproduction is mostly in a vegetative growth form (Gordon et al., 2021; Steenkamp et al., 2014). In *F. circinatum* vegetative growth occurs when mycelia undergoes mitotic division forming hyphae, some of which may also produce conidiophores bearing microconidia and/or macroconidia (Elliott, 1991; Hawker, 2016). For sexual reproduction, isolates of *F. circinatum* carrying either the MAT1-1 or MAT1-2 idiomorph may undergo plasmogamy, karyogamy, and meiosis, which collectively results in the development of perithecia bearing haploid ascospores (Leslie & Summerell, 2008). However, the sexual stage of *F. circinatum* has never been observed in the field.

For studying the population genetics of *F. circinatum*, various DNA-based markers have been used (Fru et al., 2019; Fru et al., 2017; Santana et al., 2016; Steenkamp et al., 2014; Steenkamp et al., 2012; Wingfield et al., 2008). These include markers to assay the mating type of isolates (Steenkamp et al., 2016), as well as various markers for studying the genetic diversity within collections of isolates (Fru et al., 2019). The first set of such markers were developed by Wikler and Gordon (2000), who used them to assess the genetic relationship in *F. circinatum* populations

around the world. The second set of DNA-based markers was developed by Britz et al. (2002), who subsequently used them to study the first *F. circinatum* outbreak in South Africa (Coutinho et al., 2007). Most recently, a comprehensive set of microsatellite markers were developed by Santana et al. (2009), and these have since become the population markers of choice for the pitch canker fungus (Berbegal et al., 2013; Fru et al., 2017; Santana et al., 2016). This is because combined with mating type data, microsatellites are highly informative for studying reproductive mode, population structure and population origins of a heterothallic fungus. For example, well-established populations that reproduce sexually are typically diverse with both mating types being present (Heitman, 2006, 2010; Ježić et al., 2012). By contrast, those that mainly propagate via vegetative means and/or that were introduced into a new location, mostly have limited diversity and/or are clonal, often with one of the mating types under-represented or completely absent (Fru et al., 2017; Kohn, 1995; Wang, 1997).

Application of the various population markers showed that the South African population of *F. circinatum* is generally diverse, which was initially thought to be due to sexual reproduction (Britz et al., 2001; Viljoen et al., 1994). However, various studies on recent disease outbreaks found no evidence for recombination and sexual reproduction in populations from the plantation setting using population markers (Fourie et al., 2014; Fru et al., 2017; Herron et al., 2020; Santana et al., 2016). The observed diversity in these populations was therefore ascribed to multiple independent introductions into the country (Fru et al., 2017). Therefore, it was suggested that the genetically distinct isolates that reproduce asexually may represent clones that shared the same mating type, multilocus genotype (MLG) (Herron et al., 2020; Santana et al., 2016), as well as belong to the same vegetative compatibility groups (Steenkamp et al., 2014).

A recent study by Herron et al. (2020), demonstrated that isolates that appear to be clonal differed significantly in virulence to *P. patula* seedlings during artificial inoculation experiments. This may be attributed to isolates originating from different hosts (i.e., asymptomatic grass and diseased *Pinus* tissue). The aim of this study

was therefore to determine whether the clonality observed for selected groups of isolates using microsatellite alleles also extends to phenotypic level. For this purpose, phenotypes that potentially impact the population dynamics of a plant pathogen were used (i.e., pathogenicity, growth rate, and sporulating capacity). Understanding population composition of *F. circinatum* would assist in mitigating its impact in the South African context. This study adds to the body of knowledge about the reproductive mode and how clonality relates thus enhancing our understanding of the fungus, thereby potentially providing valuable information for controlling it in South Africa.

Materials and Methods

Isolate selection

Nine *F. circinatum* isolates were used in this study (Table 1), representing four microsatellite-based genotypes (MS10, MLG11, MLG33, and MLG39). The three MS10 isolates shared the same set of alleles at all 10 of their microsatellite loci (Fru et al., 2017). The same was also true for MLG11, MLG33, and MLG39, consisting of two isolates each (Herron et al., 2020; Santana et al., 2016). Spore suspension of each isolate was plated onto water agar (20 g/L; Biolab, Midland, Johannesburg) and incubated overnight at room temperature, after which single germinating conidia were plated onto fresh potato dextrose agar (PDA; 20g/L; Sigma-Aldrich®, Steinheim, Germany). The isolate was then incubated at 25ºC for seven days from which pure cultures were produced for subsequent experiments.

Virulence assays

Virulence of the different genotypes was determined based on root, stem, and tip inoculations on three-month-old *Pinus patula* seedlings as described previously (Martínez-Álvarez et al., 2016; Mitchell et al., 2012). All three inoculation methods were conducted using a completely randomised design with 20 replicates per isolate for tip and stem inoculations, and eight replicates per isolate for all three root

inoculation methods. Each experiment was repeated once. Tip inoculations involved applying 10 µl of *F. circinatum* inoculum onto a wound created by removing the terminal growth bud of the seedling. The inoculums concentration was prepared by calculating 5×10^4 spores/ml of 15% (v/v) sterile glycerol suspension. This was done by flooding seven-day-old PDA cultures with glycerol before quantification using a haemocytometer and compound light microscope at 20x magnification. For stem inoculation, a sterile cork borer (5 mm in diameter) was used to make agar plugs of seven-day-old PDA cultures from the edge of growing cultures. The same sterile cork borer was then used to remove the bark layer of the stem, after which the agar plug was placed on the wound (with the mycelium side facing the stem). This was then carefully covered with Parafilm (parafilm 'M', American National Can™ Chicago, USA). The inoculated plants were kept at the Forestry and Agricultural Biotechnology Institute (FABI) greenhouses at temperatures ranging between 25-30ºC. For tip and stem inoculation, control treatments of sterile 15% glycerol and PDA plugs respectively were used for inoculation. For the tip and stem inoculations, a seven-by-seven insert tray was divided into two, after which twenty plants were transplanted to each side of the tray per isolate. The same tray arrangement was made for the 10 isolates used in the study plus the control treatment. They were then monitored daily for symptom development. Stem lesion lengths were measured for both inoculation techniques.

For the root inoculations, seedlings grown in sterile pine bark or water were used. Also, the plants in bark medium were inoculated with either spore suspensions or mycelial plugs, while those in water were inoculated only with spore suspensions. Therefore, this set of experiments was grouped according to the inoculation method: plug in pine bark (P), spore suspension in pine bark (S) and spore suspension in water (H). All the inoculations were in 250 ml polystyrene cups, either with holes and quarter-filled with pine bark (for the P and S treatments) or intact containing 50 ml sdH$_2$O (for the H treatment). For the S and H inoculations, 10 µl of 5×10^4 spores/ml of 15% (v/v) sterile glycerol suspension was pipetted into the bottom of eight cups with pine bark and eight cups with sdH$_2$O. The P inoculations were treated with a 5

mm wide mycelial plug placed upside down at the bottom of the cup with pine bark and covered in pine bark. Inocula were prepared as initially described.

Inoculation for the S and P treatments was accomplished by removing the plants from their conical containers and cutting off 10% of the root system (this was done for balancing the mode of entry for all three inoculation methods) with a sterile scissor and re-inserting the plants into the respective cups. To support the plants, more pine bark was added to S and P cups. For the H treatments, the seedling roots were washed with sdH$_2$O and damaged with a sterile scissor, after which the plant was inserted into relevant cups and kept upright using adhesive tape. A rating scale was created to score the severity of the disease caused by each isolate on the plants (Table 2). This was done by observing the colour of the lesions and correspondence with the allocated ratings.

After scoring disease severity on roots and stems of the plants, as another way of scoring roots and stem disease severity: root and stem fresh weights were measured separately using a fine weighing scale after which each piece was kept in a respective paper bag for drying. Paper bags containing the relevant plant tissues were left in the phytotron at 25-28ºC for four weeks, after which dry weight measurements were taken. To determine the root and stem moisture contents (RMC and SMC), the dry weights were subtracted from the fresh weights (fresh weight – dry weight = RMC/SMC). The data were recorded in Microsoft Excel and subjected to statistical analysis. After each scoring, a piece of tissue from the three points of inoculation was kept at -4ºC. After which Koch's postulate and PCR assays using *F. circinatum* specific primers were conducted.

Growth rate studies

Growth rate studies were conducted on the nine *F. circinatum* genotypes using two media types. Cultures were prepared as described by Porter et al. (2009) and inoculated on the pine extract agar (PEA) (Autoclaved pine extract liquid; PDA; 20g/L; Sigma-Aldrich®, Steinheim, Germany) and PDA (PDA; 20g/L; Sigma-Aldrich®, Steinheim, Germany) 90 mm plates. Plates were sealed with Parafilm (parafilm 'M'

(American National Can™ Chicago, USA)) and placed in growth chambers with temperatures of 20ºC, 25ºC and 30ºC. Five plates per isolate were inoculated for each of the two media and each of the three temperatures. The experiment was repeated twice. Mycelium growth was recorded by measuring the diameter of the two perpendicular lines drawn at the bottom of the 90 mm petri dish. The two values were then averaged, and generated data was used for statistical analysis. A regression test was done to determine the correlation in growth based on media type and at different temperatures using excel or the R programme (R Core Team, 2018).

The degree to which the nine *F. circinatum* genotypes produces conidia was investigated on both PEA and PDA after seven days of incubation at 25ºC. For this purpose, the respective cultures were prepared as described above after which they were flooded with 10 ml of 15% sterile glycerol. A haemocytometer was used in spore counting under a compound microscope. Spore readings were taken from three plates per isolate.

Statistical analysis

Means and the standard errors derived in excel were used to report the data. Statistical significance was evaluated by one-way analysis of variance (ANOVA) with Tukey's Multiple Comparison post-test in R- studio v.20 (Gandrud, 2018) for the tip and stem assays. The minimum significance level was set at $p < 0.001$. Multiple comparisons between groups and between assays were made using Tukey's post-hoc test in R. The correspondence among data obtained for the different isolates in the different experiments was evaluated using regression analysis in excel (Carlberg, 2016). For the root assays rating data, multiple comparisons within and between the same MLG groups were made using Chi square analysis in R. The minimum significance level was set at $P < 0.05$.

Results

Comparison among virulence assays

Virulence of the different MLG-based clones of *F. circinatum* on *P. patula* seedlings showed that within-treatment standard error (SE) varied across the various sets of experiments (Figure 2 and 3). However, these variations were mostly not significant. Based on Koch's postulate and using produced *F. circinatum* specific primers in PCR assays, lesions generated on tip, stem and root tissues were confirmed to be caused by *F. circinatum*. (Figure S1).

Similar overall trends were observed for the two experiments involving inoculation of stem and tip inoculated plant parts (Figure 2). The results for these two experiments were also positively correlated (Figure 4). By contrast, results for the three root inoculation experiments were mostly not significantly correlated with one another, nor with those of the above-ground inoculations (tip and stem) (Figure 4). The only exception was a positive but very weak correlation between the stem inoculation experiment and the H experiment (Figure 4). Additionally, compared to the tip and stem inoculation experiments, those conducted on the roots took much longer to show symptoms. The former yielded results after six and three weeks, respectively, while the root inoculation experiments took more than 12 weeks because all seedlings remained symptomless until week 13. Shoot discolouration in most of the inoculated seedlings only started in week 13 or later (Figure 5).

Neither root moisture nor stem moisture contents (RMC or SMC) provided information about the virulence of isolates on the above-ground plant parts (from the root colar to the tip of the seedling) (Figures 6 and 7). This is also evident from the lack of any correlation between the disease ratings of isolates and their RMC and SMC values (Figure 8A and B), as well as a lack of correlation between these values and lesion lengths obtained from stem and tip inoculations (Figure 8 C, D, E, and F).

Virulence among same-genotype isolates

Comparison of the lesion lengths induced by same-MLG isolates on above-ground plant parts indicated some difference between the putative microsatellite-based clones (Figure 2). For the stem inoculation experiment, the mean lesion lengths caused by the two MLG39 isolates differed significantly ($p<0.05$), while significant differences were absent within the remaining three same-MLG groups. For the tip inoculation experiment, the lesion lengths caused by the two MLG33 isolates differed significantly,

while significant differences were lacking in the three other same-MLG groups. The results for these two experiments, therefore, indicate that the apparent clonality of MLG33 isolates and MLG39 isolates do not extend to strain aggressiveness or virulence on the above-ground parts of *P. patula* seedlings.

Differences among same-MLG isolates were also observed in the results for the P, S and H root inoculation experiments. In the case of the S and H experiments, differences were observed between the disease ratings of the two isolates included in each of MLG11, MLG33 and MLG39 (Figure 3). For the P experiment, the disease ratings for one of the MS10 isolates differed significantly from the other two, while the isolates included in each of MLG39 and MLG33 differed non-significantly (Figure 3). Overall, the observed variations in response/lesion development are mostly insignificant but questionable for clonal isolates. Together, these data thus support the fact that clonality within MLG39 and MLG33 do not extend to virulence, but also suggest that this is true for MLG11 and MS10.

Growth rate

Growth rates on PDA and PEA between and among same-MLG isolates were determined at 25ºC, which falls within the optimal growth range of *F. circinatum* (Elvira-Recuenco et al., 2021). The growth rate of isolates on PDA varied both considerably and significantly within all four of the same-MLG groups (Figure 9). The only exception was for MLG11 where the two isolates' growth did not differ significantly. On PEA, however, there were no significant differences observed within

the MS10, MLG39, and MLG33 isolate groups, while one of the MLG11 isolates grew significantly faster ($p < 0.001$) than the other. This difference in the general trends observed on PDA and PEA was also reflected in the results of the regression analysis showing no (R-square close to 0.00) correlation between the growth rates on PDA and PEA (Figure 10).

Growth at suboptimal temperatures revealed significant differences among/between isolates within the various MLGs. As expected, all four groups of isolates grew faster at 25ºC than at 20ºC and 30ºC (Figure 9), with the only exception being the isolate CMW53344 (MLG39) that appeared to grow slightly faster at 20ºC than at 25ºC. However, within each of the groups, there were significant differences in growth rate among the MS10 isolates, and between the MLG33 and the MLG11 isolates at both at 20ºC and 30ºC (Figure 11). Overall, these results thus showed that the apparent clonality of the same-MLG isolates examined does not extend to the growth rate in culture and that incubation to suboptimal temperatures likely accentuates these differences.

Sporulating capacity

Comparison of the number of spores produced on PDA showed no significant differences within the MS10, MLG11 and MLG33 isolate groups (Figure 12A1, C1, and D1). Only in the case of MLG39 did one of the isolates produce significantly ($p < 0.001$) more spores on PDA (Figure 12B1). However, on PEA this difference was not observed. Indeed, sporulation capacity within each of the isolate groups did not differ significantly on PEA. There was also no correlation between the sporulating capacities on PDA and PEA ($p > 0.05$; R-square close to 0.00) (Figure 13).

Discussion

In this study, we investigated whether *F. circinatum* isolates that are thought to be clonal based on their identical multi-locus genotypes display similar saprophytic abilities in living and non-living substrates. Data from different inoculation procedures

revealed significant differences in virulence of same-MLG isolates while infecting the tip, stem, or roots of *P. patula* seedlings. Similar variations were also observed in laboratory growth and sporulation studies on different artificial media and under different temperature regimes.

Isolates from the same MLG group included in this study displayed substantially different growth rate patterns on PDA and PEA at 25ºC. This implies that the putatively clonal isolates differed in how they responded to the nutrients provided by these media. For example, there might have been differences in nutrient uptake (Meletiadis et al., 2001; Suberkropp, 1995; Tang et al., 2015) and the subsequent ability to synthesize cellular components, and ultimately replicate and grow (Vieira-Silva & Rocha, 2010). These differences observed among isolates of the same MLG group could thus be due to regulatory idiosyncrasy inherent to any one of a range of different processes.

The sporulating capacity among members of different MLG groups differed, although this trait appeared to be influenced by the growth medium used. According to (Malleck et al., 2018), sporulating capacity is higher at optimal temperatures, which for *F. circinatum* is around 25ºC (Botella et al., 2019; Elvira-Recuenco et al., 2021). However, the data presented here showed sporulation at this temperature was not always higher. Furthermore, the sporulation capacity of *F. circinatum* has not been studied in detail and even then, was expressed in terms of spore deposition. For example, Schweigkofler et al. (2004), reported that the fungus typically produces aerial spores in a range of 1×10^3 to 7×10^5 spores/m^2. More research is thus needed to understand how this would relate to our quantifications of suspensions (i.e., in spores/ml).

The above-ground and below ground virulence results on *P. patula* seedlings confirm the fact that clonality within MLG39 and MLG33 did not extend to virulence. This consensus suggests that this is also true for MLG11 and MS10 as MLG11 members which also varied significantly in virulence using the root P method of inoculation. However, the open-pollinated seedling's genotypic nature might have contributed to the non-uniform responses of pine to infection by same-genotype isolates. Taken

together these findings demonstrated that same-MLG isolates of *F. circinatum* show unique behavioural traits and that their microsatellite-based clonality does not extend to phenotype. This conforms to the results obtained in a preliminary study by Mbhele et al. (unpublished). Furthermore, Heron et al. (2020), also found significant differences among MLG11 isolates which then suggests that these might not be clonal.

The phenotypic differences observed among same-MLG isolates of *F. circinatum* may be ascribed to gene regulatory differences among clones. For example, it is well-known that the phenotypic properties of fungal strains that have been sub-cultured extensively or that have been preserved for extended periods of time in culture collections, may change (Davis et al., 2005; Russell). Most of the isolates in the current study were isolated by Fru et al. unpublished but it was done in 2016 (MS10) and Swett et al. (2014) (MLGs) from locations with different climatic conditions. This could mean that epigenetic gene regulation might influence the isolates' phenotypes. However, should the findings presented here indeed reflect the true phenotype of the fungi examined, the underlying differences in gene regulation and expression might provide valuable intuitions into the *F. circinatum*-*Pinus* interaction and the general biology of this fungus.

Another explanation for the findings presented in this study is that the same-MLG isolates examined are genetically different and that the microsatellite markers used for genotyping them do not provide sufficient resolution for identifying true clones. A number of previous studies reported that MLG data may be affected by recent mutations at microsatellite loci or a phenomenon known as size homoplasy (Arnaud-Haond et al., 2012; Estoup et al., 2002; Vaghefi et al., 2017; Yuzon et al., 2020). Both mutation and size homoplasy change the structure, length, and nature of the microsatellite. No accuracy would then be found in their use and any conclusion derived from that would be futile. Therefore, subsequent studies should seek to shed light on these issues by using genomic and transcriptomic approaches.

The findings presented in this study provided a valuable comparison of inoculation techniques for virulence assays. It demonstrated that the stem inoculation method is

less time consuming as compared to tip and root inoculation techniques and provides the best resolution, thus, of greater importance to assist in *F. circinatum*-pine pathogenicity and response investigations. The use of the stem inoculation technique provided very low to no within treatment standard errors, making these results most reliable. Most recent studies are using the stem inoculation technique (Martínez-Álvarez et al., 2016) to infect pine in pathogenicity studies (Amaral et al., 2021; Carter & Gordon, 2020; Davydenko et al., 2018; Martín-García et al., 2018; Martínez-Álvarez et al., 2016; Mullett et al., 2017; Muñoz-Adalia et al., 2018). The tip inoculation technique has been a standard inoculation procedure for these types of studies (Hernandez-Escribano et al., 2020; Herron et al., 2020; Iturritxa et al., 2017; Quesada et al., 2019; Steenkamp et al., 2012).

This is the first study to show how *P. patula* wounded roots respond to *F. circinatum* spores in water, spores in soil, and mycelium in the soil. In addition, here we present how the results from these root inoculations can be analysed. Infection trials have been previously conducted using non-wounded roots. For example, spores were applied to pine seedling substrate (Davydenko et al., 2018) and seedlings were dipped into a spore suspension for 1 minute (Swett et al., 2016).

In this study as well as in previous studies, a long lag-phase was observed between inoculation of the roots and symptom development (Swett et al., 2016). The late onset of symptoms and the faster growth of inoculated seedlings may possibly be linked to *F. circinatum*'s hemibiotrophic nature, where the pathogen is a biotroph or even a beneficial endophyte until it switches to its necrotrophic life stage (Swett & Gordon, 2017). However, the lag time between inoculation and symptom development was up to four times longer in trials where unwounded roots were inoculated compared to our trial (Swett et al., 2016). The shorter incubation period before symptom development in our experiment may have resulted from wounding the roots prior to fungal inoculation, differences in the substrate or even waterlogging which is known to enhance the infection rate (Swett & Gordon, 2017).

Conclusions

This study focused on the phenotypic traits of *F. circinatum* isolates that are considered as clones based on ten microsatellite loci. However, our phenotypic measurements show that these clonal isolates display different phenotypes during infection and vegetative growth. We might thus be dealing with a more diverse population sharing the same multilocus genotypes. Therefore, a subsequent study will use genomic and transcriptomic approaches to uncover the genetic identity of these isolates. For this purpose, a subset of the South African population of *F. circinatum* will be sequenced, and vegetative compatibility groups-based genotyping will be performed using both bioinformatics and experimental-based techniques. In addition, more intensive research is required to uncover the mechanisms underlying the observed diversity in a heterothallic pathogen with only one mating type found in the field and hence does not sexually reproduce in its invasive range.

References

Amaral, J., Correia, B., Escandón, M., Jesus, C., Serôdio, J., Valledor, L., Hancock, R. D., Dinis, L.-T., Gomez-Cadenas, A., & Alves, A. (2021). Temporal physiological response of pine to *Fusarium circinatum* infection is dependent on host susceptibility level: the role of ABA catabolism. *Tree Physiology*, *41*(5), 801-816.

Arnaud-Haond, S., Duarte, C. M., Diaz-Almela, E., Marbà, N., Sintes, T., & Serrão, E. A. (2012). Implications of extreme life span in clonal organisms: millenary clones in meadows of the threatened seagrass *Posidonia oceanica*. *PLoS One*, *7*(2), e30454.

Berbegal, M., Pérez-Sierra, A., Armengol, J., & Grünwald, N. (2013). Evidence for multiple introductions and clonality in Spanish populations of *Fusarium circinatum*. *Phytopathology*, *103*(8), 851-861.

Botella, L., Bačová, A., Dvorák, M., Kudláček, T., Pepori, A. L., Santini, A., Ghelardini, L., & Luchi, N. (2019). Detection and quantification of the air inoculum of *Caliciopsis pinea* in a plantation of *Pinus radiata* in Italy. *iForest-Biogeosciences and Forestry*, *12*(2), 193.

Britz, H., Couhnho, T., Gordon, T., & Wingfield, M. (2001). Characterisation of the pitch canker fungus, *Fusarium circinatum*, from Mexico. *South African Journal of Botany*, *67*(4), 609-614.

Britz, H., Wingfield, B., Coutinho, T., & Wingfield, M. (2002). Sequence characterized amplified polymorphic markers for the pitch canker pathogen, *Fusarium circinatum*. *Molecular Ecology Notes*, *2*(4), 577-580.

Carlberg, C. (2016). *Regression analysis microsoft excel*. Que Publishing.

Carter, J. W., & Gordon, T. R. (2020). Infection of the native California grass, *Bromus carinatus*, by *Fusarium circinatum*, the cause of pitch canker in pines. *Plant Disease*, *104*(1), 194-197.

Coutinho, T., Steenkamp, E., Mongwaketsi, K., Wilmot, M., & Wingfield, M. (2007). First outbreak of pitch canker in a South African pine plantation. *Australasian Plant Pathology*, *36*(3), 256-261.

Davis, K. E., Joseph, S. J., & Janssen, P. H. (2005). Effects of growth medium, inoculum size, and incubation time on culturability and isolation of soil bacteria. *Applied and Environmental Microbiology*, *71*(2), 826-834.

Davydenko, K., Nowakowska, J. A., Kaluski, T., Gawlak, M., Sadowska, K., García, J. M., Diez, J. J., Okorski, A., & Oszako, T. (2018). A Comparative Study of the Pathogenicity of *Fusarium circinatum* and other Fusarium Species in Polish Provenances of *P. sylvestris L. Forests*, *9*(9), 560.

Drenkhan, R., Ganley, B., Martín-García, J., Vahalík, P., Adamson, K., Adamčíková, K., Ahumada, R., Blank, L., Bragança, H., & Capretti, P. (2020). Global

geographic distribution and host range of *Fusarium circinatum*, the causal agent of pine pitch canker. *Forests*, *11*(7), 724.

Dwinell, L. D., Barrows-Broaddus, J. B., & Kuhlman, E. G. (1985). Pitch canker: a disease complex. *Plant Dis*ease, *69*, 270-276.

Elliott, C. (1991). Reproduction in fungi.

Elvira-Recuenco, M., Pando, V., Berbegal, M., Manzano Muñoz, A., Iturritxa, E., & Raposo, R. (2021). Influence of temperature and moisture duration on pathogenic life-history traits of predominant haplotypes of *Fusarium circinatum* on Pinus spp. in Spain. *Phytopathology, 111*(11), pp.2002-2009.

Estoup, A., Jarne, P., & Cornuet, J. M. (2002). Homoplasy and mutation model at microsatellite loci and their consequences for population genetics analysis. *Molecular Ecology*, *11*(9), 1591-1604.

Fourie, G., Wingfield, M. J., Wingfield, B. D., Jones, N. B., Morris, A. R., & Steenkamp, E. T. (2014). Culture-independent detection and quantification of *Fusarium circinatum* in a pine-producing seedling nursery. *Southern Forests: a Journal of Forest Science*, *76*(3), 137-143.

Fru, F. F., Steenkamp, E. T., Wingfield, M. J., & Roux, J. (2019). High genetic diversity of *Fusarium circinatum* associated with the first outbreak of pitch canker on *Pinus patula* in South Africa. *Southern Forests: a Journal of Forest Science*, *81*(1), 69-78.

Fru, F. F., Steenkamp, E. T., Wingfield, M. J., Santana, Q. C., & Roux, J. (2017). Unique clones of the pitch canker fungus, *Fusarium circinatum*, associated with a new disease outbreak in South Africa. *European Journal of Plant Pathology*, *148*(1), 97-107.

Gandrud, C. (2018). *Reproducible research with R and RStudio*. Chapman and Hall/CRC.

Gordon, T. R., Henry, P. M., Jenner, B. N., & Scott, J. C. (2021). Spontaneous changes in somatic compatibility in *Fusarium circinatum*. *Fungal Biology*.

Guerra-Santos, J., & Cibrian-Tovar, D. (1998). *El cancro resinoso por fusarium subglutinans (Wollenw y Reink) Nelson, Tousson y Marasas, una nueva enfermedad de Pinus spp. en Mexico*.

Hawker, L. E. (2016). *The physiology of reproduction in fungi*. Cambridge University Press.

Heitman, J. (2006). Sexual reproduction and the evolution of microbial pathogens. *Current Biology*, *16*(17), R711-R725.

Heitman, J. (2010). Evolution of eukaryotic microbial pathogens via covert sexual reproduction. *Cell Host & Microbe*, *8*(1), 86-99.

Hernandez-Escribano, L., Visser, E. A., Iturritxa, E., Raposo, R., & Naidoo, S. (2020). The transcriptome of *Pinus pinaster* under *Fusarium circinatum* challenge. *BMC Genomics*, *21*(1), 1-18.

Herron, D. A., Wingfield, M. J., Fru, F., Wingfield, B. D., & Steenkamp, E. T. (2020). Grasses as a refuge for *Fusarium circinatum* L.–evidence from South Africa. *Southern Forests: a Journal of Forest Science*, *82*(3), 253-262.

Iturritxa, E., Trask, T., Mesanza, N., Raposo, R., Elvira-Recuenco, M., & Patten, C. L. (2017). Biocontrol of *Fusarium circinatum* infection of young *Pinus radiata* trees. *Forests*, *8*(2), 32.

Ježić, M., Krstin, L., Rigling, D., & ĆURKOVIĆ-PERICA, M. (2012). High diversity in populations of the introduced plant pathogen, *Cryphonectria parasitica*, due to encounters between genetically divergent genotypes. *Molecular Ecology*, *21*(1), 87-99.

Kohn, L. (1995). The clonal dynamic in wild and agricultural plant–pathogen populations. *Canadian Journal of Botany*, *73*(S1), 1231-1240.

Leslie, J. F., & Summerell, B. A. (2008). *The Fusarium laboratory manual*. John Wiley & Sons.

Malleck, T., Daufouy, G., André, S., Broussolle, V., & Planchon, S. (2018). Temperature impacts the sporulation capacities and spore resistance of *Moorella thermoacetica*. *Food Microbiology*, *73*, 334-341.

Martín-García, J., Lukačevičová, A., Flores-Pacheco, J. A., Diez, J. J., & Dvořák, M. (2018). Evaluation of the susceptibility of several *Czech conifer* provenances to *Fusarium circinatum*. *Forests*, *9*(2), 72.

Martín-Rodrigues, N., Espinel, S., Sanchez-Zabala, J., Ortíz, A., González-Murua, C., & Duñabeitia, M. K. (2013). Spatial and temporal dynamics of the colonization of *Pinus radiata* by *Fusarium circinatum*, of conidiophora development in the pith and of traumatic resin duct formation. *New Phytologist*, *198*(4), 1215-1227.

Martínez-Álvarez, P., Fernández-González, R. A., Sanz-Ros, A. V., Pando, V., & Diez, J. J. (2016). Two fungal endophytes reduce the severity of pitch canker disease in *Pinus radiata* seedlings. *Biological Control*, *94*(1), 1-10.

McDonald, B. A., & Linde, C. (2002). Pathogen population genetics, evolutionary potential, and durable resistance. *Annual Review of Phytopathology*, *40*(1), 349-379.

Meletiadis, J., Meis, J. F., Mouton, J. W., & Verweij, P. E. (2001). Analysis of growth characteristics of filamentous fungi in different nutrient media. *Journal of Clinical Microbiology*, *39*(2), 478-484.

Mitchell, R. G., Steenkamp, E. T., Coutinho, T. A., & Wingfield, M. J. (2011). The pitch canker fungus, *Fusarium circinatum*: implications for South African forestry. *Southern Forests: a Journal of Forest Science*, *73*(1), 1-13.

Mitchell, R. G., Wingfield, M. J., Hodge, G., Steenkamp, E. T., & Coutinho, T. A. (2012). Selection of Pinus spp. in South Africa for tolerance to infection by the pitch canker fungus. *New Forests*, *43*(4), 473-489.

Mullett, M., Pérez-Sierra, A., Armengol, J., & Berbegal, M. (2017). Phenotypical and molecular characterisation of *Fusarium circinatum*: Correlation with virulence and fungicide sensitivity. *Forests*, *8*(11), 458.

Muñoz-Adalia, E. J., Cañizares, M. C., Fernández, M., Diez, J. J., & García-Pedrajas, M. D. (2018). The *Fusarium circinatum* gene fcrho1, encoding a putative Rho1 GTPase, is involved in vegetative growth but dispensable for pathogenic development. *Forests*, *9*(11), 684.

Nieuwenhuis, B. P., Tusso, S., Bjerling, P., Stångberg, J., Wolf, J. B., & Immler, S. (2018). Repeated evolution of self-compatibility for reproductive assurance. *Nature Communications*, *9*(1), 1-10.

Nirenberg, H. I., & O'Donnell, K. (1998). New Fusarium species and combinations within the *Gibberella fujikuroi* species complex. *Mycologia*, *90*(3), 434-458.

Pfenning, L. H., Costa, S. d. S., Melo, M. P. d., Costa, H., Ventura, J. A., Auer, C. G., & Santos, Á. F. d. (2014). First report and characterization of *Fusarium circinatum*, the causal agent of pitch canker in Brazil. *Tropical Plant Pathology*, *39*(3), 210-216.

Quesada, T., Lucas, S., Smith, K., & Smith, J. (2019). Response to temperature and virulence assessment of *Fusarium circinatum* isolates in the context of climate change. *Forests*, *10*(1), 40.

Russell, J. E. Evolving a national culture collection to meet current challenges in microbiology.

Santana, Q. C., Coetzee, M. P., Steenkamp, E. T., Mlonyeni, O. X., Hammond, G. N., Wingfield, M. J., & Wingfield, B. D. (2009). Microsatellite discovery by

deep sequencing of enriched genomic libraries. *Biotechniques*, *46*(3), 217-223.

Santana, Q. C., Coetzee, M. P. A., Wingfield, B. D., Wingfield, M. J., & Steenkamp, E. T. (2016). Nursery-linked plantation outbreaks and evidence for multiple introductions of the pitch canker pathogen *Fusarium circinatum* into South Africa. *Plant Pathology*, *65*(3), 357-368.

Schweigkofler, W., O'Donnell, K., & Garbelotto, M. (2004). Detection and quantification of airborne conidia of *Fusarium circinatum*, the causal agent of pine pitch canker, from two California sites by using a real-time PCR approach combined with a simple spore trapping method. *Applied and Environmental Microbiology*, *70*(6), 3512-3520.

Steenkamp, E., Makhari, O., Coutinho, T., Wingfield, B., & Wingfield, M. (2014). Evidence for a new introduction of the pitch canker fungus *Fusarium circinatum* in *South A frica*. *Plant Pathology*, *63*(3), 530-538.

Steenkamp, E. T., Rodas, C., Kvas, M., & Wingfield, M. J. (2012). *Fusarium circinatum* and pitch canker of Pinus in Colombia. *Australasian Plant Pathology*, *41*(5), 483-491.

Suberkropp, K. (1995). The influence of nutrients on fungal growth, productivity, and sporulation during leaf breakdown in streams. *Canadian Journal of Botany*, *73*(S1), 1361-1369.

Swett, C., & Gordon, T. (2017). Exposure to a pine pathogen enhances growth and disease resistance in *Pinus radiata* seedlings. *Forest Pathology*, *47*(1), e12298.

Swett, C. L., Kirkpatrick, S. C., & Gordon, T. R. (2016). Evidence for a hemibiotrophic association of the pitch canker pathogen *Fusarium circinatum* with *Pinus radiata*. *Plant Disease*, *100*(1), 79-84.

Swett, C. L., Porter, B., Fourie, G., Steenkamp, E. T., Gordon, T. R., & Wingfield, M. J. (2014). Association of the pitch canker pathogen *Fusarium circinatum* with grass hosts in commercial pine production areas of South Africa. *Southern Forests: a Journal of Forest Science*, *76*(3), 161-166.

Tang, W., Kuehn, T., & Simcik, M. F. (2015). Effects of temperature, humidity and air flow on fungal growth rate on loaded ventilation filters. *Journal of Occupational and Environmental Hygiene*, *12*(8), 525-537.

Vaghefi, N., Kikkert, J. R., Bolton, M. D., Hanson, L. E., Secor, G. A., Nelson, S. C., & Pethybridge, S. J. (2017). Global genotype flow in *Cercospora beticola* populations confirmed through genotyping-by-sequencing. *PLoS One*, *12*(10), e0186488.

Vieira-Silva, S., & Rocha, E. P. (2010). The systemic imprint of growth and its uses in ecological (meta) genomics. *PLoS Genetics*, *6*(1), e1000808.

Viljoen, A., Wingfield, M., & Marasas, W. (1994). First report of *Fusarium subglutinans* f. sp. pini on pine seedlings in South Africa. *Plant Disease*, *78*(3), 309-312.

Wang, X.-R. (1997). Genetic variability in the canker pathogen fungus, *Gremmeniella abietina*. Contribution of sexual compared with asexual reproduction. *Mycological Research*, *101*(10), 1195-1201.

Wikler, K., & Gordon, T. R. (2000). An initial assessment of genetic relationships among populations of *Fusarium circinatum* in different parts of the world. *Canadian Journal of Botany*, *78*(6), 709-717.

Wilson, A. M., Wilken, P. M., van der Nest, M. A., Wingfield, M. J., & Wingfield, B. D. (2019). It's all in the genes: the regulatory pathways of sexual reproduction in filamentous ascomycetes. *Genes*, *10*(5), 330.

Wingfield, M., Hammerbacher, A., Ganley, R., Steenkamp, E., Gordon, T., Wingfield, B., & Coutinho, T. (2008). Pitch canker caused by *Fusarium circinatum*—A

growing threat to pine plantations and forests worldwide. *Australasian Plant Pathology*, *37*(4), 319-334.

Yuzon, J. D., Travadon, R., Malar C, M., Tripathy, S., Rank, N., Mehl, H. K., Rizzo, D. M., Cobb, R., Small, C., & Tang, T. (2020). Asexual evolution and forest conditions drive genetic parallelism in *Phytophthora ramorum*. *Microorganisms*, *8*(6), 940.

Table 1: Number, multilocus genotype (MLG) and origin of the *Fusarium circinatum* isolates used in this study

Isolate number	MLG	Plant host	Geographic origin	Reference
FC101	MS10	*P. patula*	Montahills, KZN	(Fru et al, unpublished)
64NG	MS10	*P. patula*	Ngodwana, Mpumalanga	(Fru et al, unpublished)
FC172	MS10	*P. patula*	Pine Valley, KZN	(Fru et al, unpublished)
CMW53348	MLG11	*P. patula*	Soutpansberg, Limpopo	(Swett et al., 2014)
CMWF2632	MLG11	Grasses	Soutpansberg, Limpopo	(Swett et al., 2014)
CMWF1294	MLG33	*Grasses*	Tokai, Western Cape	(Swett et al., 2014)
CMWF1243	MLG33	*P. patula*	Tokai, Western Cape	(Swett et al., 2014)
CMW53344	MLG39	*P. patula*	Soutpansberg, Limpopo	(Swett et al., 2014)
CMWF2631	MLG39	Grasses	Soutpansberg, Limpopo	(Swett et al., 2014)

Table 2: Disease severity scale based on root appearance three months post inoculation

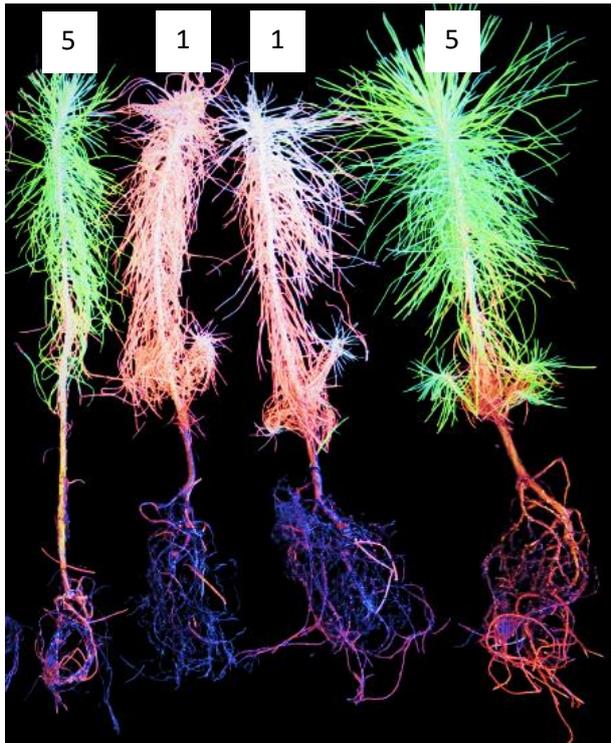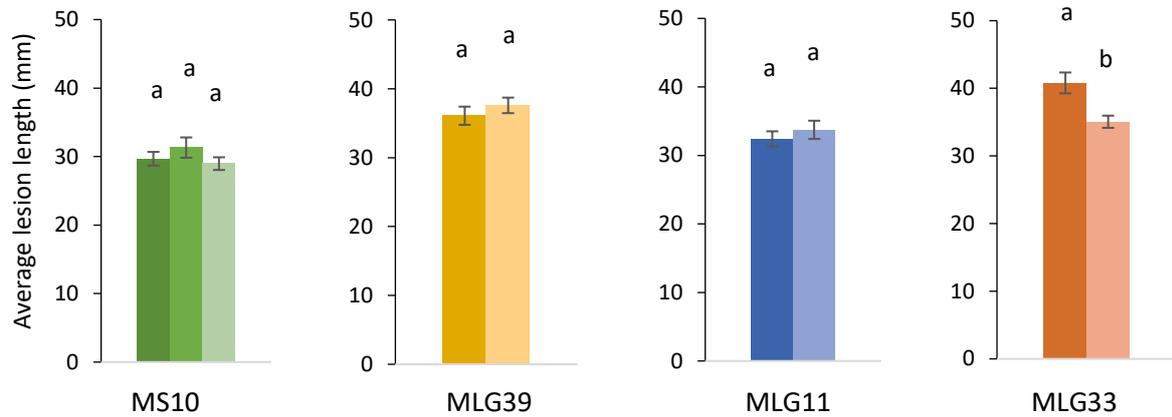| Rating	Appearance	Disease level
1	Brown roots (100%)	Severe rot
2	Brown roots (75%)	Less severe rot
3	Brown roots (50%)	Moderate rot
4	Healthy (75%)	Less rot
5	Healthy (100%)	No rot

Figure 1: Pine seedlings inoculated using the H root inoculation method showing the two extreme disease levels as per (Table 1).

A Tip inoculations
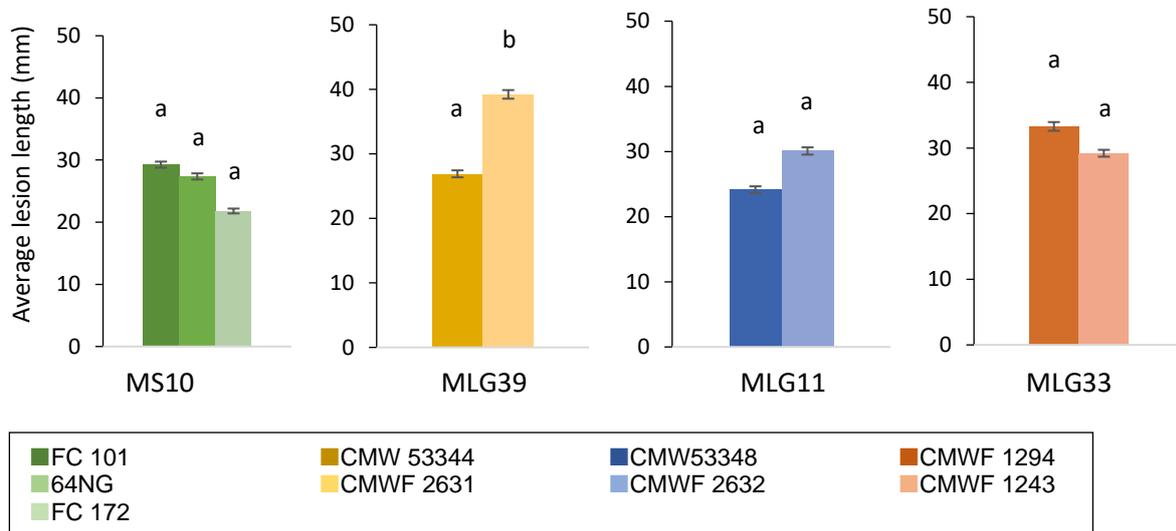

B Stem inoculations

Figure 2: Results of the two sets of inoculation experiments with nominal data for four groups (MS10, MLG11, MLG33 and MLG39) of *Fusarium circinatum* isolates previously shown to represent clones based on microsatellite analysis (A) Tip inoculations, (B) Stem inoculations. Data was collected 21 days and 6 weeks post inoculation. Isolates are colour coded according to the key provided.
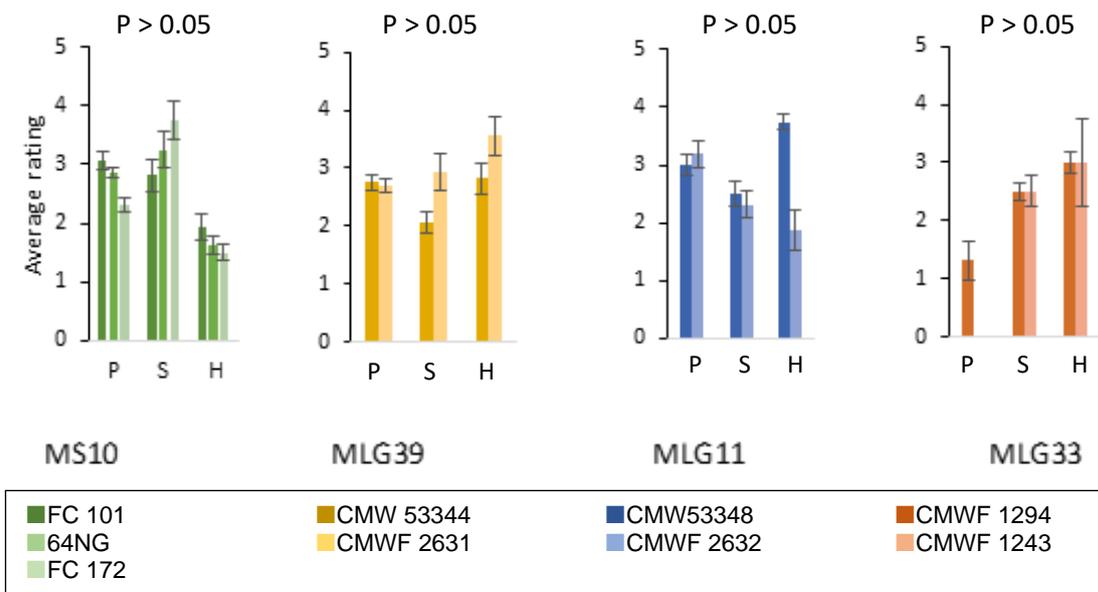
Figure 3: Results of the disease levels on roots 13 weeks post inoculation. Those performed in pine bark medium and inoculated with either mycelial plugs or spore suspensions (*ca*. 50000 spores/ml) are indicated with P and S, respectively. Those conducted in water and inoculated with spore suspensions (*ca*. 50000 spores/ml) are indicated with H. Chi-square analysis results are indicated with the p-values for each MLG group. These analyses were done within and between the isolates in each group for the three inoculation methods, all the results indicated that there was no significant difference thus only one indication is provided per MLG group.

Figure 4: Regression analysis between lesion lengths recorded in the stem inoculation experiment and lesion lengths obtained for the tip inoculation experiment (A), root rating for P treatment (B), root rating for the S treatment (C), and root rating for the H treatment (D).

Figure 5: *Pinus patula* seedlings inoculated with four groups of *F. circinatum* clonal isolates using root inoculation methods at 13 weeks post inoculation.

A Root moisture content (RMC)

B Stem moisture content (SMC)

■ FC 101	■ CMW 53344	■ CMW53348	■ CMWF 1294
■ 64NG	■ CMWF 2631	■ CMWF 2632	■ CMWF 1243
■ FC 172			

Figure 6: Results of the root inoculations RMC (A) and SMC (B) derived from root and stem weights respectively of the four groups of *F. circinatum* clonal isolates (MS10, MLG11, MLG33 and MLG39). Isolates are colour coded according to the key provided. For the root inoculation experiments, those performed in pine bark medium

and inoculated with either mycelial plugs or spore suspensions (*ca*. 50000 spores/ml) are indicated with P and S, respectively. Those conducted in water and inoculated with spore suspensions (*ca*. 50000 spores/ml) are indicated with H.
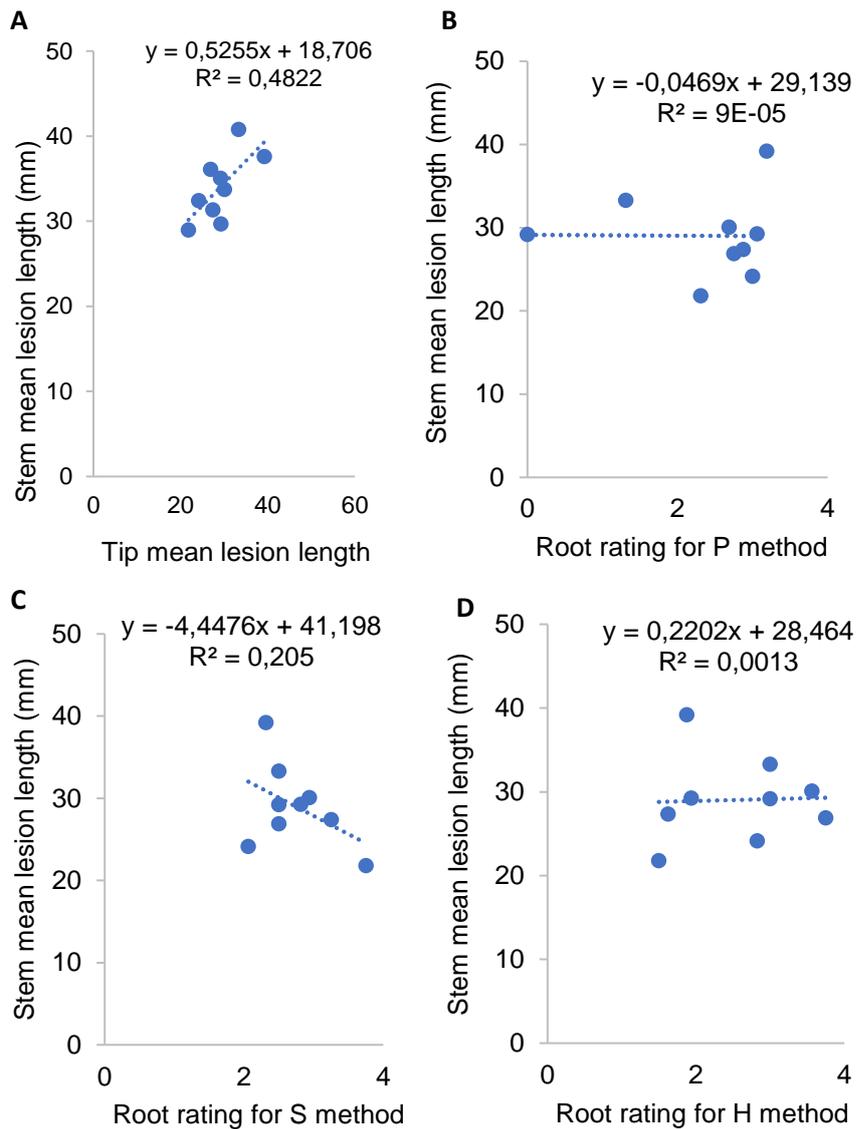
Figure 7: Regression analysis between lesion lengths recorded in the stem inoculation experiment and lesion lengths obtained for the tip inoculation experiment (A), stem moisture content for H treatment (B), and root moisture content for the H treatment (C).

C

Tip inoculation lesion length (mm)

y = -1,176x + 37,463
R² = 0,1537

Root moisture content
using P method (g/ml)

y = -1,375x + 36,666
R² = 0,0405

Root moisture content
using H method (g/ml)

y = 1,1575x + 31,496
R² = 0,0344

Room moisture content
using S method (g/ml)

D

Stem inoculation lesion length (mm)

y = 3,1681x + 22,281
R² = 0,1477

Root moisture content
using P method (g/ml)

y = 0,2798x + 28,479
R² = 0,001

Root moisture content
using H method (g/ml)

y = -2,5882x + 37,677
R² = 0,1028

Root moisture content
using S method (g/ml)

E

Tip inoculation Lesion length (mm)

y = -0,383x + 35,044
R² = 0,0064

Stem moisture content
using P method (g/ml)

y = 1,4916x + 31,688
R² = 0,0903

Stem moisture content
using H method (g/ml)

y = -0,7663x + 36,499
R² = 0,0916

Stem moisture content
using S method (g/ml)

Figure 8: Regression analysis among the four groups of *F. circinatum* clonal isolates (MS10, MLG11, MLG33 and MLG39) using the three inoculation techniques. RMC against disease rating scores in the three root inoculation methods (A), SMC against disease ratings in the three root inoculation methods (B), RMC against tip inoculations disease scores (C), RMC against stem inoculations disease scores (D), SMC against tip inoculations disease scores (E), and SMC against stem inoculations disease scores (F).

Figure 9: Growth rate comparisons among the four groups of *F. circinatum* clonal isolates (MS10, MLG11, MLG33 and MLG39) in three different temperatures on PDA. Data was collected daily. Isolates are colour coded according to the key provided.

A Growth rate on PDA

B Growth rate on PEA

Figure 10: Growth rate results of the four groups of *F. circinatum* clonal isolates (MS10, MLG39, MLG11 and MLG33) on PDA (A1-D1) and pine extracts (A2-D2) at 25ºC. Data was collected daily. Isolates are colour coded according to the key provided.

Figure 11: Four groups of *F. circinatum* clonal isolates regression analysis between the growth rates on PDA and PEA at 25ºC.

A Sporulating capacity on PDA

B Sporulating capacity on PEA

Figure 12: Sporulating capacity results for the four groups of *F. circinatum* clonal isolates (MS10, MLG11, MLG33 and MLG39) on PDA (A) and PEA (B) media at 25ºC. Data was collected 7 days post plating. Isolates are colour coded according to the key provided.

Figure 13: Four groups of *F. circinatum* clonal isolates regression between sporulating capacity analysis on 10ml ½ PDA and 10ml pine extracts.

Figure S1: Gel electrophoresis pictures showing Koch postulate's results. Tip inoculations (A), Stem inoculations (B), Root inoculations (C).

CHAPTER THREE

Identification and characterisation of vic/het genes in *Fusarium circinatum* using sequences from four model fungal species.

_____

Abstract

Vegetative compatibility is the ability of two non-sexually reproducing individuals to generate stable heterokaryons and is encoded by *het*/*vic* genes. This study aims to characterise these genes in one strain of *F. circinatum* (FSP34) to lay the foundation for their future functional characterisation in this fungus. The first step to achieving the aim was to identify orthologs of 14 HET domain-encoding *het*/*vic* genes known from four model fungi (*N. crassa*, *P. anserina*, *C. parasitica*, and *A. oryzae*) through use of sequence similarity, phylogeny, and protein domain structure. The second step aided in investigating how *F. circinatum's* het/vic gene copy number distribution differed from other fungi through sequence similarity searches of the identified number of *F. circinatum* orthologs in the genomes of the four model fungi. Phylogenetic analysis revealed that 13 of the 14 known genes have at least one ortholog in *F. circinatum* (FSP34), with *vic-6* having two and *HNWD* having seven. Except for the *HNWD* co-orthologs in *F. circinatum*, which instead of a het domain, contained a NACHT-N, practically all orthologs encoded identical functional domains, as expected. Furthermore, two of the seven *HNWD* genes in *F. circinatum* had an additional domain that was absent from the other five genes. Finally, the *AO4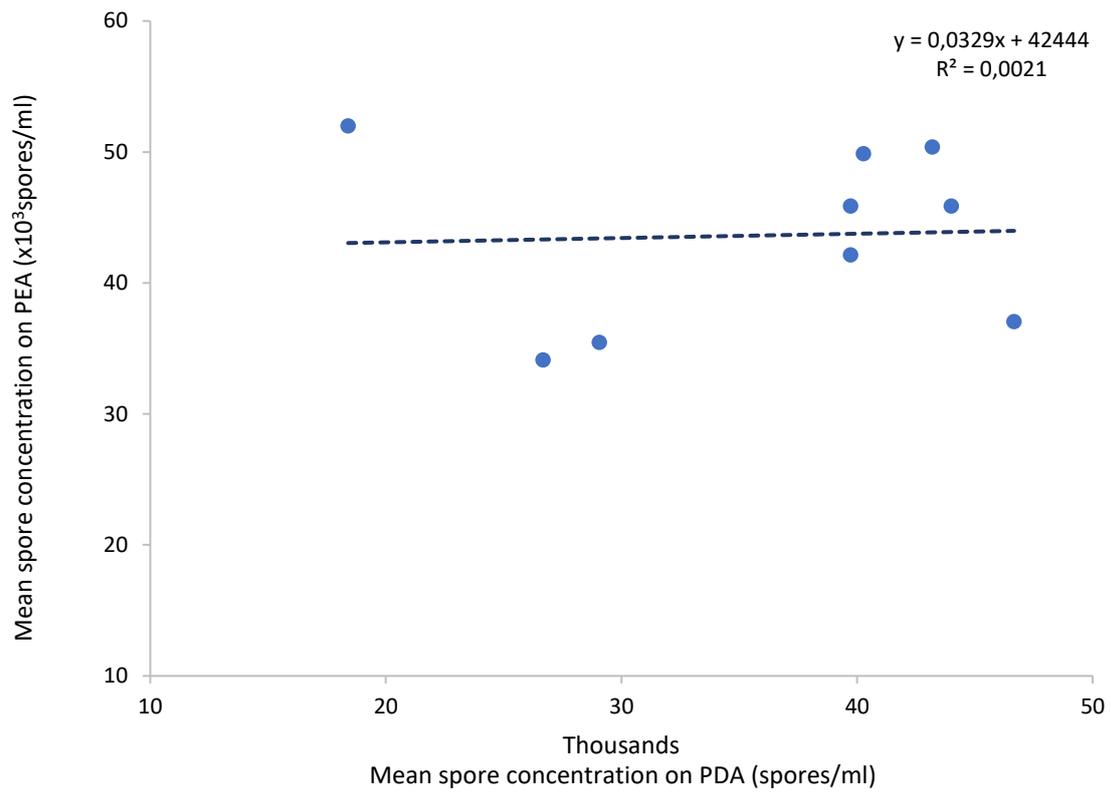04* and *pin-C* orthologs in *F. circinatum* both encoded an Ankyrin repeat domain in addition to the HET domain. In addition, most of the putative *vic*/*het* genes of *F. circinatum* occurred in higher copy number than in the four model species examined. Overall, these results showed that gene duplication combined with subsequent gene loss/multiplication and various domain fusion/shuffling events potentially shaped the development of the *het*/*vic* gene repertoire of *F. circinatum*.

_____

KEYWORDS: *In silico* **characterisation, Het domain, InterProScan.**

Introduction

Vegetative compatibility is the ability of two non-sexually reproducing fungi to form stable heterokaryons (Gonçalves et al., 2020). Individuals grow chemotropically towards each other and establish contact, then, the cell walls of the interacting cells are broken down by cell wall degrading enzymes to allow hyphal fusion and mixing of their cytoplasms (Strom & Bushley., 2016; Gonçalves et al., 2020). This fusion process is known as hyphal anastomosis, and it allows for the establishment of a distinctively linked or interconnected colony (Fischer & Glass, 2019). A colony of this type enables the efficient transfer of nutrients and organelles from one hypha to another (Hickey et al., 2002; Roper et al., 2015; Roper et al., 2013; Simonin et al., 2012). Hyphal anastomosis is essential for growth and is also thought to optimize fitness through increased colony growth rates and asexual spore generation (Bastiaans et al., 2015; Richard et al., 2012; Simonin et al., 2012; Fischer & Glass, 2019).

As a phenotypic trait, vegetative compatibility is determined by genes encoded at the so-called heterokaryon incompatibility (*het*) or vegetative incompatibility (*vic*) loci (Daskalov et al., 2020; Gordon et al., 2021; Tang et al., 2020; Zhang et al., 2020). To date, only a small number of *het*/*vic* have been identified and characterised at the molecular level. These included the seven known genes in *Podospora anserina* (*het-d, het-e, het-c, het-r, het-v, het-s,* and *het-q*) (Clavé et al., 2022; Daskalov et al., 2020; Glass et al., 2000; Saupe et al., 2000), the eight genes in *Neurospora crassa* (*het-c, pin-c, sec-9, plp-1, rcd-1, het-6, mat, and tol*) (Glass et al., 2000; Saupe et al., 2000), the five in *Cryphonectria parasitica* (*vic1-3, and vic6-7*) (Choi et al., 2012; Daskalov et al., 2019) and the three genes in *Aspergillus oryzae* (*AO370*, *AO078*, and *AO404*) (Mori et al., 2019). Of these, many represent HNWD proteins comprising of the N-terminal HET domain causes cell death, the central NACHT domain binds GTP and is required for activity, and the C-terminal WD repeat domain varies in size (number of repeats) and sequence between natural isolates and defines allele specificity. These are STAND proteins (signal transduction NTPase with multiple domains), and a fungus-specific heterokaryon incompatibility (HET) domain known to mediate cell death during vegetative incompatibility (Clavé et al.,

2022; Daskalov et al., 2020; Daskalov et al., 2019; Mori et al., 2019; Paoletti & Clave, 2007).

Two individuals that share identical alleles at most or all loci will be vegetatively compatible and able to form a stable heterokaryon (Strom & Bushley., 2016; Gonçalves et al., 2020). Vegetative compatibility is often used to study the population biology of fungal populations (Bayman & Cotty, 1991; Horn, 2003; Leslie, 1993; Milgroom & Cortesi, 1999; Papaioannou & Typas, 2015). This is because sets of compatible strains are regarded as genetically similar and therefore belonging to the same vegetative compatibility group (VCG) (Leslie & Summerell, 2008). Although these groups are analogous to those sharing the same microsatellites-based multilocus genotype (MLG), it is not yet known whether microsatellite-based MLGs and VCGs represent concordant units (i.e., whether these two methods can be used interchangeably to identify clones).

For most fungi, VCGs are determined by pairing/crossing every individual in a population with another on a suitable growth medium, where the development of a barrage or dark line at the point of contact indicates that they are incompatible, while normal growth after contact indicates that they are compatible (Leslie & Summerell, 2008). However, in other fungi such as *Fusarium* spp. this approach is not efficient, as no obvious signals of anastomosis or antagonism are readily observable (Bayman & Cotty, 1991). Therefore, approaches based on auxotrophic mutants are more commonly applied (Leslie, 1993). Viljoen et al. (1997) reported that South African *F. circinatum* strains represent at least 23 different VCGs, and Britz et al. (2005) identified an additional 6 VCGs in a subsequent study. Both studies focused on populations from the summer rainfall region of the country. For populations in the winter rainfall region, at least 46 different VCGs were reported (Steenkamp et al., 2014), but it is not known whether there was any overlap between VCGs from the two rainfall regions. Therefore, given the number of VCGs, an estimated number of 5-6 loci likely underpin the VCG diversity observed among *F. circinatum* strains in South Africa. This is because these loci are thought to be biallelic, which means that the number of VCGs would be equal to 2^n where n is the number of loci underpinning the trait (Leslie & Summerell, 2008). This estimate of the number of loci is also

similar to those reported previously (Gordon et al., 2021; Gordon et al., 2006). Indeed, in a study from the United States by Gordon et al. (2021), homologs of some of the genes thought to determine vegetative compatibility in *Podospora anserina* and *Neurospora crassa* were identified in *F. circinatum*.

Since there is currently no insight into the molecular mechanisms involved in governing VCGs in *F. circinatum* population, the first aim of this study was to identify putative *het* genes in this fungus using previously characterized *het* genes. For this purpose, inferences based on sequence similarity, phylogeny, and protein domain structure were used. The second aim was to investigate how the patterns of *het/vic* gene copy number distribution in *F. circinatum* compared to those exhibited by other fungi. For this purpose, the copy number of the identified *F. circinatum* orthologs was determined in the genomes of the four model fungi. The results of this study would thus be valuable for understanding how *F. circinatum* compare to other filamentous ascomycetes, and integration of the data generated into population genomics studies could potentially reveal which of these *het/vic* genes (if any) could serve as markers for delineating VCGs and whether these groupings are congruent with those inferred using microsatellite markers.

Materials and methods

Putative *F. circinatum het* genes were identified in the genome by using the protein sequence of the 14 known HET domain-bearing *het/vic* genes in tblastn (Gertz et al., 2006) searches against the gene nucleotide sequences from the genome of *F. circinatum* strain FSP34 using Qiagen's CLC Genomics Workbench v21 (CLC bio, Cambridge, MA) (Figure 1). Homologs were identified using expect (E)-values of $<10^{-40}$.Because these are genes under balancing selection (Aanen et al., 2010; Chevanne et al., 2009; Milgroom & Cortesi, 1999; Paoletti, 2016) and the query species were distantly related to *F. circinatum*, selections of homologs for subsequent use were made as follows: where there were more hits meeting the cut-off requirements, at most 20 hits were extracted from each blast result; and where either no or only a few hits met the requirements, at most 10 best hits were

extracted. Datasets with these best hits and the original gene sequences were compiled for further analyses.

To identify putative orthologs in *F. circinatum* for each of the known *het/vic* genes, individual datasets containing the best tblastn hits were subjected to phylogenetic analyses. For this purpose, datasets were aligned using the online multiple sequence alignment program MAFFT (Multiple Alignment using Fast Fourier Transform) v7.504 (Katoh et al., 2019). The alignments were then used to perform maximum likelihood phylogenetic analysis by using the 2021 version of the IQtree online server (Minh et al., 2013; Nguyen et al., 2015) by applying the following options: -s 'file-name'.fasta -st AA -m TEST -bb 1000 -wbt -alrt 1000. In all cases, the best-fit substitution models, according to IQtree, were used (Table 1). Branch support was estimated using ultrafast bootstraps set at 1000 replications (Minh et al., 2013). The phylograms generated were viewed and edited in Figtree v1.4.4 (Tang et al., 2020).

Datasets containing the best-hit *F. circinatum* sequences were subjected to protein domain searches using InterProScan v88.0 (Blum et al., 2020). This was done to identify the domains encoded by each of the respective genes. Furthermore, the most likely orthologs of *F. circinatum* for each of the known *het/vic* genes were used to determine the number of homologs encoded by the genomes for each of the four model fungi. This was done using the procedure as in the afore-described tblastn analysis.

Results

Homologs of known *het/vic* genes in *Fusarium circinatum*

At least one best hit for the known genes was found using tblastn searches against the *F. circinatum* genome (Table 2). The only exception was the gene AO078 from *A. oryzae* for which no homolog was detected. For the best *F. circinatum* hits, query coverage ranged from 13% to 52%, with an average of 39% of each gene identified aligning to a particular query sequence. Additionally, these best hits displayed 29-

64% protein sequence identity (35% average) to the respective query sequences. Although these query coverage and sequence identity ranges were broad, it was not unusual given that the genes of interest encode multidomain proteins that likely experience positive selection (Aanen et al., 2010; Chevanne et al., 2009; Milgroom & Cortesi, 1999; Paoletti, 2016).

Based on these criteria, multiple homologs of most of the known genes were detected in the *F. circinatum* genome (Table 2). The only exceptions were for the genes from *N. crassa*, where only one homolog of *het-C* and *het-6* were found, and three homologs of *pin-C*. There were also only three *F. circinatum* homologs for the *A. oryzae* gene *AO370*. Notably, all six of the *P. anserina* genes examined were homologous to the same set of genes in the *F. circinatum* genome, thus reflecting the fact that their protein products are paralogous members of the HNWD protein family (Paoletti et al., 2007). The remaining known genes each had sets of homologs within *F. circinatum*.

Putative orthologs in *F. circinatum* of the known *het*/*vic* genes

For most of the known genes, the phylogenetic analysis allowed for the identification of putative orthologs in *F. circinatum* (Figure 2-8). In the case of *N. crassa het-c* (Figure 3), its closest relative in *F. circinatum* was gene Fcirg_07624, suggesting an orthologous relationship between them (*i.e.*, they originate from the same ancestral gene that occurred in their last common ancestor) (Koonin, 2005). Such analyses also revealed likely orthologs for *vic-,7*, *AO370,* and *AO078* in *F. circinatum* (Figures 7-9; Table 3). Phylogenetic analyses using a broader set of sequences obtained from NCBI further confirmed that the single best tblastn hits identified using the *N. crassa het-6* and *pin-C* also likely represent orthologs of these genes (Table 3; Figures 4 and 5).

Among the *F. circinatum* homologs identified, a set of two paralogs (genes that are related by duplication) were identified for *vic-6* (Figures 6). However, following the suggestion by Koonin (2005), they were designated as co-orthologs (i.e., the ancestor of genes Fcirg_05676 and Fcirg_11997 was a *vic-6* ortholog that had

subsequently undergone lineage-specific duplication). Alternatively, the two genes can be viewed as inparalogs as they result from lineage-specific duplication after the divergence of the ancestor of the species in question (Koonin 2005).

In the case of the *HNWD* genes (*het-D*, *het-E*, *het-R*, *HNWD1*, *HNWD2*, and *HNWD3*) from *P. anserina*, they all grouped in an exclusive group that did not contain any *F. circinatum* sequences (Figure 2). However, this group of *HNWD* paralogs formed a sister-group relationship with a set of seven *F. circinatum* paralogs. In other words, the respective groups of paralogs in *P. anserina* and *F. circinatum* each represented a set of co-orthologs (or inparalogs).

Based on the bootstrap support obtained for the respective phylogenetic trees, the ortholog designation for some genes required additional confirmation. This was particularly the case for *pin-C*, *vic-6,* and *AO037* where the relevant branches received <60% bootstrap support (Figures 4, 6, and 8). Therefore, the protein domains encoded by the various homologs were investigated using an InterProScan.

The putative *F. circinatum* orthologs of *het-C*, *het-6*, *vic-6*, *vic-7,* and *AO370* encoded the expected protein domains (Figures 3, 5-8). They all encoded the HET domain (InterPro: IPR010730), although the *N. crassa het-C* and its *F. circinatum* ortholog contained the het-C superfamily (InterPro: IPR010816) domain that includes the HET domain (Figure 3). Like the *N. crassa het-6*, its ortholog in *F. circinatum* additionally also contained an ankyrin repeat domain (InterPro: IPR036770; Figure 5).

For *pin-C*, *AO404,* and the *HNWD* genes from *P. anserina*, differences were observed between the known genes and the identified orthologs from *F. circinatum* regarding domain structure. Unlike what is seen in *pin-C* and *AO404* that contained only the HET domain, their *F. circinatum* orthologs both contained an ankyrin repeat domain in addition to the HET domain (Figures 4 and 9). Furthermore, the *HNWD* co-orthologs in *F. circinatum* contained the expected NACHT nucleoside triphosphatase (NTPase; InterPro: IPR007111) and WD-40 repeat (InterPro: IPR036322) domains but lacked an identifiable HET domain and instead contained

an N-terminal domain (NACHT-N) found in the NACHT-NTPase and P-loop NTPases (InterPro: IPR031352) domain (Figure 2). Two of the *F. circinatum HNWD* genes (Fcirg_14677 and Fcirg_11350) also contained a nucleoside phosphorylase domain (InterPro: IPR000845).

Copy number of the *F. circinatum het/vic* gene orthologs in the model species

At least one best hit for the *F. circinatum het/vic* orthologs were found per species in the reference genomes of the four model fungi (Table 4). These excluded *het-6*, *pin-C*, *vic-6*, *vic-7*, and *AO370*, which did not have any significant hits in at least one of the reference genomes. All hits had significant E-values ($<10^{-40}$), but only the *het-C* gene in *F. circinatum* had a protein identity greater than 60% (Table 4).

Few putative homologs of the *F. circinatum het-C*, *het-6*, *pin-C*, and *AO370* orthologs were found in the genomes of the model species (Table 4). They all had at most two significant copies of the respective *F. circinatum* genes (Table 4). However, *F. circinatum* had substantially more putative homologs of *vic-6* (both co-orthologs) (Table 3; Figure 6), whereas in *A. oryzae* genome it was absent (Table 4).

At least two significant copies of the *het-C* and *AO404* orthologs of *F. circinatum* were detected in the four genomes of the model species (Table 4). In addition, both the best hits for *het-C* and *AO404* had E-values of $<10^{-40}$, >60% query coverage, and >46% identity values. Regarding to the analysis done using the *HNWD* ortholog of *F. circinatum*, multiple homologs were detected in the genomes of all the model species except in *N. crassa* where it was absent. However, the *F. circinatum* genome contained at least 20 homologs of *HNWD* gene (Table 2), those of *P. anserina* and *C. parasitica* and *A. oryzae* contained 10, 8, and 4, respectively (Table 4).

Discussion

The current study lays a foundation for understanding the molecular basis of vegetative/heterokaryon incompatibility in *F. circinatum*. This was achieved by characterizing the known *het/vic* genes from *N. crassa*, *P. anserina*, *C. parasitica*,

and *A. oryzae* in the reference strain (FSP34) of *F. circinatum*. The results showed that most of these known genes have at least one counterpart in *F. circinatum*. The results of phylogenetic analyses further revealed that 13 of the 14 known genes were orthologous to a *F. circinatum* gene. The only exception was *vic-6* of *C. parasitica* and *HNWD* of *P. anserina,* which had multiple co-orthologs in *F. circinatum*. As expected, almost all orthologs encoded for similar functional domains except for the *P. anserina* co-orthologs in *F. circinatum*, which did not have a HET domain but a NACHT-N instead. Also, two of the *HNWD* genes in *F. circinatum* had an extra domain. Lastly, in addition to the HET domain, the *AO404* and *pin-C* orthologs also encoded an Ankyrin repeat domain.

The information presented here showed that the *P. anserina HNWD* genes represent co-orthologs of a comparable set of co-orthologs in *F. circinatum*. In other words, these two sets of genes likely derive from an ancestral *HNWD* gene that has subsequently undergone lineage-specific duplication in the two fungi (Koonin, 2005). It is unknown whether/not these genes are potentially implicated in vegetative compatibility in *F. circinatum.* This is because the *F. circinatum* co-orthologs all encoded the expected domains but lacked the HET domain needed for mediating cell death during vegetative incompatibility (Clavé et al., 2022; Daskalov et al., 2020; Daskalov et al., 2019; Mori et al., 2019; Paoletti & Clave, 2007). This is similar to what has been observed in *Tuber melanosporum,* where the authors concluded that *HNWD* genes are not involved in vegetative incompatibility in this fungus (Iotti et al., 2012). However, some of the co-orthologs did have a nucleoside phosphorylase protein domain with known catalytic activities (GO:0003824), suggesting that they might play some other roles in the processes triggering cell death.

The fact that the putative *HNWD* genes of *F. circinatum* represent co-orthologs or in-paralogs encoding slightly different domains might be indicative of the high evolutionary rates they experience. This is because high evolutionary rates increase further duplication after the initial duplication in the ancestor, thereby increasing the likely number of in-paralogs in the subsequent duplication events (Jordan et al., 2004). Such duplicated genes further experience weak or no functional constraint

(Kondrashov et al., 2002). This might thus explain the differences in functional domains identified in the *HNWD* co-orthologs of *F. circinatum* (Blouin et al., 2003; Jordan et al., 2004).

The two *vic-6* co-orthologs identified in *F. circinatum* represent duplicated genes with a similar function. They both encode only a HET domain and nothing else, which was also found for the other homologs of this gene in *F. circinatum*. Due to the central role that this domain plays in vegetative compatibility, all *vic-6* homologs should be investigated for potential functioning in this phenotype. For example, the results of future population genomic analyses might have polymorphism patterns suggestive of those found using VCG assays, which in turn would point to the genes underpinning this trait in the populations examined.

Different *F. circinatum* genes are orthologous to similar *het/vic* genes in the model species, meaning that the FSP34 strain has more genes encoding one *het/vic* gene as compared to the four model species. As recently reported (Gordon et al., 2021), the current study confirmed the presence of eight different *vic/het* genes in the *F. circinatum* FSP34 genome, namely *het-C*, *pin-C*, *het-6*, *vic-6*, *vic-7*, *AO370*, *AO404*, and *HNWD*. These are all genes interacting with other *vic/het* genes in either an allelic or non-allelic manner to induce the vegetative incompatibility reaction (Saupe et al 2000). Here, allelic refers to when genes from the same locus interact and non-allelic to when interacting genes are from different loci. In other words, genes encoding products potentially representing the non-allelically interacting partners of these identified genes were not identified. The only exceptions were for *het-C* and *pin-C*. This could be because *het-C* is tightly linked to *pin-C* which is its "helper" during the vegetative incompatibility interaction (Kaneko et al., 2006).

Fusarium circinatum FSP34 has a higher *het/vic* genes copy number than any of the model species. Various evolutionary events within species may lead to the multiplication of genes and, if such events occurred in ancestral lineages, thereby potentially increasing gene copy numbers in their descendants. For example, gene duplication may be due to genome duplication, as was reported for *Lichtheimia corymbifera and Rhizopus oryzae* (Schwartze et al. 2014), as well as during species

divergence. For the latter, a notable instance is for *pin-C*, where the divergence of *Sordaria* from *Neurospora* was associated with the duplication of this gene in *Sordaria* (Nowrousian et al., 2010). A study on *het/vic* genes from the Basidiomycota also showed these genes often occurred in multiple copies, with subsequent expansions or losses in numerous lineages (Van der Nest et al., 2014).

Closely related genes may not encode proteins with the same function in different species, meaning that some genes can be closely related and have similar sequences but encode different functional domains. The FSP34 gene Fcirg_05676 is not the closest relative of *pin-C*, with which it shares only a HET domain and no other domains. Although other genes also have the HET domain, they also have the ankyrin repeat domain, which has a variety of functions, including transcriptional initiators, cell cycle regulators, cytoskeletal proteins, ion transporters, and signal transducers (Bartee et al., 2017; Schaffner & Sabeti, 2008). The reason why the Ankyrin repeat domain is absent in *pin-C* and Fcirg_05676 might be that in *F. circinatum*, the HET domain functionality is assisted by this protein as it is for the best hit Fcirg_08239. This could also be the case for *het-6* where all the FSP34 genes code for both the HET domain and the ankyrin repeat domain.

The ankyrin repeat domain was more frequently encountered in the putative *het/vic* genes from *F. circinatum* than in the four model species analysed. The orthologs of *A. oryzae* (*AO404*) and *N. crassa* (*pin-C*) in *F. circinatum* and other FSP34 genes encoded an ankyrin repeat domain in addition to the het domain. It is unclear why this might be the case, but it could point to a fundamental role in vegetative/heterokaryon incompatibility in *F. circinatum* as opposed to the four model species. Alternatively, the ankyrin repeat domain might be a common feature of *F. circinatum* gene architecture where it is involved in multiple processes. This idea may be supported by the fact that the domain is not defined by its function but by its structure of tandemly repeated modules of about 33 amino acids found commonly in eukaryotes (Mosavi et al., 2004). It also has no specific sequence that it recognizes in a respective species (Li et al., 2006).

As expected, the HET domain is encoded commonly throughout putative *het*/*vic* orthologs of *F. circinatum* genes. The molecular processes that determine vegetative compatibility appear to be part of a module that includes a domain that detects like/unlike components from the two interacting strains, as well as a domain that executes cell death (Paoletti, 2016). The domains from the two interacting strains might be found on the same protein or different proteins (Paoletti, 2016). Of these domains, a HET domain encoded by a heterokaryon incompatibility protein is the most common and fundamental in cell death execution. However, other domains such as a Helo domain involved in *P. anserina* gasdermin-like cell death have now been discovered (Rico-Ramírez et al., 2022). These data also show that the presence of a HET domain is not an absolute requirement for cell death execution. Therefore, other new domains, probably having a different function in the model species might carry out this function in *F. circinatum*. Overall, however, gene duplication combined with subsequent gene losses/expansions and various domain fusions/shufflings likely governed the development of the *het*/*vic* gene repertoire of *F. circinatum* as have been demonstrated for other fungi (Van der Nest et al., 2014; Paoletti, 2016).

The data emerging from this study provide a valuable foundation for research on vegetative compatibility in *F. circinatum*. Sequence diversity in genes encoding a HET domain means that their expression in either an allelic or non-allelic interaction may lead to cell death owing to a heterokaryon incompatibility reaction during anastomosis (Strom and Bushley., 2016; Fischer and Glass, 2019; Gonçalves et al., 2020). Therefore, with genomes and VCG inferences made based on this kind of work, it should be easy to identify it. This, together with comparative genomics work, will assist in concluding on the question of whether the South African population is clonal or diverse.

References

Aanen, D. K., Debets, A. J., Glass, N. L., & Saupe, S. J. (2010). Biology and genetics of vegetative incompatibility in fungi. *Cellular and Molecular Biology of Filamentous Fungi*, 274-288.

Bartee, L., Shriner, W., & Creech, C. (2017). Adaptive Evolution. *Principles of Biology*.

Bayman, P., & Cotty, P. J. (1991). Vegetative compatibility and genetic diversity in the *Aspergillus flavus* population of a single field. *Canadian Journal of Botany*, *69*(8), 1707-1711.

Blouin, C., Boucher, Y., & Roger, A. J. (2003). Inferring functional constraints and divergence in protein families using 3D mapping of phylogenetic information. *Nucleic Acids Research*, *31*(2), 790-797.

Chevanne, D., Bastiaans, E., Debets, A., Saupe, S. J., Clavé, C., & Paoletti, M. (2009). Identification of the het-r vegetative incompatibility gene of *Podospora anserina* as a member of the fast evolving HNWD gene family. *Current Genetics*, *55*(1), 93-102.

Choi, G. H., Dawe, A. L., Churbanov, A., Smith, M. L., Milgroom, M. G., & Nuss, D. L. (2012). Molecular characterization of vegetative incompatibility genes that restrict hypovirus transmission in the chestnut blight fungus *Cryphonectria parasitica*. *Genetics*, *190*(1), 113-127.

Clavé, C., Dyrka, W., Turcotte, E. A., Granger-Farbos, A., Ibarlosa, L., Pinson, B., Vance, R. E., Saupe, S. J., & Daskalov, A. (2022). Fungal gasdermin-like proteins are controlled by proteolytic cleavage. *Proceedings of the National Academy of Sciences*, *119*(7).

Daskalov, A., Dyrka, W., & Saupe, S. J. (2020). NLR function in fungi as revealed by the study of self/non-self recognition systems. In *Genetics and Biotechnology* (pp. 123-141). Springer.

Daskalov, A., Gladieux, P., Heller, J., & Glass, N. L. (2019). Programmed cell death in *Neurospora crassa* is controlled by the allorecognition determinant rcd-1. *Genetics*, *213*(4), 1387-1400.

Gertz, E.M., Yu, Y.K., Agarwala, R., Schäffer, A.A. and Altschul, S.F. (2006). Composition-based statistics and translated nucleotide searches: improving the TBLASTN module of BLAST. *BMC Biology*, *4*(1), pp.1-14.

Glass, N. L., Jacobson, D. J., & Shiu, P. K. (2000). The genetics of hyphal fusion and vegetative incompatibility in filamentous ascomycete fungi. *Annual Review of Genetics*, *34*(1), 165-186.

Gordon, T. R., Henry, P. M., Jenner, B. N., & Scott, J. C. (2021). Spontaneous changes in somatic compatibility in *Fusarium circinatum*. *Fungal Biology*.

Gordon, T. R., Kirkpatrick, S. C., Petersen, J. C., & Friel, C. J. (2006). Potential diversity in vegetative compatibility groupings in the California population of *Gibberella circinata*. *Mycological Research*, *110*(8), 936-940.

Henikoff, S., & Henikoff, J. G. (1992). Amino acid substitution matrices from protein blocks. *Proceedings of the National Academy of Sciences*, *89*(22), 10915-10919.

Horn, B. W. (2003). Ecology and population biology of aflatoxigenic fungi in soil. *Journal of Toxicology: Toxin Reviews*, *22*(2-3), 351-379.

Iotti, M., Rubini, A., Tisserant, E., Kholer, A., Paolocci, F., & Zambonelli, A. (2012). Self/nonself recognition in *Tuber melanosporum* is not mediated by a heterokaryon incompatibility system. *Fungal Biology*, *116*(2), 261-275.

Jordan, I. K., Wolf, Y. I., & Koonin, E. V. (2004). Duplicated genes evolve slower than singletons despite the initial rate increase. *BMC Evolutionary Biology*, *4*(1), 1-11.

Kalyaanamoorthy, S., Minh, B. Q., Wong, T. K., Von Haeseler, A., & Jermiin, L. S. (2017). Model Finder: fast model selection for accurate phylogenetic estimates. *Nature Methods*, *14*(6), 587-589.

Kaneko, I., Dementhon, K., Xiang, Q., & Glass, N. L. (2006). Nonallelic interactions between het-c and a polymorphic locus, pin-c, are essential for nonself recognition and programmed cell death in *Neurospora crassa*. *Genetics*, *172*(3), 1545-1555.

Katoh, K., Rozewicki, J., & Yamada, K. D. (2019). MAFFT online service: multiple sequence alignment, interactive sequence choice and visualization. *Briefings in Bioinformatics*, *20*(4), 1160-1166.

Kondrashov, F. A., Rogozin, I. B., Wolf, Y. I., & Koonin, E. V. (2002). Selection in the evolution of gene duplications. *Genome Biology*, *3*(2), 1-9.

Koonin, E. V. (2005). Orthologs, paralogs, and evolutionary genomics. *Annual Review of Genetics*, *39*, 309-338.

Le, S. Q., & Gascuel, O. (2008). An improved general amino acid replacement matrix. *Molecular Biology and Evolution*, *25*(7), 1307-1320.

Leslie, J. F. (1993). Fungal vegetative compatibility. *Annual Review of Phytopathology*, *31*(1), 127-150.

Leslie, J. F., & Summerell, B. A. (2008). *The Fusarium laboratory manual*. John Wiley & Sons.

Li, J., Mahajan, A., & Tsai, M.-D. (2006). Ankyrin repeat: a unique motif mediating protein− protein interactions. *Biochemistry*, *45*(51), 15168-15178.

Milgroom, M. G., & Cortesi, P. (1999). Analysis of population structure of the chestnut blight fungus based on vegetative incompatibility genotypes. *Proceedings of the National Academy of Sciences*, *96*(18), 10518-10523.

Minh, B. Q., Nguyen, M. A. T., & von Haeseler, A. (2013). Ultrafast approximation for phylogenetic bootstrap. *Molecular Biology and Evolution*, *30*(5), 1188-1195.

Mori, N., Katayama, T., Saito, R., Iwashita, K., & Maruyama, J.-i. (2019). Inter-strain expression of sequence-diverse HET domain genes severely inhibits growth of *Aspergillus oryzae*. *Bioscience, Biotechnology, and Biochemistry*, *83*(8), 1557-1569.

Mosavi, L. K., Cammett, T. J., Desrosiers, D. C., & Peng, Z. y. (2004). The ankyrin repeat as molecular architecture for protein recognition. *Protein Science*, *13*(6), 1435-1448.

Müller, T., & Vingron, M. (2000). Modeling amino acid replacement. *Journal of Computational Biology*, *7*(6), 761-776.

Nguyen, L.-T., Schmidt, H. A., Von Haeseler, A., & Minh, B. Q. (2015). IQ-TREE: a fast and effective stochastic algorithm for estimating maximum-likelihood phylogenies. *Molecular Biology and Evolution*, *32*(1), 268-274.

Nowrousian, M., Stajich, J. E., Chu, M., Engh, I., Espagne, E., Halliday, K., Kamerewerd, J., Kempken, F., Knab, B., & Kuo, H.-C. (2010). De novo assembly of a 40 Mb eukaryotic genome from short sequence reads: *Sordaria macrospora*, a model organism for fungal morphogenesis. *PLoS Genetics*, *6*(4), e1000891.

Paoletti, M. (2016). Vegetative incompatibility in fungi: From recognition to cell death, whatever does the trick. *Fungal Biology Reviews*, *30*(4), 152-162.

Paoletti, M., & Clave, C. (2007). The fungus-specific HET domain mediates programmed cell death in *Podospora anserina*. *Eukaryotic Cell*, *6*(11), 2001-2008.

Paoletti, M., Saupe, S. J., & Clavé, C. (2007). Genesis of a fungal non-self recognition repertoire. *PLoS One*, *2*(3), e283.

Papaioannou, I. A., & Typas, M. A. (2015). High-throughput assessment and genetic investigation of vegetative compatibility in *Verticillium dahliae*. *Journal of Phytopathology*, *163*(6), 475-485.

Rico-Ramírez, A. M., Gonçalves, A. P., & Glass, N. L. (2022). Fungal Cell Death: The beginning of the end. *Fungal Genetics and Biology*, 103671.

Saupe, S. J., Clavé, C., & Bégueret, J. (2000). Vegetative incompatibility in filamentous fungi: *Podospora* and *Neurospora* provide some clues. *Current Opinion in Microbiology*, *3*(6), 608-612.

Schaffner, S., & Sabeti, P. (2008). Evolutionary adaptation in the human lineage. *Nature Education*, *1*(1), 14.

Schwartze, V. U., Winter, S., Shelest, E., Marcet-Houben, M., Horn, F., Wehner, S., Linde, J., Valiante, V., Sammeth, M., & Riege, K. (2014). Gene expansion shapes genome architecture in the human pathogen *Lichtheimia corymbifera*: an evolutionary genomics analysis in the ancient terrestrial mucorales (Mucoromycotina). *PLoS Genetics*, *10*(8), e1004496.

Steenkamp, E., Makhari, O., Coutinho, T., Wingfield, B., & Wingfield, M. (2014). Evidence for a new introduction of the pitch canker fungus *Fusarium circinatum* in South Africa. *Plant Pathology*, *63*(3), 530-538.

Tang, J. W., Tambyah, P. A., & Hui, D. S. (2020). Emergence of a novel coronavirus causing respiratory illness from Wuhan, China. *Journal of Infection*, *80*(3), 350-371.

Van der Nest, M., Olson, Å., Lind, M., Velez, H., Dalman, K., Durling, M. B., Karlsson, M., & Stenlid, J. (2014). Distribution and evolution of het gene homologs in the basidiomycota. *Fungal Genetics and Biology*, *64*, 45-57.

Viljoen, A., Wingfield, M.J., Gordon, T.R. and Marasas, W.F.O., 1997. Genotypic diversity in a South African population of the pitch canker fungus *Fusarium subglutinans* f. sp. pini. *Plant Pathology*, *46*(4), 590-593.

Zhang, J., Zhang, X., Han, W., Fan, X., Wang, Y., Xu, D., Zhang, Y., Ma, J., Liang, C., & Ye, N. (2020). Identification of genes under positive selection reveals evolutionary adaptation of Ulva mutabilis. *Acta Oceanologica Sinica*, *39*(10), 35-41.

Table 1: The best-fit models according to the Bayesian information criterion (BIC) as performed in IQtree (Nguyen et al., 2015)

Dataset	Number of sequences	Model	Model reference	The proportion of invariable sites (I)	Empirical base frequencies (F)	Gamma correction for among site rate variation
Het C	4	VT	(Müller & Vingron, 2000)	Yes	Yes	No
Het 6	11	LG	(Le & Gascuel, 2008)	Yes	No	Yes
Pin C	11	LG	(Le & Gascuel, 2008)	Yes	Yes	Yes
Het D	21	VT	(Kalyaanamoorthy et al., 2017)	Yes	Yes	Yes
Het E	21	VT	(Müller & Vingron, 2000)	No	Yes	No
Het R	21	VT	(Müller & Vingron, 2000)	No	Yes	No
HNWD1	21	VT	(Müller & Vingron, 2000)	No	Yes	No
HNWD2	21	VT	(Müller & Vingron, 2000)	Yes	Yes	Yes
HNWD3	21	VT	(Müller & Vingron, 2000)	Yes	Yes	Yes
Vic 6	11	LG	(Le & Gascuel, 2008)	Yes	Yes	Yes
Vic 7	11	LG	(Le & Gascuel, 2008)	Yes	Yes	Yes
AO404	11	Blosum62	(Henikoff & Henikoff, 1992)	No	Yes	Yes
AO370	11	LG	(Le & Gascuel, 2008)	Yes	Yes	Yes

Table 2: Homologs in *F. circinatum* of the 14 HET-domain encoding *vic/het* genes previously characterized in model ascomycetes.

Species	*vic/het* gene	NCBI Accession number[1]	*F. circinatum* (FSP34)[2]	E-value	Identity (%)[3]	Query coverage (HSP/query)[4]	Number of hits
Neurospora crassa	*het-C*	AAF08294.1	Fcirg_07624	0.00	64.62	21	3
			Fcirg_01689	9.21E-142	42.45	31	
			Fcirg_08454	9.91E-86	34.16	31	
	het-6	CAD37033.1	Fcirg_05558	1.90E-99	35.77	32	1
	pin-C	ABC46541.1	Fcirg_11570	1.29E-46	29.23	13	1
Podospora anserina	*het-D*	CAL30216.1	Fcirg_11350	0.00	43.33	30	20
			Fcirg_08680	4.17E-152	30.31	36	
			Fcirg_14595	2.13E-133	29.77	35	
			Fcirg_11141	2.70E-125	35.85	33	
			Fcirg_05581	5.14E-122	37.00	33	

Species	*vic/het* gene	NCBI Accession number[1]	*F. circinatum* (FSP34)[2]	E-value	Identity (%)[3]	Query coverage (HSP/query)[4]	Number of hits
			Fcirg_12012	1.16E-85	28.89	33	
			Fcirg_14567	1.06E-70	39.43	33	
			Fcirg_10819	1.33E-59	47.32	33	
			Fcirg_14677	5.66E-58	25.10	34	
			Fcirg_05914	2.05E-56	45.49	38	
			Fcirg_14532	1.14E-55	48.23	34	
			Fcirg_12012	3.03E-55	35.99	34	
			Fcirg_02359	2.20E-54	48.00	33	
			Fcirg_04013	3.73E-54	31.31	37	
			Fcirg_08274	5.28E-54	47.09	33	
			Fcirg_06736	7.96E-54	45.13	36	
			Fcirg_12299	3.13E-51	32.28	33	
			Fcirg_04013	5.70E-51	38.06	38	
			Fcirg_07090	1.33E-50	45.19	35	
			Fcirg_12012	1.44E-50	39.18	33	

Species	*vic/het* gene	NCBI Accession number[1]	*F. circinatum* (FSP34)[2]	E-value	Identity (%)[3]	Query coverage (HSP/query)[4]	Number of hits
	het-E	CAL30215.1	Fcirg_11350	1.14E-154	51.45	32	19
			Fcirg_11141	4.79E-122	45.49	32	
			Fcirg_05581	3.63E-115	41.28	32	
			Fcirg_14595	3.15E-109	42.60	31	
			Fcirg_08680	4.93E-105	40.03	33	
			Fcirg_14567	5.14E-90	44.91	33	
			Fcirg_10819	1.47E-61	50.88	33	
			Fcirg_07090	1.61E-55	45.70	35	
			Fcirg_05914	1.97E-55	44.49	38	
			Fcirg_12009	3.60E-55	48.51	33	
			Fcirg_14532	5.24E-55	42.80	32	
			Fcirg_02359	1.04E-53	47.53	33	
			Fcirg_08274	1.33E-52	45.26	34	
			Fcirg_12299	2.44E-52	46.15	33	

Species	*vic/het* gene	NCBI Accession number[1]	*F. circinatum* (FSP34)[2]	E-value	Identity (%)[3]	Query coverage (HSP/query)[4]	Number of hits
			Fcirg_01059	3.16E-50	44.13	34	
			Fcirg_09454	1.15E-49	46.38	37	
			Fcirg_02056	1.10E-47	38.77	36	
			Fcirg_11515	6.6E-46	41.33	40	
			Fcirg_05706	2.05E-43	43.50	33	
	het-R	ACM48730.1	Fcirg_11350	0.00	44.76	35	20
			Fcirg_08680	1.36E-162	31.22	37	
			Fcirg_05581	1.00E-134	33.33	34	
			Fcirg_14595	2.39E-129	28.05	36	
			Fcirg_11141	7.56E-129	30.91	34	
			Fcirg_12012	4.51E-83	27.80	33	
			Fcirg_14567	1.85E-74	38.44	33	
			Fcirg_10819	6.49E-63	45.09	32	
			Fcirg_14677	4.36E-59	25.18	35	

Species	*vic/het* gene	NCBI Accession number[1]	*F. circinatum* (FSP34)[2]	E-value	Identity (%)[3]	Query coverage (HSP/query)[4]	Number of hits
			Fcirg_04013	6.38E-59	33.78	38	
			Fcirg_06736	5.16E-58	40.40	36	
			Fcirg_14755	1.42E-57	34.05	32	
			Fcirg_12009	3.97E-55	24.64	34	
			Fcirg_05914	5.65E-54	49.80	36	
			Fcirg_14532	1.12E-51	39.64	32	
			Fcirg_12299	1.46E-51	39.74	35	
			Fcirg_08274	6.85E-51	32.71	33	
			Fcirg_01059	2.43E-50	38.41	35	
			Fcirg_09454	2.85E-50	43.51	36	
	HNWD1	CAL30203.1	Fcirg_11350	0.00	47.72	33	20
			Fcirg_08680	1.48E-158	33.06	30	
			Fcirg_14595	3.87E-147	32.36	32	
			Fcirg_05581	8.63E-129	32.59	33	

Species	vic/het gene	NCBI Accession number[1]	F. circinatum (FSP34)[2]	E-value	Identity (%)[3]	Query coverage (HSP/query)[4]	Number of hits
			Fcirg_11350	5.28E-124	43.00	36	
			Fcirg_11141	6.52E-122	30.27	35	
			Fcirg_14567	7.16E-87	44.06	32	
			Fcirg_14677	1.65E-82	24.48	33	
			Fcirg_12012	5.89E-71	26.91	32	
			Fcirg_10819	8.39E-62	49.78	32	
			Fcirg_06736	8.74E-61	40.13	33	
			Fcirg_05914	4.02E-59	39.40	35	
			Fcirg_12012	1.73E-57	38.51	33	
			Fcirg_09454	8.83E-57	47.06	32	
			Fcirg_14532	2.80E-56	40.40	30	
			Fcirg_04013	3.52E-56	35.87	35	
			Fcirg_02359	1.35E-55	50.43	32	
			Fcirg_12009	1.67E-55	40.07	33	
			Fcirg_12299	1.76E-55	47.56	36	

Species	vic/het gene	NCBI Accession number[1]	F. circinatum (FSP34)[2]	E-value	Identity (%)[3]	Query coverage (HSP/query)[4]	Number of hits
			Fcirg_07090	4.47E-55	35.19	32	
	HNWD2	CAL30202.1	Fcirg_11350	0.00	46.97	32	20
			Fcirg_08680	8.45E-135	37.38	34	
			Fcirg_05581	1.52E-129	35.85	32	
			Fcirg_11141	2.06E-128	36.47	35	
			Fcirg_14595	6.00E-106	31.55	32	
			Fcirg_14567	9.00E-76	38.44	33	
			Fcirg_10819	1.27E-63	45.09	33	
			Fcirg_12009	3.32E-55	49.39	33	
			Fcirg_05914	1.81E-54	39.64	35	
			Fcirg_14532	7.13E-52	43.51	32	
			Fcirg_12299	7.97E-52	44.24	33	
			Fcirg_08274	3.60E-51	47.06	32	
			Fcirg_01059	1.61E-50	42.92	34	

Species	vic/het gene	NCBI Accession number[1]	F. circinatum (FSP34)[2]	E-value	Identity (%)[3]	Query coverage (HSP/query)[4]	Number of hits
			Fcirg_09454	1.76E-50	44.09	33	
			Fcirg_07090	4.14E-50	39.45	32	
			Fcirg_02359	9.47E-50	42.92	33	
			Fcirg_02056	9.39E-47	36.94	32	
			Fcirg_12056	1.93E-45	24.37	34	
			Fcirg_12012	6.90E-45	38.64	35	
			Fcirg_11515	2.91E-44	24.81	33	
	HNWD3	CAL30201.1	Fcirg_11350	0.00	45.58	33	20
			Fcirg_08680	3.48E-172	32.42	32	
			Fcirg_14595	8.25E-156	35.49	34	
			Fcirg_05581	3.92E-151	33.91	34	
			Fcirg_11141	2.69E-148	35.41	33	
			Fcirg_14567	1.97E-92	43.42	33	
			Fcirg_12012	1.51E-80	28.15	32	

Species	*vic/het* gene	NCBI Accession number[1]	*F. circinatum* (FSP34)[2]	E-value	Identity (%)[3]	Query coverage (HSP/query)[4]	Number of hits
			Fcirg_10819	1.98E-65	53.88	33	
			Fcirg_14677	8.91E-65	25.43	32	
			Fcirg_04013	2.87E-60	35.81	33	
			Fcirg_05914	1.17E-59	45.91	35	
			Fcirg_06736	1.78E-59	41.39	34	
			Fcirg_14532	1.52E-58	51.77	32	
			Fcirg_12009	3.67E-58	41.39	33	
			Fcirg_02359	5.50E-58	51.13	34	
			Fcirg_12299	3.79E-57	41.39	33	
			Fcirg_07090	1.95E-55	35.28	35	
			Fcirg_01221	1.64E-54	50.22	32	
			Fcirg_01059	1.28E-53	48.03	33	
			Fcirg_08274	3.30E-53	46.22	34	
Cryphonectria	vic-6	AET07139.1	Fcirg_11323	8.54E-57	33.33	35	10

Species	*vic/het* gene	NCBI Accession number[1]	*F. circinatum* (FSP34)[2]	E-value	Identity (%)[3]	Query coverage (HSP/query)[4]	Number of hits
parasitica			Fcirg_14134	1.55E-56	33.67	31	
			Fcirg_05676	2.80E-53	34.01	33	
			Fcirg_11997	5.93E-51	32.53	30	
			Fcirg_13663	1.05E-50	34.45	33	
			Fcirg_14563	1.59E-49	31.28	32	
			Fcirg_11570	1.39E-48	28.54	34	
			Fcirg_13201	3.13E-46	31.31	32	
			Fcirg_15261	3.27E-46	32.12	32	
			Fcirg_05610	4.05E-43	29.66	31	
	vic-7	QHN64381.1	Fcirg_15095	3.31E-92	44.90	34	1
Aspergillus oryzae							
	AO078	AO090001000078	none	-	-	-	0
	AO370	AO090701000370	Fcirg_15261	5.94E-51	29.83	31	3

Species	*vic/het* gene	NCBI Accession number[1]	*F. circinatum* (FSP34)[2]	E-value	Identity (%)[3]	Query coverage (HSP/query)[4]	Number of hits
			Fcirg_13927	6.51E-43	29.41	31	
			Fcirg_11570	2.25E-40	27.06	33	
	AO404	AO090701000404	Fcirg_14532	3.60E-98	32.34	34	10
			Fcirg_12299	8.51E-54	34.94	40	
			Fcirg_08274	6.57E-50	41.16	44	
			Fcirg_09952	5.28E-47	44.70	34	
			Fcirg_09454	5.20E-45	40.08	46	
			Fcirg_07090	7.54E-44	38.08	45	
			Fcirg_12009	5.07E-42	31.81	40	
			Fcirg_10819	2.67E-41	36.56	52	
			Fcirg_01059	2.85E-41	38.52	41	
			Fcirg_02359	4.35E-41	36.92	45	

[1] National Centre for Biotechnology Institute (https://www.ncbi.nlm.nih.gov) accession numbers.

[2] Identified using the *het/vic* gene in tblastn searches against the genome of *F. circinatum* isolate FSP34

[3] Percentage identity: the determinant of how similar the query and the hit sequence are.

[4]The percentage query coverage (High-scoring segment pair [HSP] length/query length *100), the determinant of how much of the query sequence is covered by the hit sequence.

Table 3. Gene number and genome position for putative orthologs of the known HET domain-encoding *vic/het* genes identified in *F. circinatum*.

Model species	*vic/het* gene	*F. circinatum* gene[1]	Position in the genome FSP34[2]
N. crassa	*het-C*	Fcirg_07624	Chromosome 4: 1580319-1582889
	het-6	Fcirg_05558	Chromosome 5: 15885-160826
	pin-C	Fcirg_11570	Chromosome 8: 895280-897626
P. anserina	*het-D, het-E,*	Fcirg_11350	Chromosome 8: 359267-363902
	het-R, HNWD1,	Fcirg_08680	Chromosome 6: 100512-105287
	HNWD2, HNWD3	Fcirg_14595	Chromosome 11: 334152-340394
		Fcirg_11141	Chromosome 7: 324973-3210650
		Fcirg_05581	Chromosome 5: 208037-211991
		Fcirg_12012	Chromosome 8: 2133397-2137752
		Fcirg_14677	Chromosome 11: 513905-519406`
C. parasitica	*vic-6*	Fcirg_05676	Chromosome 5: 430849-432451
		Fcirg_11997	Chromosome 8: 2096256-2098248
	vic-7	Fcirg_15095	Chromosome 11: 1644971-1647228
A. oryzae	*AO370*	Fcirg_05610	Chromosome 6: 2340225-2342183
	AO404	Fcirg_14532	Chromosome 11: 176925-179045

[1] Identified using a phylogeny-based approach (see Figures 2-9).

[2] Nucleotide position of the putative *vic/het* gene orthologs in the genome of strain FSP34 of *F.circinatum.*

Table 4: Number of homologs of the *F. circinatum het*/*vic* orthologs detected in genomes of four model fungi.

Reference fungi	*vic/het* gene	*F. circinatum* query [2]	Number of tblastn hits	Best hit information			
				Accession number	E-value	Identity (%)	Query coverage (%) [3]
N. crassa	*het-c*	Fcirg_07624	2	NC_026502	0.00	80.00	95.00
	het-6	Fcirg_05558	3	NC_026502	2.08E-101	36.98	51.45
	pin-C	Fcirg_08239	No hit	-	-	-	-
	vic-6	Fcirg_05676	1	NC_026506	7.73E-51	34.82	51.53
	vic-6	Fcirg_11997	4	NC_026507	1.96E-57	34.08	51.26
	vic-7	Fcirg_15095	No hit	-	-	-	-
	AO370	Fcirg_05610	1	NC_026503	8.83E-87	33.73	47.59
	AO404	Fcirg_14532	2	NC_026504	8.18E-82	51.08	70.56
	HNWD representative	Fcirg_11350	No hit	-	-	-	-
P. anserina	*het-c*	Fcirg_07624	2	NW_001914857	3.46E-121	52.72	69.39
	het-6	Fcirg_05558	2	NW_001914834	3.61E-147	39.05	56.90
	pin-C	Fcirg_08239	2	NW_001914834	1.82E-45	31.40	49.03
	vic-6	Fcirg_05676	1	NW_001914854	4.49E-48	30.70	45.63
	vic-6	Fcirg_11997	1	NW_001914857	6.99E-41	30.24	46.11
	vic-7	Fcirg_15095	No hit	-	-	-	-
	AO370	Fcirg_05610	2	NW_001914837	1.60e-46	32.07	46.56
	AO404	Fcirg_14532	12	NW_001914846	1.35E-80	52.72	69.39

	HNWD representative	Fcirg_11350	10	NW_001914858	0.00	100	57.36
C. parasitica	het-c	Fcirg_07624	2	NW_024468912	0.00	70.24	80.36
	het-6	Fcirg_05558	No hit	-	-	-	-
	pin-C	Fcirg_08239	2	NW_024468909	6.42E-45	33.42	48.77
	vic-6	Fcirg_05676	3	NW_024468911	3.07E-54	34.63	50.39
	vic-6	Fcirg_11997	2	NW_024468911	2.18E-47	32.48	49.00
	vic-7	Fcirg_15095	1	NW_024468914	8.23E-96	38.92	53.63
	AO370	Fcirg_05610	2	NW_024468912	1.80E-47	35.64	48.24
	AO404	Fcirg_14532	4	NW_024468911	2.41E-75	46.82	60.90
	HNWD representative	Fcirg_11350	4	NW_024468910	0.00	69.32	50.10
A. oryzae	het-c	Fcirg_07624	2	NC_036438	8.71E-163	61.97	78.87
	het-6	Fcirg_05558	1	NC_036440	6.03E-54	29.36	42.35
	pin-C	Fcirg_08239	2	NC_036438	5.20E-48	38.54	51.56
	vic-6	Fcirg_05676	No hit	-	-	-	-
	vic-6	Fcirg_11997	No hit	-	-	-	-
	vic-7	Fcirg_15095	No hit	-	-	-	-
	AO370	Fcirg_05610	No hit	-	-	-	-
	AO404	Fcirg_14532	6	NC_036441	6.73E-159	50.84	68.23
	HNWD representative	Fcirg_11350	8	NC_036440	2.05E-79	70.00	22.35

[1] The identified *het*/*vic* gene orthologs of *F. circinatum* isolate FSP34 used in the tblastn search sequences of the against fungi.

[2] National Centre for Biotechnology Institute (https://www.ncbi.nlm.nih.gov) accession numbers.
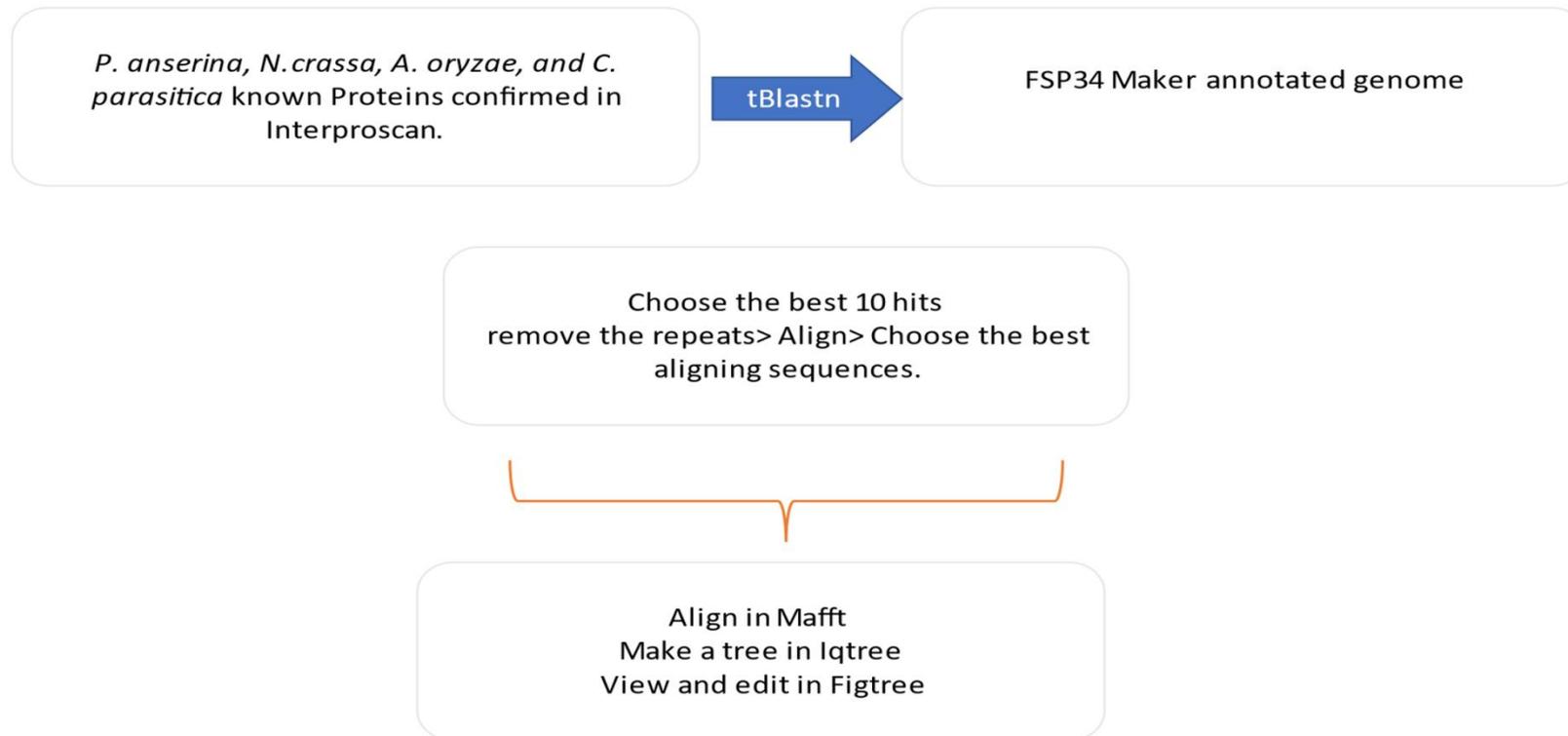
P. anserina, N.crassa, A. oryzae, and C. parasitica known Proteins confirmed in Interproscan.

tBlastn

FSP34 Maker annotated genome

Choose the best 10 hits
remove the repeats> Align> Choose the best aligning sequences.

Align in Mafft
Make a tree in Iqtree
View and edit in Figtree

Figure 1: Overview of the methodology used to identify orthologs of the known HET-domain containing het/vic genes from four model fungi.

Figure 2: Phylogenetic tree showing the relationships among the *Podospora anserina* het domain coding genes such as *Het-D*, *Het-R*, *Het-E*, *HNWD1*, *HNWD2*, *HNWD3* and their blast hits and domains they code for in *F. circinatum* FSP34 isolate. Each coloured star represents a different protein domain that was identified using the InterProScan per gene in the phylogenetic tree.
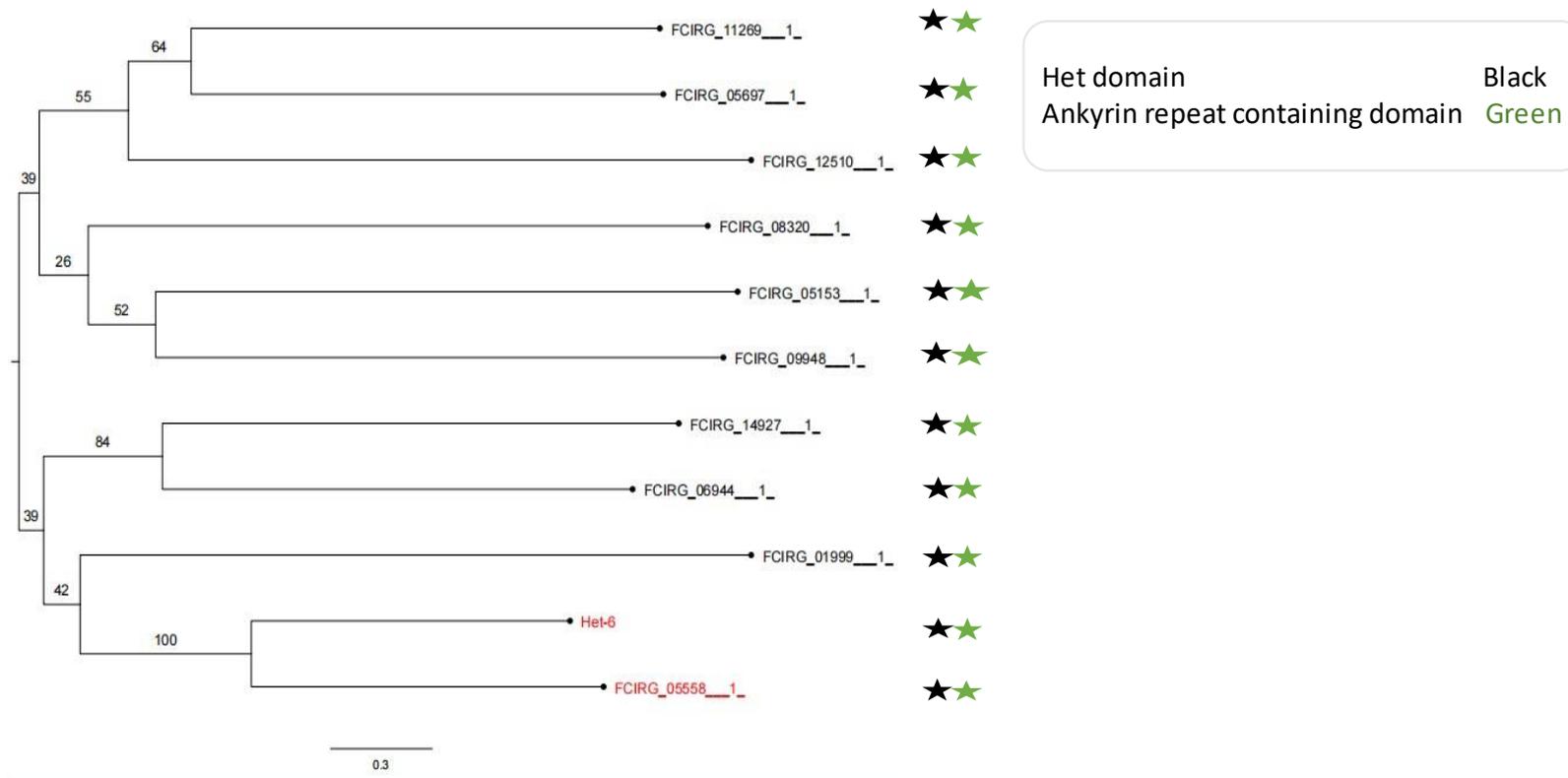
Figure 3: Phylogenetic tree showing the *het-C* homolog and domains they code for in *F. circinatum* FSP34 isolate. Each coloured star represents a different protein domain that was identified using the InterProScan per gene in the phylogenetic tree.
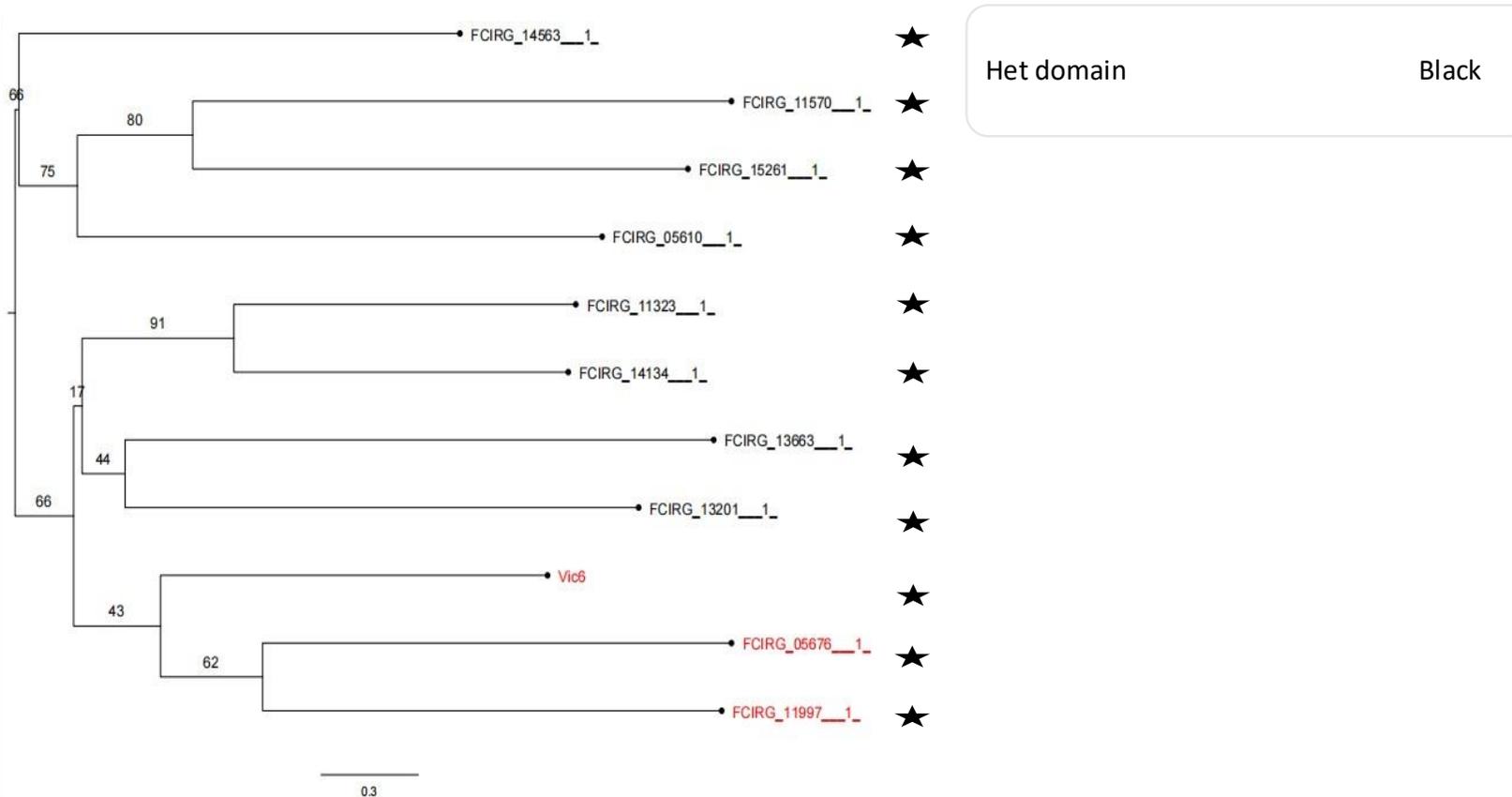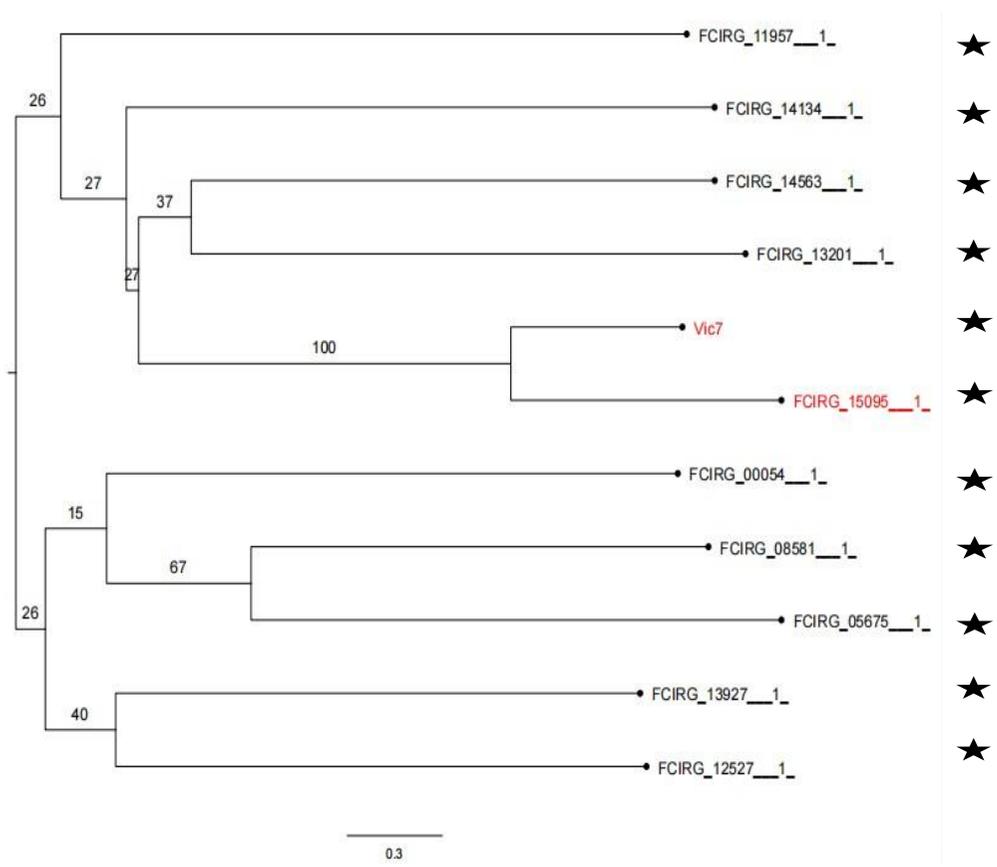
Figure 4: Phylogenetic tree showing the *Pin-C* homolog and domains they code for in *F. circinatum* FSP34 isolate. Stars represent a different protein domain that was identified using the InterProScan per gene in the phylogenetic tree.

Figure 5: Phylogenetic tree showing the *het-6* homolog and domains they code for in *F. circinatum* FSP34 isolate. Each coloured star represents a different protein domain that was identified using the InterProScan per gene in the phylogenetic tree.

Figure 6: Phylogenetic tree showing the *vic-6* hits and domains they code for in *F. circinatum* FSP34 isolate. Each coloured star represents a different protein domain that was identified using the InterProScan per gene in the phylogenetic tree.
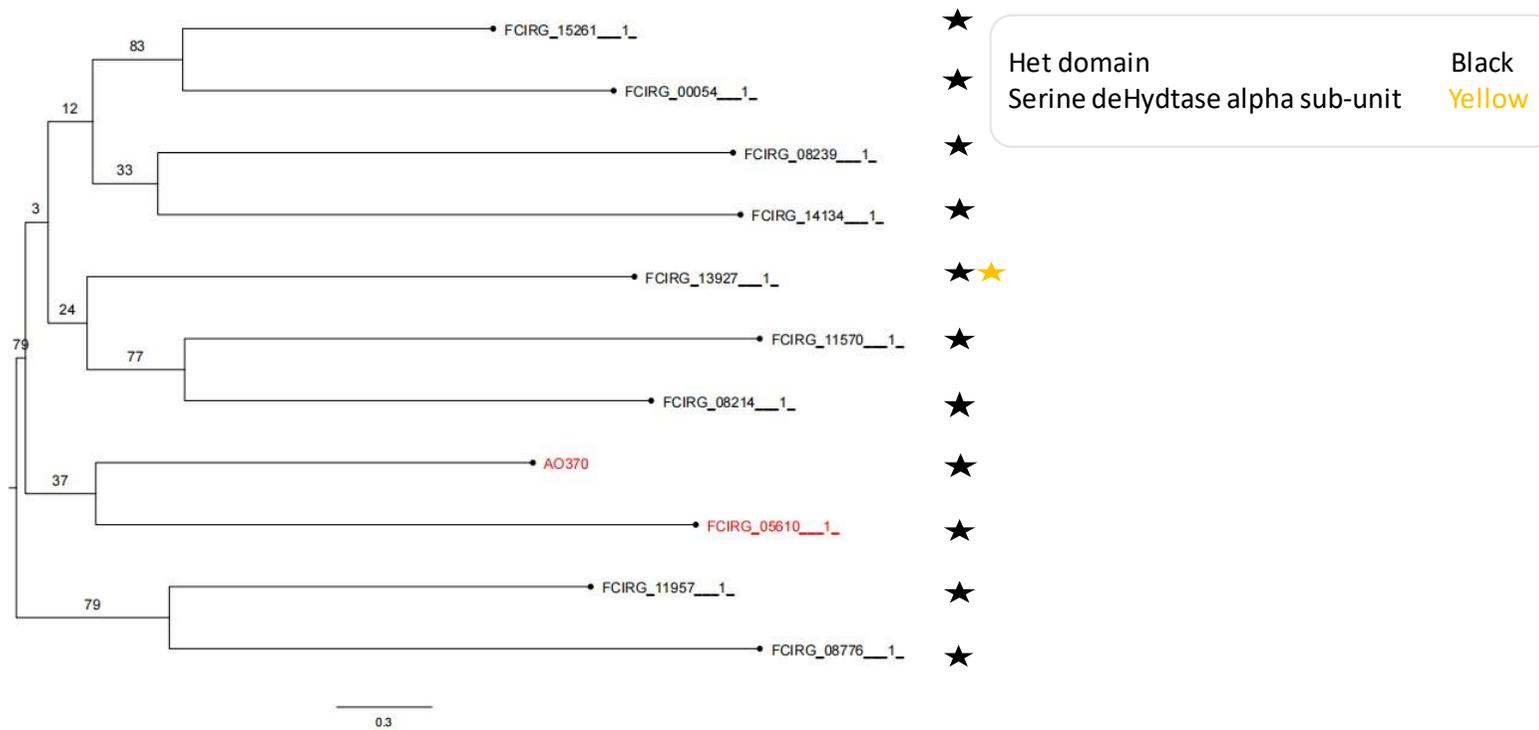
Figure 7: Phylogenetic tree showing the *vic-7* homolog and other close hits, and domains they code for in *F. circinatum* FSP34 isolate. Each coloured star represents a different protein domain that was identified using the InterProScan per gene in the phylogenetic tree.

Figure 8: Phylogenetic tree showing the *AO370* homolog and other close hits, and domains they code for in *F. circinatum* FSP34 isolate. Each coloured star represents a different protein domain that was identified using the InterProScan per gene in the phylogenetic tree.
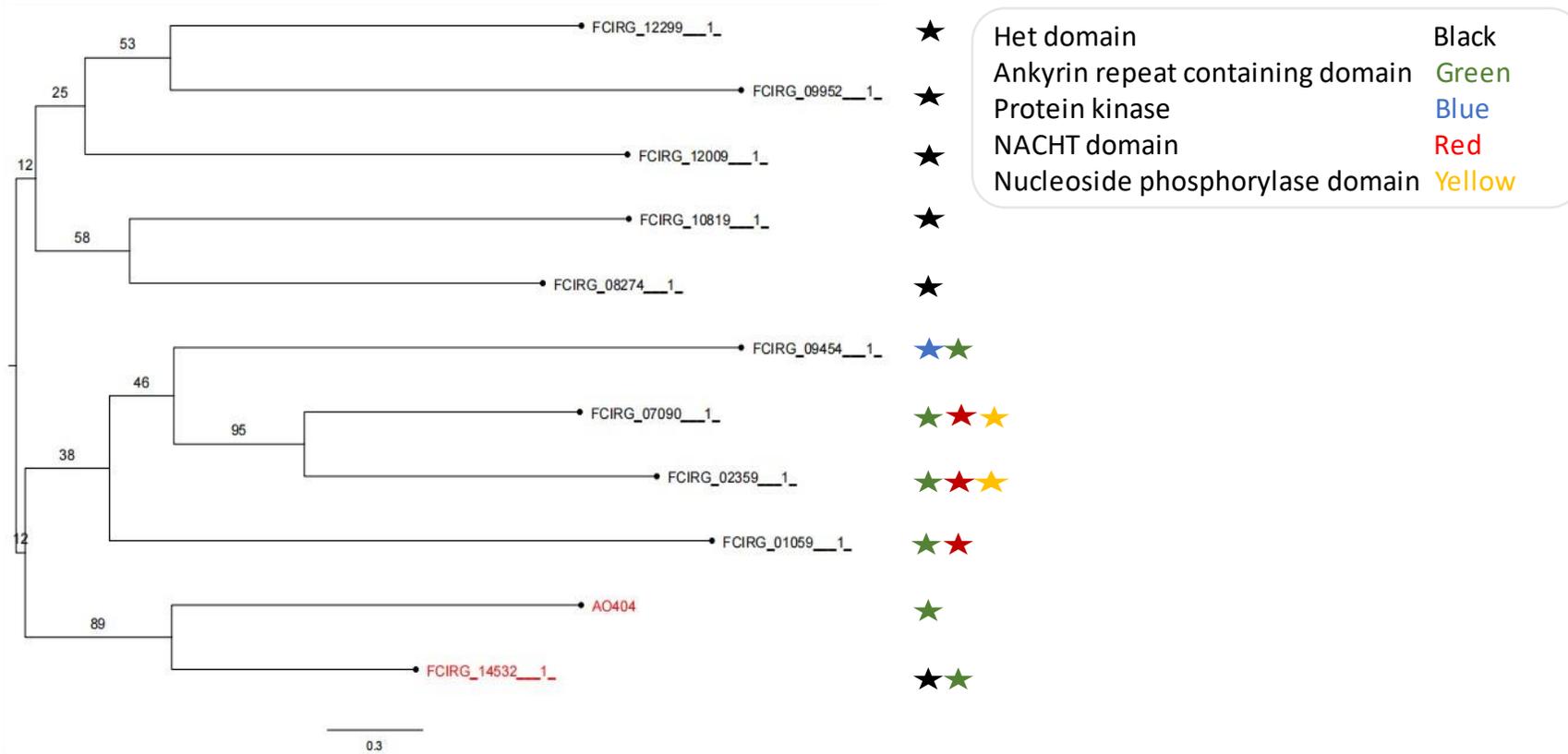
Figure 9: Phylogenetic tree showing the *AO404* hits and domains they code for in *F. circinatum* FSP34 isolate. Each coloured star represents a different protein domain that was identified using the InterProScan per gene in the phylogenetic tree.

SUMMARY

The population of *Fusarium circinatum* in South Africa is large and diverse, yet relatively few isolates have sequenced genomes or have been genotyped using microsatellites. Indeed, only one strain so far has a draft genome that is fully annotated. However, there has been significant progress in studies to better understand the population biology of this fungus in order to develop effective disease control measures for it in the local pine-based forestry industry. This study established a foundation for guiding subsequent full characterisation of the entire *F. circinatum* population using vegetative incompatibility. The literature review included here outlines and summarizes what is currently known about *F. circinatum* populations and the knowledge gap.

The first research chapter (Chapter Two) focused on the phenotypic traits of *F. circinatum* isolates that were considered clonal based on ten unlinked microsatellite loci. The results showed that isolates thought to be clonal based on microsatellites differed significantly on a phenotypic level. This implies that we might be dealing with a more diverse population sharing the same multilocus genotypes. Two possible concluding hypotheses were drawn: previous genotyping methods were either not sensitive enough to delineate true clones or the phenotypic differences observed were due to differential gene regulation. Therefore, a subsequent study should use genomic and transcriptomic approaches to uncover the genetic identity of these isolates. For this purpose, after the South African population of *F. circinatum* isolates is sequenced, vegetative compatibility groups-based genotyping could be performed using both bioinformatics and laboratory-based techniques.

The second research chapter (Chapter Three) lays the groundwork for understanding the molecular basis of vegetative/heterokaryon incompatibility in *F. circinatum*. This was accomplished by characterizing the known het/vic genes from *N. crassa*, *P. anserina*, *C. parasitica*, and *A. oryzae* in the *F. circinatum* reference strain (FSP34). The findings revealed that most of these known genes have at least one putative homolog in *F. circinatum*. Phylogenetic analyses also revealed that 13 of the 14 known genes had orthologs in *F. circinatum*. The only exceptions were *C.*

parasitica's *vic-6* and *P. anserina*'s *HNWD* genes, both of which had multiple co-orthologs in *F. circinatum*. Almost all orthologs encoded similar functional domains, apart from the *P. anserina* co-orthologs in *F. circinatum*, which did not encode a HET domain but rather a NACHT-N. In addition, two of the *HNWD* genes in *F. circinatum* had an extra domain. Finally, in addition to the HET domain, *F. circinatum* orthologs of the *AO404* and *pin-C* genes encoded an ankyrin repeat domain.

This dissertation thus adds valuable information into the population structure of *F. circinatum*. Future studies can focus on the molecular validation of the genes involved in vegetative incompatibility by production of knock-out mutants and the bioinformatic analysis of *het*/*vic* loci of more isolates. In addition, transcriptional and genomic characterization of isolates from the same multilocus genotype will reveal the basis for their phenotypic variation.